Lake Sturgeon (*Acipenser fulvescens*) Myotome Development: The Proliferation of Satellite Cells in the Developing Sturgeon

by

Amber Hiebert

A thesis submitted to the Faculty of Graduate Studies

in partial fulfillment of the requirements to the degree of

MASTER OF SCIENCE

Department of Biological Sciences

University of Manitoba

Winnipeg, Manitoba

Contents

Abstract

The Lake Sturgeon (*Acipenser fulvescens*) continues to grow throughout life, though the process by which muscle stem cells, called satellite cells (SCs) contribute to formation of fibers in the myotome is largely unknown in this endangered fish. Since muscle function and growth are critical to survival, it is important to understand the functional basis of fiber growth, and how SCs provide daughter cells that fuse into fibers in myotome development and regeneration. The hypotheses are that during aging: the cell cycle of SCs lengthens, the ratio of SCs to myonuclei decreases, and myonuclear domain increases. This experiment used the single fiber model and a pulse-chase design in which exposure to bromodeoxyuridine (BrdU) labeled S-phase for the first 2 hr in culture. Myofibers were isolated from 20-40 fish per age (1-6 months post-hatch). After fiber culture for 24 hours, fibers were fixed and stained for BrdU or Pax7 (expressed by myogenic stem cells) with colour detection. The number of Pax7- or BrdU-positive nuclei and the total number nuclei associated were counted per fiber in 8-20 fibers per dish. Results showed a significant change in the ratio of Pax7+ SCs to myonuclei as the fish age ($p < 0.05$) with an apparent decrease in cell cycle duration with increasing age ($p < 0.05$). This investigation adds to our understanding of SC contributions to myofiber growth in the developing Lake Sturgeon and results will be a new foundation for future research on the role of environmental influences on muscle in Lake Sturgeon.

Acknowledgements

I want to thank several people for helping me through the past 2 years of graduate school, and for continual support, guidance and encouragement. My research and this thesis would not have been possible without the people in my life.

I must start by thanking my advisor, Judy Anderson. I cannot thank you enough for your patience, guidance and support though my research and writing, but also in my personal life. Your expertise and understanding made it possible to work on and complete research on this topic that was of great interest to me. It was such a pleasure to work with you.

I am grateful to the members of my committee, Dr. Peeler and Dr. G. Anderson. Your guidance and help contributed greatly to this project.

Thank you to the members of the lab, Ziba and Nasibeh. Your assistance, support and company were appreciated daily.

Thank you to the funding provided by the NSERC Discovery grant program and the Graduate Enhancement of Tri-Council Stipends program at the University of Manitoba (both to Dr. Judy Anderson), as well as collaborative support of research funding to Dr. Gary Anderson (NSERC-Manitoba Hydro Industrial Research Chair; NSERC Discovery grant program). Thank you also to the sturgeon-rearing facilities and staff of the Biological Sciences Animal Holding Facility at the University of Manitoba.

Finally, and most importantly, a huge thank you to my family and my amazing boyfriend Peter, for their patience and encouragement, and also to the Almighty God, for his guidance and grace in me. This would not have been possible without all of you.

List of Tables

List of Figures

Introduction

Skeletal muscle provides the means for mobility and allows fish to interact with and move through their environment. Red muscle uses mitochondria and oxidative aerobic metabolism for slow, endurance swimming, whereas white muscle utilizes glycolytic anaerobic metabolism for quick, burst swimming. Muscle has an innate ability to regenerate following injury, a characteristic provided by the muscle stem cells, also termed satellite cells (SCs) that surround the muscle. As well as regeneration, SCs are responsible for post-natal muscle development. Satellite cells, found between the basement membrane and the plasma membrane of the muscle fibers, have the ability to self-renew, and provide a muscle precursor cell in the same proliferation event (Chang & Rudnicki, 2014). During initial stages of post-natal mammalian myogenesis, SCs are very active, but they become quiescent in adult muscle, at least in mammals. Even though they remain inactive for the majority of a mammal's life, they are able to become activated when resident muscle becomes damaged (Qu-Petersen et al., 2002) or in response to mechanical stretching and exercise (Leiter et al., 2012; Leiter & Anderson, 2010). The activation of SCs is a very regulated process, and can occur due to mechanical means such as by resistance muscle training, by electrical stimulation, or by chemical means such as by myogenic regulatory factors (MRFs) like Myf5, MyoD, myogenin and MRF4 (Kern et al., 2014; Zammit et al., 2001).

Muscle development is a very important process in any animal. Without proper development of skeletal muscle, movement will be impaired, which affects survival. Especially in fish this is important, since fish must be able to swim to find food and evade predators as soon as they hatch. Unlike muscle development in teleosts, or bony fish, which

is well studied, the same in not as well studied in ancient fish. The most traditional method of muscle research is at the cellular level, using histological techniques to study sections cut from muscle, though the isolation of myofibers instead of sections allows for additional focus on the fiber unit, which can be viewed to track myosatellite cell location and proliferation status as well as molecular-level features of metabolism (such as fiber typing) or gene and protein expression (such as applied in this thesis project).

The Lake Sturgeon (*Acipenser fulvescens*) is a freshwater fish residing in North America and has become a conservation focus due to its risk for extinction. With a skeleton made of cartilage and an armoured body, it is thought of as a living fossil. Although it is an evolutionarily old species, not a lot is known about its development. This research project aimed to describe and document the size and growth pattern of skeletal muscle fibers in Lake Sturgeon as well as show the rate at which SCs are incorporated into the skeletal muscle.

Chapter 1: Literature Review

1.1 Skeletal Muscle Development

Skeletal muscle development in amniotes and teleosts (bony fish) is a remarkably conserved process. In both, muscle development occurs through several steps or waves of myogenesis, but the timing of those steps differs in the two clades. There are also other commonalities such as the formation of somites and myotomes, molecular signals that advance commitment and differentiation, as well as the exhibition of muscle fibers with different contractile characteristics (Rossi & Messina, 2014). Some specific differences of teleost muscle development from amniotes are: processes at the early stage of muscle

commitment, the very different proportions of fast- and slow-contracting fibers, and the capability for some species to have indeterminate growth, or growth throughout much of their ontogeny (Rossi & Messina, 2014). Embryonic myogenesis also occurs earlier in teleosts than in amniotes, which could be due to the necessity to produce momentum as soon as they hatch (Johnston et al, 2011).

1.1.1 Mammalian Development

Undifferentiated cells from the mesoderm-derived somites proliferate to produce the first muscle cells in mammalian embryonic myogenesis. The stages of amniote development are categorized into pre-natal and post-natal, each of which is defined by a different set of myogenic precursor cells. In pre-natal development, fetal and embryonic myoblasts, derived from somites, are involved in myogenesis, and satellite cells (SCs) govern myogenesis in post-natal development. Different than satellite cells, somites are ball-like blocks of tissue containing the initial proliferating cells in the embryo that form embryonic muscles (Epstein et al., 2017). The cells that make up the skeletal muscles of the trunk and limbs come from the dermomyotome (Schäfer & Braun, 1999). The dermomyotome part of somites in amniotes gives rise to hypaxial muscles of the body, and some muscles of the head, though the fate of these cells is determined by the surrounding environment (Dietrich et al., 1999). The myotome portion of the dermomyotome gives rise to the epaxial muscles of the body.

The steps that somites of the myotome must take in each myogenetic wave before they differentiate into muscle cells are delamination, migration, proliferation and determination (Buckingham et al., 2003). Delamination is the process that occurs as myoblasts leave the dermomyotome; it is controlled by the transcription factor Pax3 and

the gene c-met, the hepatocyte growth factor receptor (HGFR) (Dietrich et al., 1999; Epsteinet al., 2017). Both c-met and Pax3 are involved with long distance migration of myoblasts and many experiments have aimed to explain their involvement. In Pax3-deficient mice, both delamination and migration are absent (Schäfer & Braun, 1999). Pax3 has many functions in development as a regulatory transcription factor. It controls the delamination and migration of muscle precursor cells, and also regulates c-met expression (Dietrich et al., 1999). Although Pax3 is very involved in development of limb and trunk muscles, it doesn't appear to play a role in development of face and head muscles (Tajbakhsh et al., 1997).

Pax3 also appears to be involved with migration of somitic cells during development, along with c-met, its ligand hepatocyte growth factor (HGF), and Ladybird Homeobox 1 (Lbx1). C-met and Pax3 have several roles in regulation during several steps of muscle development, though Lbx1, a homeobox transcription factor, mainly has a role only in migration of somites (Schäfer & Braun, 1999). Some somites and derivatives of somites need to migrate a distance to develop skeletal muscle, and subsequently have high expression of Lbx1. This transcription factor is a very important factor in designating the migratory fate, as well as the migratory path of cells derived from somites (Schäfer & Braun, 1999). Cells in non-migratory somites do not express Lbx1, but still do express c-met and Pax3 (Dietrich et al., 1999). Embryos that are deficient in Lbx1 display somites that delaminate but stay in the local area of their origin. These cells adopt a different cell fate that depends upon their niche (Schäfer & Braun, 1999). Though the expression of c-met and Pax3 is not required to regulate migration, mutations in these genes can affect the delamination and migration of somites destined to migrate (Dietrich et al., 1999).

The step following migration in muscle development is proliferation of the somitic cells called myogenic precursor cells (Marics et al., 2002). Cells that migrate from their location of origin express pax3, c-met, and Lbx1, and develop independently of the expression of myogenic regulatory factors (MRFs). During development, the somites sequentially start to express the MRFs Myf5, myogenin, Myf-6 and MyoD (Braun et al., 1994; Tajbakhsh & Buckingham, 2017). Proliferation of the muscle progenitor cells (MPCs) is regulated by Pax3, c-met, Myf5, MyoD, Six1 and Six4 transcription factors (Delfini et al., 2000). It appears as though Myf5 is the first transcription factor to be expressed in myogenic progenitors, and its expression actually commits the cell to the myogenic lineage (Kablar et al., 1999). The MRFs have such a strong influence on cell fate that if ectopically expressed or overexpressed (in transgenic mice) they are able to convert non-muscle progenitor cell types, such as chondroblasts, fibroblasts, smooth muscle and epithelial cells into myoblasts and multinucleated myotubes (Choi et al., 1990). Once the cell starts expressing Myf5 and MyoD, this increases the expression of Mox2, Six1 and Six4 regulatory transcription factors (Mootoosamy & Dietrich, 2002). Mox2, a homeobox protein, is critical for regulation of skeletal muscle development in the embryo. It is expressed in myoblasts that have migrated, and is regulated by Pax3 and Myf5 (Mankoo et al., 1999). Experiments so far show that the Six1 and Six4 transcription factors are involved minimally in regulating proliferation, but rather have more of a preventative role in apoptosis (Grifone et al., 2005). Somitic cells deficient in Six1 and Six4 homeoproteins display a much higher rate of apoptosis, exhibiting the importance of Six homeoproteins in cell survival (Grifone et al., 2005). This combination of increased proliferation and decreased cellular apoptosis works to promote growth and development.

Myf5 and MyoD are very important MRFs, but studies show that the expression of these two proteins alone is not enough to activate the differentiation pathway (Delfini et al., 2000). In addition to these myogenic regulatory factors being critical in muscle growth and development, Notch signalling has also been shown to repress MyoD transcription, allowing a delay in the expression of MyoD and therefore a delay in differentiation (Delfini et al., 2000).

There is a very complex regulatory framework in which many parts must all work together within the MPCs to get the cells to their migratory destination, and expressing all the correct proteins (Mankoo et al., 1999). Since there are so many regulatory factors involved, removal of one of them won't necessarily negate muscle development completely, but rather the embryo would show a defect in specific area(s) (Tajbakhsh & Buckingham, 2017). Embryonic muscle development is coordinated by combinations of several regulatory transcription factors, rather than one master factor (Cornelison & Wold, 1997).

The dermomyotome provides the cells for muscle development in the early embryo; however, once this structure disappears, the secondary muscle progenitors that form muscles must come from somewhere else, namely from the early muscle stem cells. Later in development, after fibers are formed, satellite cells surrounding the skeletal muscle fibers are the source of further muscle progenitors (Gros et al., 2005). Somitic cells from the dermomyotome delaminate and migrate to the location of their involvement in muscle development, reducing the size of the dermomyotome structure, until it no longer exists. Satellite cells, also thought to be somitic in origin, are a type of stem cell that provides

muscular growth and repair in the post-natal organism (Seale et al., 2000) and they populate the nascent muscle fibers in a second wave of in-migration toward the muscle anlagen.

During myogenesis the initial myoblasts that fuse together are termed the primary myofibers and they provide the framework for other myoblasts to adhere to (Kelly & Zacks, 1969). This is the first of two main waves of myoblast fusion that occur in vertebrate myogenesis. Developed from late myoblast populations, the secondary muscle fibers form around the primary muscle fibers (Miller & Stockdale, 1986). Both amniotes and teleosts exhibit two waves of myogenesis, though in teleosts myogenesis occurs earlier.

1.1.2 Teleost Development

Somitic formation occurs in fish, just as it does in amniotes, and those cells contribute to the formation of MPCs. The difference between the two groups is that in fish the specification of the MPCs by the expression of MyoD and Myf-5, and therefore muscle development, begins before somitogenesis commences (Rescan, 2005). Initially the expression of MyoD is confined to medial (adaxial) cells of the paraxial mesoderm, followed by the expression of myogenin in the same cells. In contrast, the expression of Myf-5 is in both the lateral and adaxial cells of the paraxial mesoderm (Rescan, 2005). In the paraxial mesoderm, during somatic development the precursors for fast and slow muscle types are already divided (Steinbacher et al., 2006).

There are three phases of muscle development in fish. The first occurs in the embryonic stage, and involves the formation and fusion of embryonic myofibers, the second is during the larval stage when there are distinct phases of ventral and dorsal muscle development (Johnston, 1999). The third and final stage of fish muscle growth requires

the muscle satellite cells on the surface of the embryonic myofibers to be activated and fuse together with the existing fibers or fuse together and create new fibers.

Differing from mammalian skeletal muscle, fish have very distinct regions of slow (red) and fast (white) muscle. The slow, oxidative fibers, derived from adaxial cells lie superficial to the fast, glycolytic fibers which are derived from lateral presomitic cells (Rescan, 2005). The precursors to the slow muscle fibers migrate to their final location in a two-step process. Beginning with a dorso-ventral expansion of the cells at the medial surface, the final established location of the slow muscle precursors at the lateral surface occurs by medio-lateral migration (Steinbacher et al., 2006). In mature teleosts, red and white fibers themselves seem to have a finite size that they can grow to, and are not often seen larger than 50 and 200 μm respectively in diameter (Johnston, 1999). In comparison with mammals that are born with a fixed number of skeletal muscle fibers, several fish species are known to continue to grow throughout their life span by the addition of new muscle fibers (Johnston, 2006; Rescan, 2005).

1.2 Myofiber Characteristics

1.2.1 Types of Myofibers

Myofibers can be categorized into fast twitch and slow twitch muscle types. Fast and slow twitch muscles differ both functionally and metabolically (Puthucheary et al., 2011). Muscle fiber classification is done according to the activities of oxidative or glycolytic enzymes, level of ATPase activity and the isoforms of myosin heavy chain (MHC) they express (Close, 1972; Larsson et al., 1991). Slow-twitch, or type I muscles, are all oxidative, and fast twitch muscles can be classified as fast-twitch glycolytic (type IIa) or fast-twitch oxidative-glycolytic (type IIb), the latter also being termed intermediate

fibers (Rui et al., 2016). Fast-twitch fibers do not have as many mitochondria, and use mainly glycolysis for quick energy production, and as a result, they fatigue quickly in comparison to slow-twitch fibers. They also have a high activity of ATPase and appropriately have a fast contraction time (Close, 1972). In contrast, the slow, type I muscle fibers are low in ATPase activity and high in oxidative enzymes. They also have many mitochondria, a much higher concentration of myoglobin and take longer to become fatigued (Brooke & Kaiser, 1970). The higher concentration of myoglobin in slow-twitch muscle fibers gives them a red colour, and the lower concentration of myoglobin in glycolytic, fast-twitch muscles give them a white-ish appearance (Brown et al., 1976).

The colour that is observed of different muscle types is due to the density of myoglobin in the muscle as a result of the metabolic properties. Slow-twitch muscle fibers have a high activity of oxidative enzymes, and because of that they require more oxygen which is provided by the higher density of capillaries (Sjogaard, 1982). The glycolytic fast twitch muscle fibers rely mainly on glycolysis for energy, therefore do not require as high a density of capillaries for oxygen transport (Brown et al., 1976). This contrast in capillary density is most pronounced in animals such as rats, rabbits and guinea pigs, where density is 2-3 times greater in slow twitch than in fast twitch muscles, though this disparity is lessened in humans (Sjogaard, 1982).

The proportions of fiber types are not consistent over time and can actually change through physical muscle training to either increase or decrease the expression of proteins associated with functions of slow-twitch fibers. Staron et al. (1991) showed that the muscle fiber types in humans can actually convert from glycolytic to more oxidative fiber types with training (Staron et al., 1991). These fiber-type conversions occurred over the course

of a 20-week training regime of high-intensity weight lifting (Staron et al., 1991). The literature on the effect of aging on muscle fiber proportions is quite controversial. There are some studies that have also shown changes in the fiber type proportions with age, but there are also several that show no change (Houmard et al., 1998).

Neuromuscular junctions (NMJs), the location on fibers where a nerve interacts with the muscle fiber and stimulates its contraction, are different between different fiber types. The NMJs of slow-twitch fibers (type I) demonstrate a high measure of neuronal sprouting, whereas the other fiber types show very little (Winter et al., 2006). The neurons synapsing with the slow-twitch fibers also have a very shallow pre-synaptic region in comparison with the bulbous pre-synaptic membrane of the neurons attaching to the fast-twitch fibers (Ellisman et al., 1976). At the NMJs, the density of voltage-gated sodium channels is much higher than in other areas of membrane surrounding the muscle fiber (Wood & Slater, 1995). The junction where a nerve innervates a muscle fiber is the point at which depolarization starts in order to stimulate contraction of the muscle.

1.2.2 Anatomy and Physiology

Skeletal muscle is a very ordered organ that covers the skeleton and is controlled by reflex response and conscious thought. In all systems structure determines function, and skeletal muscle is no exception. The different sizes and types of skeletal muscle give rise to different extensibility and contractility (Lieber & Friden, 2000). Skeletal muscle is made up of many bundled fascicles, which in themselves are bundles of muscle cells, or myofibers. Each myofiber is a multinucleated cell that contains myofibrils running parallel to the cell and contain the contractile elements of the muscle, termed sarcomeres (Rome, 1997). Sarcomeres, the smallest units of muscle, produce contraction by the action of

overlapping thick and thin myofilaments. Thick filaments, made of myosin, create cross bridges with thin filaments, made of actin, and "ratchet" along the thin filament, shortening the sarcomere (Rome, 1997).

Initially described by Huxley and Niedergerke in 1954, the sliding filament model of contraction details how myosin and actin filaments work together to shorten the sarcomeres of the myofiber (Huxley & Niedergerke, 1954). When stimulated by motor neurons, the myosin heads attach to the actin filaments creating a "cross bridge". The heads shift, creating tension in the long axis of the sarcomere, and shortening the sarcomere. The filaments themselves don't shorten, but rather their overlap increases, which shortens the length of the entire sarcomere (Lieber, 1993). The cross bridges form and break many times repeatedly during a single muscle contraction, generating a gradation of tension, and allowing the muscle to generate force between its attachments to bone and/or tendon (Lieber, 1993).

Muscle contraction is very calcium-dependent, as without calcium no cross bridges can be created. When activated by a motor neuron, an action potential (AP) is propagated along the sarcolemma, opening calcium channels, increasing intracellular calcium concentrations. The calcium is then able to bind to troponin, resulting in the active sites of the actin being exposed and available to bind to the myosin heads (Baylor & Hollingworth, 1998). The binding of calcium acts as a trigger for contraction, and the myosin heads bind to the actin active sites. The myosin heads then shift, generating a power stroke, and are released from the actin myofilament once ATP binds (Holmes & Geeves, 2000).

Myofibers don't appear to have as many organelles as non-syncytial cells, but the structures are dispersed between fibrils, including mitochondria, rough and smooth

endoplasmic reticulum, Golgi apparatus, and lysosomal vesicles. Fibers contain several to hundreds of myonuclei per fiber, a population that is controlled by mechanisms that are largely unknown; however, the number is thought to be influenced by concentrations of m-cadherin (Abmayr & Pavlath, 2012). The muscle-fiber nuclei regulate protein synthesis and its degradation via the Golgi and rough endoplasmic reticulum, and the many mitochondria in each fiber (especially numerous in slow-twitch fibers) are essential for producing ATP for the energy to drive force production and respiration. When SCs are activated they proliferate and fuse to each other, or to existing myofibers resulting in a multinucleated cell, or syncytia (Choi et al., 1990). The distribution of myonuclei within a myofiber is observed to be equally spaced, which is thought to minimize the distance from any area of the fiber to a nucleus (Bruusgaard et al., 2010). In experiments by Bruusgaard et al. (2006) it was determined that the distribution of myonuclei is not random. In fact the distance between the nuclei in mammals is influenced by their so-called repulsive properties towards each other and works to minimize long distance travel of molecules (Bruusgaard et al., 2006).

The same lab did experiments looking at the correlation between the number of nuclei per myofiber and the size of the fiber. They found there to be a direct correlation in young mice, but the correlation was lost as the mice grew older toward middle age (Bruusgaard et al., 2006). Though this could be due to the sedentary life that most lab mice live as they age, it is still of note, and requires more research to understand well in context of muscle fiber development and growth. Bruusgaard et al. also determined that different muscle types exhibit contrasting trends in the distribution of myonuclei per unit of fiber volume, though without significantly large differences in the number of myonuclei per

millimetre. The soleus muscle, a slow-twitch muscle with mostly type I (oxidative) fibers, was shown to have a much less ordered distribution of myonuclei than the extensor digitorum longus (EDL), a fast-twitch muscle composed largely of glycolytic type IIb fibers and oxidative-glycolytic type IIa fibers (with only a few type I fibers) (Bruusgaard et al., 2006; Soukup et al., 2002). The distribution and number of myonuclei in myofibers was established to be regulated by fiber type and mouse age (Soukup et al., 2002).

The myonuclear domain, or the amount of sarcoplasm controlled by a single myonucleus, is correlated with myosin heavy chain (MyHC) expression as well as muscle fiber type, as stated prior. The red or slow muscle types exhibit a smaller domain than that of fast or white muscle (Rosser et al., 2002). Because of this it is thought that fibers that have a high rate of protein synthesis need to have more nuclei per unit volume, and therefore have smaller domains (Rosser et al., 2002).

1.2.3 Innervation

Before the growth cone of a neuron has reached its target muscle fiber during development, the muscle fiber itself has already started to prepare for receiving the innervating signal. It begins to express receptors for the neurotransmitters that the neuron will discharge (Lin et al., 2001). Using α-bungarotoxin, a toxin that specifically binds to the acetylcholine receptor (AchR), Bevan and Steinbach (1977) demonstrated the even distribution of AChR in fetal rats, which modifies to clustering of AChR at the NMJ in the adult (Bevan & Steinbach, 1977). Fetal muscle fibers are observed to be innervated by several nerve axons, though usually in a clustered area, or motor endplate, in order to maintain post-synaptic specialization (Lin et al., 2001).

In the post-natal period, muscle eliminates the multiplicity of motor neuron synapses in the motor endplate until there is only one synapse per muscle fiber (at least in mammals), as seen in mature muscle. Mono-neuronal innervation is important for acute muscle activation, and synapse elimination acts to reduce the number of innervating neurons and incoming axons until only one remains (Thompson, 1986). Bevan and Steinbach (1977) determined the initial post-natal diameter of rat NMJs was 30 µm, whereas in the adult they measured NMJs that were 90 µm in size. Each adult muscle fiber is innervated by the axon from a single neuron, and the synaptic length on the muscle grows as the muscle grows (Bevan & Steinbach, 1977).

1.3 Satellite Cell Characteristics

Derived from somitic cells, SCs are mononucleated cells that are responsible for post-natal skeletal muscle development and regeneration following injury (Chang & Rudnicki, 2014). In mammals, SCs are potentially available throughout the adult life and are capable of asymmetrical division, the process that gives rise to two daughter cells with different cell fates. In indeterminate growing fish, SCs continue to proliferate and contribute to the muscle fibers throughout the life span. SCs can proliferate to create another satellite cell with stem-cell potential (for self-renewal of that population, or it can go back to quiescence), and also produce a second daughter cell that is committed toward myogenesis, the formation of muscle fibers. During the adult life of mammals, most SCs are quiescent, and in the G_0 phase, but can be activated by several different factors such as physical muscle training, electrical stimulation or chemically by MRFs (Kern et al., 2014; Zammit et al., 2001).

SCs are distinguished by their conserved location and morphological characteristics, in addition to their function as the tissue-resident stem cell in skeletal muscle. Observable cellular traits are a large nuclear to cytoplasmic ratio, a small nucleus, and a greater volume of heterochromatin in the nucleus compared to that of the myonuclei in the myofiber (Anderson, 2000). These characteristics of satellite cells indicate satellite cell quiescence in that they are less transcriptionally active than nuclei in proliferating myoblasts and the myonuclei inside the fused fibers (Chargé & Rudnicki, 2004).

Initially named due to their close relation to the muscle fiber, they were first discovered as cells residing between the basement membrane and muscle fibers in frogs (*X. laevis*; Mauro, 1961). Up until 1997, there were no specific markers known for SCs. In 1997, Cornelison and Wold described mRNA and protein expression of the c-met receptor as the first markers of SCs found in both the quiescent and activated states in their location around skeletal muscle fibers (Cornelison & Wold, 1997). Now SCs are characterized as having their own unique microenvironment, or niche, and to express specific surface proteins and transcription factors (Engler et al., 2004). Most SCs express Pax3, Myf5, Barx2, c-met, M-cadherin, CD34, CXCR4, and many other transcription factors and surface proteins, though all satellite cells express Pax7 (Cornelison & Wold, 1997).

Pax7, a paired-box transcription factor, is involved in controlling several developmental processes (Seale et al., 2000). The main role of Pax7 is to commit stem cells to become specified as myogenic myoblasts (Halevy et al., 2004; Seale et al., 2000). The stem cells are committed to being myoblast-producing satellite cells and proliferate to produce myoblast daughter cells to make up muscle fibers.

Satellite cells can divide three different ways. A symmetric division will produce two stem daughter cells, or two myoblast daughter cells. An asymmetric division will produce a committed myoblast, and another more stem-like self-renewing myogenic satellite cell. There are several differences between self-renewing SCs and myoblast daughter cells including transcription factor expression and chromosome division. The daughter cell that continues on to be another satellite cell maintains the expression pattern $Pax7^{+}/Myf5^{-}$, while the daughter cell that will differentiate into a myoblast expresses both genes in the $Pax7^{+}/Myf5^{+}$ pattern (Kassar-Duchossoy et al., 2005). When the chromosomes separate during division, the "older" or original-template strand of DNA in the chromosomes stay with the self-renewing daughter cell that is going to become a SC, and the "newer" DNA strand of the chromosomes are isolated to the myoblast (committed myogenic) daughter cell (Conboy et al., 2007). SCs can complete symmetric or asymmetric division, and the distance of the nucleus during division from the muscle fiber (i.e., either the cell divides parallel to and along the fiber underneath, or perpendicular to the fiber) determines which type of division occurs (Kuang et al., 2007).

In recent work done by Dumont and colleagues (2015), asymmetric division was found to be key in developing a population of self-renewing myogenic precursors. Asymmetric division is influenced by dystrophin, a rod-shaped protein that connects the cytoskeleton of the myofibers to the extracellular matrix. In activated SC, dystrophin is segregated to one side of the cell 24 hours after activation and is only expressed in the differentiated SC following division (Dumont et al., 2015). Mark2, a transcription factor, is an important regulator of cell polarity and is regulated itself by dystrophin. Without dystrophin, Mark2 is dysregulated and lacks polarity, and therefore asymmetric division is

impaired (Dumont et al., 2015). This polarity of division is important for differentiating between the myogenic precursor daughter cell and the stem daughter cell. Without the polarity of dystrophin and Mark2, atypical mitotic spindle orientation occurs, and there is a decrease in the required apicobasal divisions. Ultimately the reduction in cellular polarity results in a decrease in asymmetrical divisions, and thus a decrease in the myogenic precursor population. Consequently, without dystrophin, not only is the integrity of the myofiber jeopardized, but the SC populations are not repopulated when they divide in response to muscular injury or stress. Muscular dystrophy occurs in these cases and can develop into dystrophic diseases such as Duchenne muscular dystrophy (DMD) (Dumont et al., 2015).

Satellite cells in mammals and fish are quite conserved and are seen to have the same MRFs and transcription factors. In a study conducted on rainbow trout, Gabillard and colleagues (2010) showed similarities in the expression of MyoD and myogenin in isolated SCs compared with that of mice and chickens (Gabillard et al., 2010). The difference they observed was that in the trout muscle, myogenin expression continued even after the myogenic myoblasts were fused to the myofiber, unlike in the amniotes where myogenin expression in the myofiber has a different purpose (Gabillard et al., 2010).

1.3.1 Satellite Cell Heterogeneity

The satellite cell niche includes a region of extracellular matrix superficial to the fiber sarcolemma and deep to a layer of laminin, but its functional characterization also includes cell-cell interactions and intrinsic transcription factors (Collins et al., 2005). The niche is made up of extrinsic factors such as integrins, cytokines, and other molecules that affect SCs (Deasy et al., 2003). These extrinsic factors work alongside factors inside or

intrinsic to the SCs to regulate their fate (Table 1). Though SCs are all found in similar areas relative to the muscle fiber they surround, they are not all the same. Depending on what types of muscles they surround, and the stem cell niche, SCs display differential molecular and functional heterogeneity.

Such heterogeneity is seen in studies that compare the SCs of the head muscles with SCs in all other skeletal muscles including the diaphragm (Anderson et al., 1998), pharyngeal and extraocular muscles (McLoon & Wirtschafter, 2002) and even the masseter and fast-twitch extensor digitorum longus (EDL) or slow-twitch soleus muscles [for example as described by (Harel et al., 2009; Mootoosamy & Dietrich, 2002; Motohashi & Asakura, 2014)].

Table 1. Intrinsic and extrinsic regulatory factors that influence satellite cell fate

This is an incomplete list of regulatory factors that influence satellite cell activity (Motohashi & Asakura, 2014; Watt & Hogan, 2000; Yin et al., 2013).

Location	Factor	Control/Target	Function
Quiescent Satellite Cells	microRNA-489	Inhibit Dek expression	Maintains the SC in quiescent state
	Spry1	Inhibits FGF signalling	Supresses proliferation
	Wnt7a	Wnt7a/PCP pathway	Maintains symmetric cell division
	Notch3	Notch signalling	Supresses proliferation
Activated Satellite Cells	Spectrins/ cyclin A	Mitotic spindle orientation	Aids in asymmetric cell division
	Notch	Notch signalling	Asymmetric division
	Numb	Downstream Notch signalling	SC differentiation and self-renewal
Extracellular Matrix	HGF (hepatocyte growth factor)	HGF/Scatter Factor signalling	Regulation of migration and cell growth
	FGF (Fibroblast growth factor)	FGF/FGFR signalling	Increases proliferation and delays differentiation
	IGF (insulin-like growth factors)	IGF-I and IGF-II signalling	Differentiation, proliferation and migration promotion

Molecular heterogeneity stems from the fact that not all SCs express the same genes with the same pattern in time. For example, not all SCs express M-cadherin, CD34 or the active phosphorylated form of Myf5 (Kuang et al., 2007). They also may or may not express the same gene set throughout their entire existence, for as a muscle matures and changes, so do the surrounding SCs (Chakkalakal et al., 2012). In different species, muscle stops growing at different points in the organism's life. For example, whereas the muscle in an indeterminate grower continues growing for the lifespan of the organism, a determinate grower's muscle does not (Johnston et al., 2011). SCs surround all types of muscle fibers and the muscles each have unique muscle-specific architecture, contractile patterns, metabolic capabilities and innervation pattern. Just as muscles are heterogeneous, so are the SCs that reside near them, and in cultures of SC-derived myoblasts, they do not necessarily give rise to myoblasts that will differentiate toward the same phenotype (e.g., fiber type) as the muscle fiber of origin.

SCs surrounding extrafusal muscle fibers, which form the vast bulk of muscle fibers, have different characteristics than those that reside near intrafusal muscle fibers. Innervated by motor and sensory neurons, intrafusal muscle fibers make up the muscle spindle and are proprioceptors which detect the change in length of a muscle fiber (Maeda et al., 1983). Another proprioceptor that detects the change and rate of change of muscle length is the Golgi tendon organs which are comprised of collagen that connects the muscle to bone. Though muscle movement and position are regulated with a combination of the function of both the Golgi tendon organs and muscle spindles, it is the intrafusal muscle fibers that are developed by and regulate SCs (Kirkpatrick et al., 2008). The SCs that surround the muscle spindle fibers are thought to be in an "immature state" since they have

an expression pattern close to that of embryological myogenic cells, where the muscle is still developing and growing (Walro & Kucera, 1999). Extrafusal muscle fibers, innervated only by motor neurons (since intrafusal fibers function in the sensory arm of the primary reflex arc), are far more numerous than intrafusal fibers, and have large roles in locomotion and posture (Walro & Kucera, 1999). The extrafusal fibers can be made up of slow or fast contracting fibers, which each have their own resident stem cells (in a typical niche). SCs derived from fast and slow twitch muscles display very similar patterns of AchE following culture (Boudreau-Larivière et al., 2000).

1.3.2 Satellite Cell Activation and Proliferation

The regulation of SCs in embryonic and post-natal muscle development have many similarities, such as the regulatory factors required, but SC regulation in these two phases of mammalian development also have many differences. Pre-natal and pre-hatch development in amniotes and fish respectively are characterized by both hyperplasia (the increase in myofiber number) and hypertrophy (growth of existing myofibers), but they differ in their development after birth (amniotes) or hatching (fish) (figure 1). In amniotes, the myofiber number is fixed following birth, so muscle development continues by the hypertrophy of individual fibers. In contrast, the post-hatch development of white muscle in most fish is ongoing and continues by both fiber hypertrophy and fiber hyperplasia (Koumans et al, 1993; Rossi & Messina, 2014; White et al, 2010). During post-hatch development, the satellite cells that are resident on the muscle fibers are responsible for providing myoblasts that will contribute nuclei into fibers for significant fiber hypertrophy over time and the building blocks that fuse into new fibers that is hyperplasia in fish.

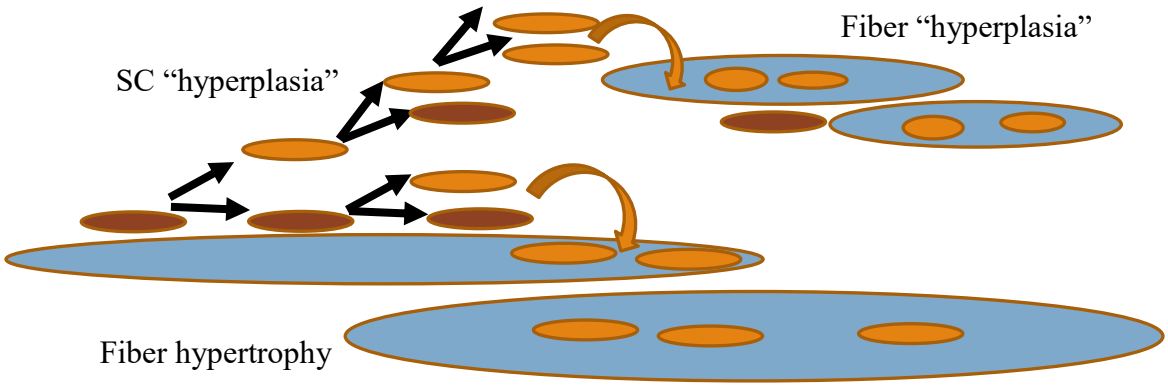

Figure 1. Hyperplasia versus Hypertrophy in Skeletal Muscle

Myofiber hyperplasia, or the addition of new myofibers, is a process that is completed by satellite cell (SC) hyperplasia (proliferation) and fusion together. Myofiber hypertrophy is the growth of the myofiber by increase in the sarcoplasm, or by the addition of new nuclei from SCs.

Post-natal mice have a SC population that accounts for about 30% of the sublaminar muscle nuclei inside and also resident upon all myofibers (Chargé & Rudnicki, 2004). As mice age, the proportion of observable SCs drops to less than 5% of all nuclei under the layer of laminin in the basement membrane around fibers at just 3 weeks of age. This change in the ratio of SC to sublaminar muscle nuclei is most often due to the large increase in myonuclei with age, though in glycolytic fibers in mammals there is also a decrease in SC number (Chargé & Rudnicki, 2004). SCs stay inactive, or quiescent for the majority of the lifespan of amniotes, and are only activated to proliferate during times of stress (Cornelison & Wold, 1997; Franchi et al, 2017; Imaoka et al, 2015). Quiescence is very important for survival and longevity of SCs in amniotes. Without the maintenance of the quiescent state, the muscle stem cells activate prematurely, and the long term renewal abilities of the SC population is greatly diminished (Cheung et al., 2012). Quiescence keeps the cell in a low metabolic state, and also keeps the cell resistant to DNA damage (Chakkalakal et al., 2012). Since this dormancy is so important to the long term ability of SCs to make an effective response to injury or demand throughout life, there are regulatory factors that maintain the quiescent state. The first factor that was determined to provide this function was pulsatile nitric oxide (NO) release from the resident myofiber (Anderson, 2000).

More recent research has determined that quiescence is dependent upon many factors, including the expression of NO and specific transcription factors and microRNAs (Cheung et al., 2012). MicroRNAs are cellular RNA molecules that destroy mRNA before it is translated, and they have a large role in maintaining the quiescent state of SCs. Cells deficient in DICE R1, a microRNA processor endoribonuclease, rapidly fall out of

quiescence, and are unsuccessful at reproducing myocytes following an injury event (Cheung et al., 2012). The primary microRNA that works to retain the dormancy of SCs is the micoRNA-489. The key target for microRNA-489 is the gene for Dek, a cell cycle protein (Cheung et al., 2012). When microRNA-489 is active within the cell, it destroys Dek mRNA and consequently helps to keep the cell from leaving the G_0 phase. Another microRNA that has a role in quiescence is microRNA-31. This microRNA targets the gene that codes for myf5, and represses its transcription (Crist et al., 2012). Instead, microRNA-31 stores the myf5 mRNA within a messenger ribonucleoprotein particle (mRNP), where it is kept until the SC is activated (Crist et al., 2012). This action keeps the cell from re-entering the cell cycle, but also allows for quick cell cycle re-entry when the SC is activated since the mRNA molecules are ready to be translated and do not have to be transcribed.

There are transcription factors that inhibit the expression of proteins that push the cell into entering the cell cycle, and proteins that inhibit the introduction into the cell cycle themselves. Low levels of cyclins and cyclin-dependent kinases (CDKs) are maintained to keep the cell from entering the proliferation phase (Fukada et al., 2007). This inhibition is preserved by transcription factors that inhibit the transcription of these proteins. Cell cycle inhibiting proteins, such as the CDK inhibitor p27/Kip1 and p130/Rbl2 are upregulated (Cao et al., 2003). SPRY1, a factor that inhibits effects of fibroblast growth factor 2 (FGF2), is another protein that is upregulated in quiescent SC and downregulated after SCs are activated (Shea et al., 2010). This combination of signals that upregulate some genes and downregulate others, works to amplify the quiescent state.

Satellite cells can be activated by mechanical or chemical stimulation, though the two methods are interconnected (Yamada et al., 2008). The most common mode of

muscular growth and regeneration is done by mechanical stress (muscular stretch or contraction due to load), which activates a chemical cascade of SC activation, though *in vitro* tests have shown the sole introduction of chemical signals can also activate SCs (Yamada et al., 2008). Different types of stimuli act on the muscle such as shear force, stretching, overload exercise and injury and can all affect muscular development. The protein nitric oxide synthase (NOS) is upregulated during these types of stimulation on the muscle, and once activated produces the small molecule, nitric oxide (NO) (Anderson, 2000; Wozniak & Anderson, 2007). NO is very important in activation of SCs, but also has a role in differentiation, fusion and hypertrophy from muscle overload. NO is expressed in both quiescent and active SCs, but activation is only seen at high and low concentrations of NO (Wozniak & Anderson, 2007). The mechanical stimulation of stretching muscle opens calcium channels. The influx of calcium ions activates NOS, which synthesizes then releases NO. The increased concentration of NO is a large factor that activates satellite cells (Yamada et al., 2008).

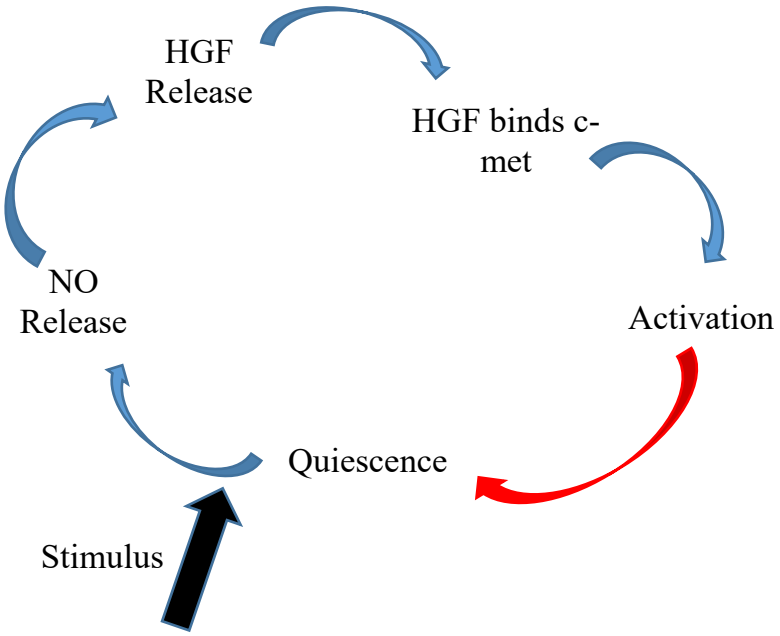

Figure 2. Chemical pathway from SC Quiescence to Activation

The possible chemical signalling cascade that starts when a stimulus acts upon a quiescent satellite cell (SC). Once the stimulus occurs, it triggers the release of nitric oxide (NO), which subsequently releases hepatocyte growth factor (HGF). The HGF then can bind to c-met, causing the activation and subsequent proliferation of the SC. The SC daughter cell can then return to quiescence, while the myoblast daughter cell fuses to another myoblast cell to create a new myofiber, or that daughter cell can fuse to an existing myofiber (adapted from Wozniak et al., 2005).

Once NO is synthesized, it activates matrix metalloproteases (also called metalloproteinases), such as MMP-2, which cleave heparin-sulphate proteoglycans (Yamada et al., 2008). MMPs, zinc-dependent endopeptidases, release the HGF that is tethered to the extracellular matrix, making it available to bind to its receptor on quiescent SCs, c-met (Yamada et al., 2008). C-met is an immediate-early gene that mediates quick activation of SCs (Wozniak & Anderson, 2007). The binding of HGF to c-met induces proliferation of the SC (Figure 2), and ultimately initiates activation and introduction back into the cell cycle (Yamada et al., 2008). HGF is a cytokine that has many roles in muscle development inducing proliferation by binding to c-met, and delaying differentiation by promoting the expression of TWIST, a transcription factor that delays differentiation until there are sufficient number of proliferated myoblasts (Leshem et al., 2000).

Myoblasts that originate by proliferation from SCs are committed muscle cell precursors and fuse together, performing a crucial step in muscle development (Abmayr & Pavlath, 2012). Before fusion can occur though, myoblasts must identify and adhere to other myoblast cells (Przewoźniak et al., 2013). M-cadherin, an adhesion molecule is fundamental in the fusion process. It allows the initial and prolonged contact between cells while several other transcription factors and signalling molecules work to create pores and connections between the two cell membranes (Chargé & Rudnicki, 2004). M-cadherin, along with nephrin, integrin and metalloprotease-12 are all found localized to the contact point of two fusing cells (Przewoźniak et al., 2013). Since fusion is such a highly regulated process, there are several regulatory factors that control the remodelling of the actin cytoskeleton, including Nap1/Hem, Filamin C and the Neural Wiskott-Aldrich syndrome protein (N-WASP; Nowak et al., 2009).

1.4 Lake Sturgeon Development

1.4.1 Sturgeon Life History and Development

The Lake Sturgeon *(Acipencer fulvescens*) is a very large North American freshwater fish with K-selection life history strategy traits (Barth & Anderson, 2015). These traits include reaching reproductive maturity late in life, having a long life span and spawning periodically. This type of evolutionary strategy means that the females are very large and old by the time they reach reproductive maturity (Winemiller & Rose, 1992). The males are also very large, though they have shorter periods between spawning seasons. Partially due to their large distribution in North America, there is variation in spawning behavior between and within populations. Theim and colleagues collected data from previous studies and combined it with the data obtained from the 51 Lake Sturgeon they captured along the Richelieu River, Quebec, to compare reproductive age, spawning time and location as well as egg production (Thiem et al., 2013). From their study, they determined that female Lake Sturgeon reach reproductive age at about 26 years, and the males are reproductively mature earlier, being only 18-20 years old. Since spawning is such an "expensive" feat, females may spawn only every 3-5 years, and males every 1-2 years (Thiem et al., 2013).

Though they are relatively small when hatched, Lake Sturgeon can grow to be several thousand millimetres in length. Lake sturgeon eggs measure about 2.5-3.5 mm in diameter, and depending on the temperature of the water, they hatch in about 8-14 days (Peterson et al., 2007).

1.4.2 Sturgeon Muscle Development

Little is known about the development of sturgeon muscle, but in other aspects of development and structure they do have similarities to teleost fish. As indeterminate growers, both Lake Sturgeon and several species of teleosts do not stop growing once they have reached a "predetermined" size. In indeterminate fish, muscles continue to grow for the whole adult life of the fish by increasing both in fiber number (hyperplasia) and size (hypertrophy) (Johnston et al., 2012).

Water temperature is thought to be one of the most important factors determining the growth rate of fish in general, but specifically sturgeon (Hardy & Litvak, 2004). Although Lake Sturgeon can grow to be very large, during the first stages of development post-hatch they are relatively small and are influenced greatly by the environment. The temperature of the water impacts the age at which they are able to escape predators, and search for food once their yolk-sac is gone (Hardy & Litvak, 2004).

In a study done by Hardy and Litvak (2004) where they looked at Shortnose and Atlantic Sturgeon, they showed that higher temperatures (18 and 21^{o} C) reared longer body size, but it was at the colder test temperatures (13 and 15^{o} C) that reared longer survival times (Hardy & Litvak, 2004). A larger total length earlier on in life may assist in escape from predators, but it seems the larger fish have a lower overall survival rate. These temperature-based differences in size seemed to become negligible at the first escape response age (Hardy & Litvak, 2004).

1.5 Isolated fibers in culture as a model system

Isolated myofibers are used as a model system to observe SCs in both active and quiescent states. The protocols used to isolate fibers preserve the SCs in their natural position between the basal lamina and the sarcolemma of the muscle (Anderson et al., 2012). The muscle fibers can be stained for Pax7 to observe all SCs, and additionally with BrdU to stain for the activated SCs. Both Pax7 and BrdU will be seen only in SCs if the fibers are fixed before the daughter cell fuses to the myofiber. The single-fiber isolation method is used as a model for observing SCs because it preserves the attachments and interactions between the SCs and myofiber yet it removes the interactions that SCs have with cells in other tissues such as nerves and blood vessels (Anderson et al., 2012).

There are other cell markers that are applicable for viewing SCs, including c-met and MyoD. MyoD would be useful in the examination of activated SCs, though not quiescent. This marker has also been reported to be expressed in myofibers, so the drawback would be a high probability of background staining. C-met, just like Pax7, is a marker that can be used to view both quiescent and activated SCs. Other proteins that can show proliferation would be cyclin A and Ki67. Like BrdU, these proteins are able to be used to mark proliferating cells and be used to calculate a cell cycle. Other than MyoD, which has a high probability of large background staining, all other mentioned SC and proliferation markers would be acceptable for viewing the respective cells.

Muscle development and satellite cells specifically have been studied using several different methods. In vivo studies allow the most detailed analysis of SCs in their natural environment, though the interactions with non-muscle tissues, and other variables within different animals can cause a lot of variability in the data. Histological sections allow for

nuclei and fibers to be easily stained and observed, and the sections are a lot thinner than the thick, isolated fibers. A drawback of sections is that the muscle fibers are quite dense, and do not allow adequate viewing of the satellite cells between them.

When done properly the fiber isolation method can be very useful and provide suitable data for studying resident satellite cells. Developed by Bekoff and Betz (1977) the isolation of fibers allows for the control and consistency of cellular extrinsic factors such as electrical stimulation and ionic environment (Bekoff & Betz, 1977). This method does have some drawbacks as the isolation of the fibers can cause agitation and therefore activation, and it can also be damaging to the fibers themselves (Cornelison & Wold, 1997). When done carefully, isolated fibers provide a clean view of the myofibers and the resident SCs between the sarcolemma and basal lamina. Using minimal agitation, quiescent SCs can be preserved and fibers can be maintained in controlled medium that preserved the SC-myofiber interactions.

1.6 Research Question/Rationale

While the development of muscle in mammals and zebrafish has been examined in many research inquiries, there has been far less exploration into the features of muscle fiber development and growth, including the proliferation of satellite cells, in Lake Sturgeon muscle, even though muscle makes up much of the body size. This research project aims to characterize muscle development in Lake Sturgeon according to the proliferative activities and the number of SCs on fibers. Since it has already been determined by previous research that fish SCs express Pax7, this protein will be an appropriate marker to identify SCs in their position, resident on myofibers. BrdU, being an analog of the

nucleoside thymidine, is incorporated into new DNA in any cell undergoing S-phase during exposure; it will be used to detect the proliferation of SCs.

The objective of this project is to characterize the populations of SCs and myonuclei in individual myofibers at different ages of sturgeon to better understand the growth trends in Lake Sturgeon as they age. The numbers of SCs and myonuclei will also be examined in context of simultaneous changes in fiber diameter and fiber length to determine if there is a distinct relation between those parameters that remains stable or changes as the fish ages.

Specific hypotheses are as follows:

1. The satellite cell to myonuclear ratio will decrease as age increases;
2. The cell cycle duration of SCs will increase with age; and
3. The myonuclear domain in fibers will increase as the sturgeon age.

The results obtained by testing these hypotheses will provide new information regarding the development of the juvenile Lake Sturgeon, specifically relating to the activation and proliferation of satellite cells. Calculating the ratio of SCs to myonuclei will determine the rate of hypertrophy from the addition of nuclei. It is hypothesized that the cell cycle of the SCs would increase in length as the fish age, as they have a large growth spurt in the first year, post-hatch. The resolution of the cell cycle would provide information to determine if the SCs change their cycle over time. The myonuclear domain, demonstrating the amount of sarcoplasm that is controlled by each myonuclei, is important to determine the range each nuclei has and if it changes with age.

Theoretically, these hypotheses can be tested by *in vivo* injection of BrdU before euthanasia to track the proliferative cells. Though this would give a much more detailed description of the myofiber development, the interactions with other cells *in vivo* is not predicable and not able to be controlled. In this project, experiments were conducted using cultures of single, isolated sturgeon fibers exposed to a BrdU-containing medium directly following dissection in order to achieve the same results as an *in vivo* study would allow, without the degree of complexity that comes with it. The SCs could be fixed and have their activation and cycles tracked while still maintaining location and interaction.

Since muscle function and growth are critical to a Lake Sturgeon's growth and survival, it is important to understand the functional basis of fiber growth, satellite cell activation and proliferation in this endangered species. This investigation provides additional knowledge of SC contributions to myofiber growth in the developing Lake Sturgeon and the results will be a new foundation for future research. The results of this study can also conceivably be applied for conservation advancement of this evolutionarily important endangered species (Pollock et al., 2015).

Chapter 2: Methodology

2.1 Dissection

Muscle tissue was collected under a protocol approved for use by Dr. Judy Anderson's laboratory (Protocol # F16-031) from sturgeon reared under Dr. Gary Anderson's animal protocol at 16^{o}C in the animal holding facility at the University of Manitoba. Nine age groups were used for sampling: 0.5, 1, 2, 3, 4, 5, 6, 17, and 29 MPH (months post-hatch). Depending on the size of the fish, between 5-50 were used for

sampling at each age group MPH. Small fish (<120 mm) were euthanized with an MS-222 overdose (90 mg/125 ml), then dipped in 10% bleach solution to cleanse the scutes and skin, rinsed in saline (0.9%) and blotted dry. The large fish (>120 mm) were euthanized by a sharp blow to the head. The standard length and weight of the fish were measured and then the fish were decapitated right behind the operculum. Under the dissecting microscope, spring scissors were used to cut open the abdomen of the small fish from the anterior to the posterior end. The dissection of the large fish was done without the use of the dissecting microscope and dissecting scissors and medium forceps were used. The viscera were removed using forceps and discarded. The skin was removed by severing the connective tissue between the skin and the muscle tissue using very fine to medium forceps, depending on the size of the fish. While holding the skin with one pair of forceps and inserting a second pair of closed forceps between the skin and muscle, the connective tissue was severed by carefully opening the second pair of forceps. The fins and extra skin were removed carefully without damaging the muscle below.

Once the skin, head and viscera were removed on the small fish, the rest of the fish was put into 0.2% collagenase (appendix). On the larger fish the skin, head and viscera were removed in the same way as the small fish, though the skin was much thicker and took longer to remove. Once the skin was removed, the muscle was cut on the outside of two adjacent myosepta about two centimeters deep so that intact muscle fibers were removed. Two muscle blocks were taken from each of the 5 fish at the 17 MPH and 29 MPH age groups and combined per age into the conical tube with 0.2% collagenase.

2.2 Fiber Isolation

Muscle tissue was put into a 15 mL plastic conical Falcon centrifuge tube with 0.2% collagenase for 3 hours in a 37ºC water bath. Following incubation, the collagenase was decanted, being careful not to lose any tissue, then the tissue was combined with a small amount of basal medium (BM; appendix) containing L-15 medium, 1% antibiotic/antimycotic and 2% fetal bovine serum at 7.4 pH, and carefully poured into an autoclaved glass petri plate. Using a flamed, wide-bore glass pipette, the tissue was triturated to further separate individual fibers, but done carefully so as not to break the fibers. If the fibers took more than 10 triturations to separate fairly completely, the remaining intact tissue was moved to another dish and triturated further; this avoided damaging the already-isolated fibers. This technique allowed deeper fibers to be removed from the tissue without damaging the superficial fibers that were already separated from the skeleton.

Once most of the fibers were separated from the skeleton, the skeleton, spinal cord and debris were removed with fine forceps under a dissecting microscope. Using an autoclaved, flamed, wide-bore pipette, all the solution containing fibers was moved into a glass conical test tube (15 mL) and subsequently covered with tin foil. These were used for gravity sedimentation so the fibers in the tube could settle for 10 minutes to the bottom of the tube.

Starting from the top of the liquid meniscus, the BM was removed from the tube until about 2.5 cm of solution was left covering the myofiber pellet. Fresh BM was then added until the tube was approximately ¾ full, and the pellet was resuspended by gently

flicking the bottom of the tube. The tube was left for another 10 minutes so fibers would again settle into a pellet.

During the gravity sedimentation steps, the bromodeoxyuridine (BrdU) solution, acid alcohol, TBS, HS, and the solvent for the collagen solution (containing everything but the collagen) were prepared (solution recipes and the source of each reagent are found in the appendix). Following the 10-minute gravity sedimentation, most of the BM in the conical tube was removed using the same method as previously, leaving about an inch of solution above the pellet once again. The fibers were resuspended in the remaining solution by gently flicking the tube, and then carefully poured into a 60-mm glass petri plate.

The petri plate was tipped slightly by resting one side on the top of another glass petri dish. While the fibers were settling in the petri plate, the collagen was added to the collagen-solvent solution, and the cell culture dishes were prepared.

2.3 Myofiber Plating

The required number of cell culture dishes was determined in advance by multiplying the number of time points in the experiment by 6 (35x10mm) plastic cell culture plates for each time point. This allowed for 3 dishes at each time point that would be used for each type of incubation: in medium containing BrdU, and for immunostaining for Pax7. Each entity would identify satellite cell nuclei using the method of immunostaining involving colour detection using horseradish peroxidase, peroxide, and diaminobenzidiene (HRP-DAB) staining, so stained fibers could be viewed at any time without concern about photobleaching of fluorescence. This approach was necessary as viewing and counting nuclei (see below) by focusing through a thick fiber to see all labelled

nuclei, would not be reliable if epi-fluorescent staining was used (e.g., in a double-staining procedure for Pax7 and BrdU together). A single, washed and autoclaved coverslip was put into each 35x10mm cell culture dish.

The collagen solution was then prepared by putting the collagen into the PBS/NaOH solution right before the plates were ready for the collagen (for recipe, see appendix). Using 0.1M NaOH, 0.1M HCl and pH tape, the collagen solution was quickly brought to pH 7.0. In this neutralized state, the collagen gels by itself in about 5 minutes, so it was important to work quickly. Onto each coverslip, 100 μL of the dissolved collagen solution was pipetted and spread past the edges using a fine glass pipette tip prepared over a flame into a "hockey stick" (bent L) shape.

Using a flamed wide-bore pipette tip and micropipettor, 30 μL of the solution of BM containing myofibers was dispersed onto each coverslip on top of the collagen. After covering each dish, dishes were placed together onto clean, plastic trays, and placed into a 37^{o}C incubator for 70 minutes, or until the myofibers no longer moved when the plates were tilted (as collagen had gelled).

The plates were all removed from the incubator at that time. Then, half the dishes received 500 μL of BM pipetted carefully into each dish, and dishes were placed in the 16^{o}C incubator (for immunostaining for Pax7, n=3 per experiment). The other half of the dishes each received 500 μL of BrdU solution (appendix) by pipette (n=3 per experiment). All plates containing BrdU were then placed in the 16^{o}C incubator for 2 hours. Following the 2-hour incubation time, the cell culture plates were removed from the incubator and the BrdU solution was removed and replaced with 2 mL of BM. When solution was added or

removed, care was taken to direct the pipette tip into the corner of the petri plate and to pipette the solution slowly, so as not to dislodge the imbedded fibers.

A classic pulse-chase experiment was used to track the satellite cells that were dividing at any point in time. Putting the fibers in BrdU-containing medium for 2 hours was considered to be the "pulse", in which all SCs that were in S-phase during that time took up the BrdU into their DNA and were later stained for that label. The "chase" portion of the experiment consisted of putting the isolated fibers into medium not containing BrdU following the 2-hour pulse period, then fixing fibers at specific time points to capture the dividing SCs at that time. Following the pulse-chase experiment, the fibers were stained for the satellite cell-specific cell marker, Pax7 and for the incorporation of the proliferation marker, BrdU (section 2.5.1).

The time points for the pulse-chase experiment were chosen to be 0, 1, 3, 5, 7, 9, 12, 15, 20 and 24 hours to allow staining at each time point to follow any change in activation and cycling by tracking incorporation of BrdU into the SCs. At each time point, 6 plates were removed from the 16^{o}C incubator and fibers were fixed. This was completed by first removing the BM, and then rinsing each plate with 2 mL of PBS. Acid alcohol was then added to each plate in the amount of 2 mL and was left to sit for 20 minutes in the BSC. The acid alcohol was then removed and the plates were left in the BSC to dry for 45 minutes. TBS with horse serum (2 mL) was added to each plate following the drying step, and the plates were all placed in the 4^{o}C refrigerator until ready to stain.

2.4 Cryosectioning

A sample of muscle tissue from 2-3 fish at each age group was collected for cryosectioning at the same time the fiber isolation was done. Directly after dissection, the tissue was placed in 4% PFA for 24 hours, then moved to cryoprotectant (30% sucrose in PBS) until the tissue sunk to the bottom of the tube.

At least 30 minutes before freezing the sample, a block of dry ice was prepared and isopentane was poured into a metal can. The isopentane can was placed in a Styrofoam box on top of the block of dry ice, and was left to sit for at least 20 minutes for the isopentane to cool to -50^{o}C. Once the liquid had come down to temperature, each muscle-tissue sample was removed from the cryoprotectant solution and blotted dry. Using a cryomold that was only slightly larger than the tissue sample, the mold was filled with cryomatrix embedding compound and the tissue was gently submerged into the matrix using forceps. Care was taken to align the samples so they were straight and flat in the matrix gel, in preparation for longitudinal sections.

Using 12" forceps, each mold was placed in the -50^{o}C isopentane and frozen into a block. The blocks were then transferred onto the block of dry ice while the other samples froze. After wrapping each block in tin foil and appropriately labelling them, the samples were put into the -20^{o}C freezer until sectioning.

Using a cryostat set to -21^{o}C, the samples were cut to a thickness of 7μm; 8 sections from each block were placed onto gelatin-coated, pre-cleaned microscope slides. The slides were left to dry overnight, and then stained with hematoxylin and eosin (H&E) for observations of muscle histology.

2.5 Staining

2.5.1 IHC Staining for Isolated Myofibers (HRP-DAB)

On day 1 of the immunohistochemistry (IHC) staining protocol (IHC World protocols, as reported by Mizunoya, et al. 2011), the cover slips of fixed fibers were first removed from the freezer and allowed to dry and come to room temperature for 30 minutes. Wash steps were always done 3 times for 2 minutes each time and completed in the cell culture petri plate using 1mL of solution; the incubation steps with antibody solutions were done by removing the coverslip from the petri plate, putting the slip on top of the plate lid (labelled), and adding 100-200µL of solution.

The coverslips were washed 3 times for 2 minutes each time with PBS, then incubated for 30 minutes at room temperature (RT) with 1% Triton X-100 (diluted in PBS). Coverslips were then incubated for 1 hour at RT with 2M hydrochloric acid (HCl) to denature DNA, then washed with PBS. Using a blocking solution (containing normal goat blocking serum, 2M glycine and Fab unconjugated-mouse in a ratio of 20:1:1) at RT, the cover slips were incubated for 1 hour. The blocking step is crucial in preventing nonspecific binding of the secondary antibody at a later step. A wash step with TBS-T 3 times for 2 minutes each time followed.

The coverslips were incubated for 15 minutes at RT with 0.01% Avidin in PBS, then rinsed once with PBS. Following the washing, the coverslips were incubated with 0.001% Biotin in PBS for 15 minutes at RT, followed by washing with TBS-T. The coverslips were then incubated with primary antibody (AB) solution (i.e., primary AB in primary dilution buffer – appendix) overnight in the fridge. Mouse anti-BrdU was used for half of the coverslips and mouse anti-Pax7 was used for the other coverslips, using the

ratios of 1:50 and 1:200 respectively. For this incubation, coverslips were in petri dishes, covered with lids, and boxed to prevent drying.

On the second day, the coverslips were washed with TBS-T. The coverslips were then incubated with 4',6-diamidino-2-phenylindole (DAPI) solution (1:10.000 ratio in ddH_2O) for 1 hour to counterstain DNA in all nuclei, and subsequently washed with TBS-T. Hydrogen peroxide (H_2O_2; diluted to 3% in PBS) was then added to each plate and left to incubate for 10 minutes at RT (to quench endogenous peroxidase activity in the fibers); this was followed with washing in TBS-T. The coverslips were incubated with biotin-conjugated goat anti-mouse antibody in secondary antibody-dilution buffer (1:200) for 1 hour at RT. After washing with TBS-T, coverslips were incubated for 20 minutes with a solution of HRP-streptavidin (1:500 ratio in PBS) at RT. TBS-T was used to wash the coverslips, and 1mL of the DAB working solution (appendix) was added to each petri plate. DAB solution was left on the coverslips for 5 minutes at RT, then removed and disposed of correctly (appendix). Double-distilled water (ddH_2O) was used to wash the petri plates 5 times and the waste discarded correctly.

The coverslips were removed from the petri plates one at a time, turned fiber-side down over glass slides, and mounted onto the slides using ImmunoMount. The plates were kept at 4^oC in the dark until ready to view under a bright field microscope. Negative control plates were processed as above with the omission of primary antibody. Positive controls were sections of mouse, lamprey, and zebrafish muscle that showed nuclei positive for both Pax7 and BrdU within mononuclear cells directly adjacent to myofibers,

2.5.2 H&E Staining for Sections

Hematoxylin and eosin (H&E) staining was used on tissue sections from each age group, to observe histological features of the fibers, SCs and myonuclei. Longitudinal sections were used to observe the location, size and thickness of the satellite cells on the myofibers. With this staining, one could also see the location of myonuclei within fibers, as well as the size of the myofiber.

The slides each had 8 sections on them. Slides were removed from the freezer and left on a clean bench top to come to RT for 30 minutes. Then slides were placed in a rack and immersed into 2 changes of absolute ethanol for 5 minutes each, followed by 95% ethanol for 2 minutes and ddH_20 for 5 minutes. Following the water wash, the slides were stained in Harris' hematoxylin solution for 4.5 minutes, then washed in ddH_20 for 5 minutes. The slides were then dipped into acid alcohol (1%) slowly and carefully, dipping 5 times before gentle rinsing with ddH_20 for 5 minutes. Slides were then placed into a saturated solution of lithium carbonate for 2 minutes and put in ddH_20 for 5 minutes. Using eosin as a counterstain, the slides were immersed into the eosin solution for 2 minutes. The slides were then dehydrated by dipping gently into 70% ethanol 10 times, 95% ethanol 15 times, and then placing into 2 changes of 100% ethanol for 2 minutes each. The slides were then put into 2 changes of SlideBright solution for 2 minutes each, and mounted under coverslips with Permount mounting medium.

2.6 Counting

Originally the method chosen to view the isolated fibers was a DAPI/DAB combination in order to see the total number of nuclei within the fiber (using DAPI), as well as seeing which of those nuclei were also Pax7 or BrdU positive (using DAB). Once

the experiment commenced it became apparent that this approach was not feasible. The DAB staining interfered with the DAPI, and the time frame to view the fluorescent DAPI was too narrow (due to photobleaching) within the frequency of the experiments that were planned. Subsequently the fibers were only stained with DAB, and the low-level background staining by DAB in the fibers was available for counting myonuclei (e.g., see Zhang & Anderson, 2014).

Slides containing 2 coverslips of fibers were viewed without knowledge of time point or fish age, using an Olympus Microscope (BH-2, Olympus, Tokyo, Japan). Darkly stained DAB-positive nuclei were counted in the SCs on each fiber (8-20 per coverslip) on each coverslip using magnification by the 40x objective lens. Counts were made for every time point (in the pulse-chase BrdU-labelling experiments) at each age group. The same counting method was used for both anti-BrdU staining and anti-Pax7 staining of nuclei in SCs on fibers. The total number of myonuclei was counted for the same fibers, by focusing through the different planes of the fiber to make sure that all nuclei were counted.

The length and diameter of 40 fibers (randomly chosen from fibers at each age group) were also measured from photographs using an Olympus digital camera (Model: UC50, Olympus, Tokyo, Japan) at 20x objective lens, and the mean length and diameter were calculated and compared. The distribution of positively-stained SC nuclei, fiber length and diameter, etc. was also determined. Myonuclear population was examined in relation to fiber length, diameter and volume. Fiber volume was calculated by dividing the width of the myofiber in two, squaring that value, then multiplying it my pi and the length. This was done for each myofiber and then averaged for each age. All these calculations

served as indicators of fiber growth rate, and trends in SC activity (e.g., the ratio of mean $BrdU^+$/fiber divided by the mean $Pax7^+$/fiber).

Additional myofiber characteristics that were analyzed included the features of the muscle fiber terminus. Fibers were categorized into 3 groups based on whether they were tapered on one end or both ends, or if both ends were blunted. The tapered nature of the fibers did not change the volume calculations, as the length of the fibers was taken at the middle of the terminus, regardless of whether it was tapered or not. These data were combined with the SC activity data for further comparisons.

2.7 Statistical Analysis

Statistical analysis of means (ANOVA) was used to determine whether there were statistical differences in myonuclear population and fiber and SC characteristics among different ages of fish. Statistical tests were completed with Excel and SPSS using an $\alpha = 0.05$ to indicate statistical significance. A one-way ANOVA was used to determine differences in the mean number of nuclei among the seven age groups; when the ANOVA was significantly different, a post hoc test was performed to determine the significance of pair-wise comparisons of means for each group.

Linear regressions were used to determine correlations between variables. Scatterplots were graphed and Pearson correlation values were calculated for each pair of variables. Correlation coefficients were categorized as negligible, low, moderate, high and very high according to previous reports (Mukaka, 2012) in ranges 0.0-0.3, 0.3-0.5, 0.5-0.7, 0.7-0.9, and 0.9-1.0 correlation coefficient values respectively. The residuals were also graphed for each regression to determine confidence of reliability.

Chi-square tests were used to determine differences between the myofiber terminal characteristics between and within ages. Analysis was done to determine goodness of fit using a significance value of $p < 0.05$.

Chapter 3: Results

The results of experiments on fish that are reported here, are interpreted as representative of Lake Sturgeon reared in the animal holding facility at the University of Manitoba; they were collected from animal holding tanks by random sampling.

3.1 Body length and weight

Fish were measured prior to dissection; therefore, weight measurements included the head and viscera, and the length measurements included the head and full tail. Ages used for experimentation were 0.5, 1, 2, 3, 4, 5, 6, 17, and 29 months post-hatch (MPH).

Figure 3 depicts the changes in fish mass and length (mean, SEM), representing the overall pattern of growth with age. Both length and weight significantly increased with age overall (ANOVA, $p < 0.001$). The length increased linearly with age, but the weight increased slowly in a curve with a small plateau between 4 and 5 MPH. Between individual age groups there were significant increases in both length and weight (t-test, $p < 0.01$), except for between 4 and 5 MPH, in which there was no significant increase in either length nor weight (t-test, $p > 0.1$). The length verses age showed a positive linear trendline and a strong correlation between the variables with a very high Pearson correlation coefficient (r) of 0.993 and an R^2 value of 0.986 ($p < 0.01$). Figure 3B illustrates the curved trend that was seen when the weights were plotted against age. Compared to the 17 and 29 MPH fish, there were smaller changes in the younger ages. From 6 MPH to 17 MPH, weight

increased by more than 30-fold, which was consistent with initial observations. From 17 MPH to 29 MPH weight increased more than 2-fold, which was not what was thought was the fish were observed in the tank initially. In order to see the changes at the younger ages clearly, the older 2 ages (17 and 29 MPH) were removed from the graph to make figure 3C. The increase in weight up to 6 MPH, appeared polynomial in nature, with a slight plateau between 4 and 5 MPH (figure 3C). The length and weight were very highly correlated (Pearson correlation (r) = 0.948; $p < 0.01$) and had an adjusted R^2 value of 0.884 when plotted in a linear regression (figure 4).

There were differences in Lake Sturgeon growth rate between the fish reared at the animal holding facility at the University of Manitoba (UofM) and the fish reared at the Grand Rapids (GR) Manitoba Hydro hatchery that were sampled by fellow graduate student, Catherine Brandt (figure 5). Mean fish length and weight at different ages showed similar trends in both sets of fish and were always highest in the fish hatched in 2017 at the GR hatchery. The next largest were seen in the 2016 UofM fish, and the smallest overall sizes over the course of 6 MPH were seen in the 2017 fish from the UofM facility. There was such a variation between the locations in the 2017 hatching year, even at 2 weeks post-hatch (figure 6). The fish reared in the GR hatchery were significantly longer (ANOVA, $p < 0.001$) and heavier (ANOVA, $p < 0.001$) at each age group than those reared in the UofM hatchery. The only age that there wasn't a significant difference in the GR fish over the UofM fish was the weight of the 1 MPH fish (t-test, $p = 0.078$), though the length of the fish at that age did show a significant difference between locations (t-test, $p < 0.05$). The fish reared at UofM in 2017 were the only fish used for all analysis except for the analysis in creating figures 5 and 6.

3.2 Fiber length, width, volume, and configuration

Following euthanasia and dissection, muscle tissue was removed from the fish in a manner that ensured myofibers were damaged as little as possible (hopefully intact). Myofibers were affixed on coverslips, cultured for a pre-set time, then fixed and stained, and placed on slides for viewing and counting. Depending on how many fibers stuck to the coverslip, between 8 and 20 fibers per coverslip were measured and counted for nuclei.

The length and width of myofibers were measured from photographs of individual fibers, taking measurements of length along the longer dimension and width along the shorter dimension. The myofiber length and width varied greatly between different-aged fish, consistent with direct viewing of the fibers by microscopy. The length of fibers increased linearly as the fish aged, and plateaued after 17 MPH (figure 7A). Between 6 MPH and 17 MPH the increase in fiber length was significant (t-test, $p < 0.05$). The width of fibers, on the other hand, displayed a parabolic change with fish age (figure 7B), that is, the trend line decreased up to about 12 MPH, then increased. Though in regression studies, fiber width did not fit a trend line well, the calculated mean volume of the myofibers showed a moderate fit with a linear trend line as age increased with a R^2 value of 0.663 and a high correlation (figure 8; Pearson correlation (r) = 0.814, $p < 0.01$). As well, there was a noticeable relationship between mean myofiber length and mean total length of fish. The linear regression between these two variables showed a very high Pearson correlation coefficient (r) of 0.917 and an adjusted R^2 value of 0.818 ($p < 0.01$) (figure 9). What is interesting is that the correlation between the mean myofiber volume and mean total fish length is also a strong a correlation, with a correlation coefficient (r) of 0.803 ($p < 0.01$) (figure 10).

Fiber configuration was determined by observing photographs of individual fibers and classified according to whether a fiber had blunted or tapered ends (figure 11 illustrates different profiles of fiber). Although the pictures were not used for counting the number of positively-stained nuclei, the DAB+ nuclei can be easily observed in the images

The myofibers were varied in their end-terminal characteristics, and not all were blunt ended or tapered. When examining the isolated fibers, most had at least a single end that was tapered, although some were noted to have two tapered ends. When the data were compiled, it was revealed that at 2, 3, 6, 17 and 29 MPH, there were statistically more fibers that were blunt at both ends ($p < 0.01$); however, in the 4 MPH fish, the majority of fibers were tapered at only one end ($p < 0.01$; figure 12). The fibers isolated from the 5 MPH fish showed no statistical difference in their terminal characteristics ($p > 0.05$). Between different ages each of the myofiber terminal characteristics showed significant differences ($p < 0.001$). The tapered nature of the fibers did not change the volume calculations, as the length of the fibers was taken at the middle of the terminus, regardless of whether it was tapered or not.

3.3 Muscle histology in sections

Longitudinal sections of the muscle were cut and stained with H&E to look at the characteristics and locations of SCs surrounding the myofiber, and how it compared with the viewing of isolated fibers. With H&E staining, the nuclei come up purple and the rest of the muscle tissue stains pink (figure 13). With this you can see the nuclei in and around the myofiber, as well as the sarcomeres within the fiber. The nuclei indicated by the arrows are possibly SCs due to their location outside the myofiber. Though in most sections the fibers are quite dense, therefore you can't see SCs.

3.4 Immunohistochemistry

IHC staining was utilized to view and count the SCs on isolated myofibers in two ways. Cycling SCs were detected with anti-BrdU staining to visualize BrdU incorporation into actively dividing SCs, whereas myonuclei are post-mitotic and not darkly stained. Myogenic precursors were detected with anti-Pax7 staining as it distinguishes myogenic cells resident on fibers from internal myonuclei and nuclei in any other adherent cells that might be attached around the myofibers. Counts of the Pax7+ and BrdU+ nuclei were done at the microscope so that all nuclei could be counted by changing the plane of view through the whole fiber. The slides were examined while they were coded to remove bias, but the number of DAB+ nuclei within the fibers varied quite a bit.

3.4.1 Satellite cell cycling – BrdU+ satellite cells

A pulse-chase experiment using anti-BrdU was utilized to monitor the incorporation of BrdU and subsequent dividing of SCs. That data were then used to determine if the cell cycle time of SCs changes as the fish ages. The 'pulse' consisted of the fibers submerged in BrdU-solution for 2 hours, and the 'chase' involved the fibers in media without BrdU for 24 hours. The mean number of BrdU+ nuclei per myofiber at each determined time interval was plotted at each fish age against time. It was anticipated that the BrdU+ nuclei value would double as time progressed since the dividing SCs would incorporate the BrdU and divide into two cells, and then both daughter cells would be positive for BrdU. On some fibers there were examples of two BrdU+ nuclei right next to each other, which were counted as two separate cells, though this was only observed a couple times.

At each age, the BrdU+ nuclei on the myofibers isolated from the Lake Sturgeon were counted and subsequently graphed. Each graph of the number of BrdU+ nuclei/myofiber (that is the number of dividing SCs per myofiber) verses the chase time showed a sinusoidal curve. There were peaks and troughs denoting the number of BrdU+ SCs for each age as a function of time. To determine the SC cell cycle time at each age, the time from peak to peak was measured (figure 14A). The primary findings of the pulse-chase study were that each age showed a different cycle period, or amount of time between peaks.

The graphs produced by plotting the data points of the BrdU+ per myofiber against chase time were also fitted with a line connecting each point. The following were the observations of those graphs at each age. At 1 MPH there wasn't enough data to accurately represent the cycle, but at 2 MPH there appeared to be a sinusoidal curve, with an increase in BrdU+ cells from 0 to 1-hour post-chase (PC), then a trough at 12-hours and another peak at 15-hours post-chase. There were large peaks observed at 0 and 24-hours post-chase at 3 MPH, with a smaller peak at 12-hours PC. At 4 MPH the peaks were not as distinct as prior ages, and were a bit more difficult to deduce a cycle, but there were still peaks observed at 5 and 14-hours PC with a trough at 11-hours PC. There were 3 peaks observed for the 5 MPH fish myofiber SCs. These were at 0, 5 and 9-hours PC. At 6 MPH the peaks were at 0 and 7-hours PC. The peaks for 17 and 29 MPH were observed at 3 and 9, and 1 and 7-hours PC respectively.

The expected graph, as stated earlier, being a consistent population size and then doubling, did not occur. Instead the graphs that displayed BrdU+ SC/myofiber populations over time showed curved trend lines with peaks and troughs (figure 14A). The cell cycle

times were determined by taking the amount of time between two peaks in the curve. This was done for each age. Where there were more than 3 peaks, the average was taken between the two periods to determine an mean cell cycle time (done for 3 and 5 MPH).

The determined cell cycle times were statistically different between ages ($p < 0.001$). At 2 MPH it was the highest, being 14 hours, and continues to go down as fish age increases. The cell cycle times for each age group were as follows: 2 MPH = 14 hours (hrs), 3 MPH = 12 hrs, 4 MPH = 9 hrs, 5 MPH = 4.5 hrs, 6 MPH = 7 hrs, 17 MPH = 6 hrs, 29 MPH = 6 hrs. Once those times were decided upon from viewing the graphs, chase times were chosen for each age to be used in the reminder of the analyses (denoted the 'analyses chase times'). The times were chosen so that one full cell cycle would be completed (from the beginning of the 'pulse'), but not so long that two cycles were completed. Specifically, the data used for all the analyses was taken from the following chase times: 2 MPH = 12 hrs, 3 MPH = 12 hrs, 4 MPH = 9 hrs, 5 MPH = 5 hrs, 6 MPH = 7 hrs, 17 MPH = 5 hrs, 29 MPH = 5 hrs (figure 14C). This was done to standardize the comparisons against cycle time.

Testing that a sinusoidal curve was truly present in the graphs, the sin function of the y-axis (the number of BrdU+ nuclei per myofiber) verses the chase time was graphed. If there was one cycle within the data, one would expect to see a flat, straight line when the sine function is graphed. This was the case for all the age groups except for 5 and 17 MPH (figure 14B). When the sine function of the BrdU+ nuclei per myofiber versus chase time was graphed, 2, 3, 4, 6, and 19 MPH showed relatively flat lines, but the 5 and 17 MPH data still showed peaks.

Since the chosen chase times were used for all the analyses, the BrdU+ numbers of each age at those chase times was also graphed. The dividing SC (BrdU+) populations peaked at 3 MPH, dropped at 4 MPH, peaked at 5 MPH, and then gradually dropped off again all the way to 29 MPH (figure 15A). Since the 17 and 29 MPH showed to have a large influence in the graphed data, those data points were removed to observe what was happening up to 6 MPH (15B). There is a general upward trend observed in the BrdU+ nuclei the first 6 months of the fish's life, though there are peaks and troughs. From 2 to 6 MPH, the graph showed a linear positive trend with an R^2 value of 0.4751 ($p < 0.01$). In fact, the peak at 5 MPH is a significant increase from the populations observed at 4 MPH ($p < 0.05$). This is similar to the trend that was expected in the dividing SCs since the fish grow a lot in the first year.

Using the determined analyses chase times, populations of SCs and total nuclei per fiber were also counted and averaged. These population values were then also used for comparisons.

3.4.2 Myogenic precursor cells – Pax7+ satellite cells

The number of Pax7+ SCs per fiber was expected to be relatively constant or to decrease slightly as the fish aged, since when the SCs asymmetrically divide to produce a myogenic precursor cell, they also produce another SC, therefore keeping the SC populations relatively constant. However, the Pax7+ SC populations increased from 2 MPH up to 17 MPH, and then decreased at 29 MPH (figure 16A). To view the populations of Pax7+ SC from 2 to 6 MPH only, a graph was constructed without 17 and 29 MPH (figure 16B). There is quite a distinct positive trend in the Pax7+ SC populations, with an much higher positive outlier at 3 MPH. Though with 3 MPH, the linear line of fit is very

strong, from 2 to 6 MPH the R^2 value is 0.0001 ($p < 0.01$). The number of Pax7+ nuclei per myofiber started low in the 2 MPH (1.325 ± 0.24 mean nuclei/myofiber), rose to 2.55 ± 0.16 mean nuclei/myofiber at 3 MPH, then back down to 1.6 ± 0.25 mean nuclei/myofiber at 4 MPH. Following 4 MPH there was a very gradual increase to 6 MPH (1.75 ± 0.17 mean nuclei/myofiber), then there was a large jump in Pax7+ SC population numbers to 17 MPH (5.1 ± 0.54 mean nuclei/myofiber). The jump in the SC population between 6 MPH and 17 MPH was statistically significant ($p < 0.001$). At 29 MPH there was a drop in the Pax7+ SC population numbers (2.33 ± 0.43 mean nuclei/myofiber). This drop in the population numbers between 17 and 29 MPH was also significant ($p < 0.001$).

3.4.3 Fiber myonuclei and myonuclear domains

The population of total nuclei (SC plus myonuclei) is plotted in figure 17. All nuclei were counted that were in and directly adjacent the myofiber. There was quite a variation in myofiber populations that was observed during counting. The mean population of total nuclei associated with a fiber displayed a relatively regular trend which showed a linear increase with increasing age, an R^2 (coefficient of determination) value of 0.9313 and a very high Pearson correlation coefficient (r) of 0.965 ($p < 0.001$). The values start at 7.4 ± 0.68 total nuclei per myofiber, and increase in a linear trend with the number of total nuclei being 15.95 ± 2.3 at 29 MPH. To remove the high weight that the data from 17 and 29 MPH fish had, a graph was created that showed the number of myonuclei per myofiber from 2 to 6 MPH only (figure 17B). There is a positive linear increase in the first 6 months, with an R^2 value of 0.7633 ($p < 0.01$).

The volume of each myofiber was used to calculate the myonuclear domain. Myonuclear domain is described as the average amount of sarcoplasm regulated by a single

nucleus, and was calculated by taking the volume of each myofiber (calculated from the length and width) and dividing it by the number of myonuclei within that fiber. The total number of nuclei that is used for all calculations includes the DAB-stained nuclei (ie. Pax7+ SCs and BrdU+ dividing SCs) and the nuclei within the fiber that weren't stained dark. The volume of the myonuclear domain showed a positive linear increase with increasing age (figure 18A). The trend line of a regression of myonuclear domain versus fish age had a high correlation ($r = 0.755$), and an adjusted R^2 value of 0.508 ($p < 0.05$). When the data from 17 and 29 MPH were removed, the graphed slower a slight linear decreasing trend in the myonuclear domain for the first 6 months (figure 18B). This linear decrease shows a linear line of best fit with an R^2 values of 0.157 ($p < 0.01$).

3.5 Ratio of satellite cells to total nuclei

To see if there were consistencies in the ratios of the mean Pax7+ SCs to total nuclei or dividing (BrdU+) SCs to total nuclei, the ratio of Pax7+ SC or BrdU+ SCs with the total number of nuclei in a fiber (SC plus myonuclei) were calculated for fibers at each age. These ratios were then plotted against age.

The ratio of SCs (Pax7+) to total nuclei started low at 2 MPH (0.190 ± 0.03), had a sharp peak at 3 MPH (0.341 ± 0.02), dropped to a trough at 4 MPH (0.187 ± 0.02), then gradually increased over time to the 29 MPH age (0.317 ± 0.05; figure 19A).

The ratio of dividing (BrdU+) SCs to total nuclei showed a similar trend to the data for the number of dividing (BrdU+) SCs considered alone. In particular, there is a peak at 3MPH from 2 MPH (0.237 ± 0.02 and 0.139 ± 0.04 respectively) and again at 5 MPH (0.243 ± 0.02) with a trough at 4 MPH (0.138 ± 0.02), then after the 5 MPH peak there is

a gradual drop to 17 MPH (0.170 ± 0.02), and a slight increase to 29 MPH (0.203 ± 0.06; figure 19B).

Re-evaluating the findings for fiber configuration in relation to the staining for dividing (BrdU+) SCs, the majority of fibers were observed under microscope to have a single, tapered end. As well, the myofibers with both ends tapered appeared to have fewer positively-stained diving (BrdU+) SC nuclei.

The ratio of dividing (BrdU+) SCs to total nuclei was plotted against fish age, separating the fibers according to their terminal characteristics, results were consistent with initial observations. The plots revealed that at 3, 5, 17 and 29 MPH, the fibers that were tapered at only one end had the highest ratio of dividing SCs to total nuclei when compared with fibers with only blunt or tapered ends (figure 20). The remaining ages, 2, 4 and 6 MPH had the highest ratio of dividing (BrdU+) SCs to total nuclei in fibers that were blunt at both ends. Though the graph shows a visual difference between the terminal characteristics within and between ages, there is no statistical difference. The only age showing a statistical significant difference between the fiber configurations within the age is at 5 MPH (ANOVA, $p < 0.05$). When looking at the same myofiber terminal configuration between age groups, there is significant difference with the fibers tapered at one end and the fibers tapered at both ends (ANOVA, $p < 0.01$ and $p < 0.05$ respectively), but no statistical difference with the blunted end myofiber data ($p > 0.05$).

3.6 Other relationships

To further explore possible mathematical relationships as well as test interactions of different variables several other linear regressions were conducted, although they did

not have high correlation values. The comparisons of these pairs of data sets can better determine whether particular interpretations were consistent with results considered in tandem, or whether a multiple regression would provide a more complete understanding of correlations.

The regression between the number of total nuclei (SCs and myonuclei) per myofiber and the number of Pax7+ SCs per myofiber showed a non-significant Pearson correlation coefficient (r) of 0.489 and an adjusted R^2 value of only 0.087 ($p = 0.266$; figure 21). This regression showed no statistical significance at all.

The ratio of dividing (BrdU+) SC to total nuclei was expected to be highly correlated with the ratio of Pax7+ SC to total nuclei, but there was almost no correlation, with a non-significant Pearson correlation coefficient (r) of 0.206, with an adjusted R^2 value of -0.149 ($p = 0.658$; figure 22).

The number of dividing (BrdU+) SCs per fiber was regressed against the number of Pax7+ SCs per fiber. These two values had the smallest relationship, with a Pearson correlation coefficient of only 0.072 (non-significant, $p > 0.05$) and an adjusted R^2 value of -0.194 ($p = 0.878$; figure 23).

Myofiber length was correlated with the mean number of SCs (Pax7+) per myofiber to determine if there was any trend observed as the fibers increased in length (figure 24). Although there was an observable positive linear trend with an adjusted R^2 value of 0.41 and a Pearson correlation (r) of 0.713, both were statistically non-significant.

Results demonstrate overall, that there were many changes in cell cycling time, and the population of myonuclei and SCs on fibers, detected with the single-fiber culture experiments.

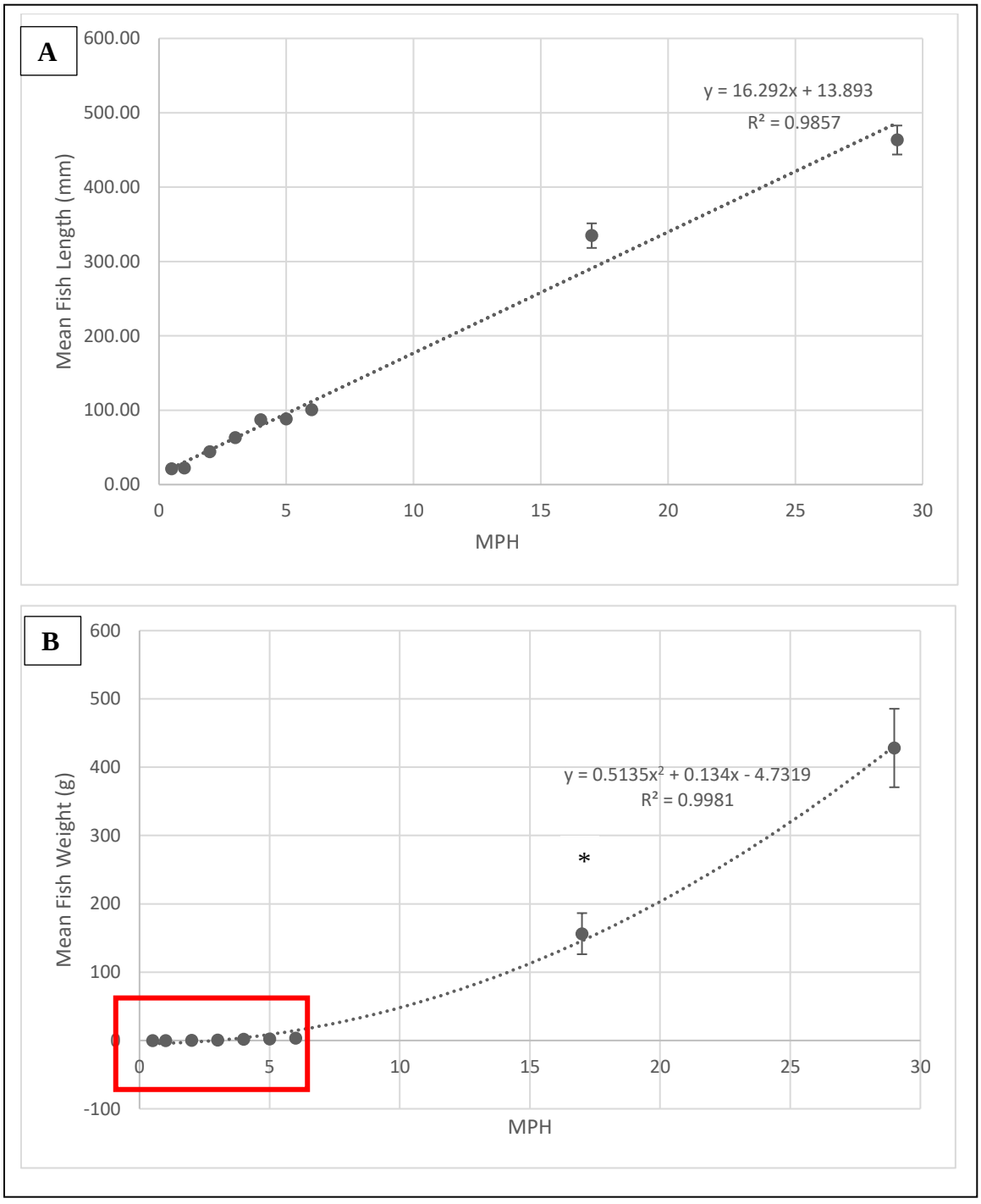
A
600.00
500.00
400.00
300.00
200.00
100.00
0.00
Mean Fish Length (mm)
y = 16.292x + 13.893
R² = 0.9857
0
5
10
15
20
25
30
MPH
B
600
500
400
300
200
100
0
-100
Mean Fish Weight (g)
y = 0.5135x² + 0.134x - 4.7319
R² = 0.9981
*
0
5
10
15
20
25
30
MPH

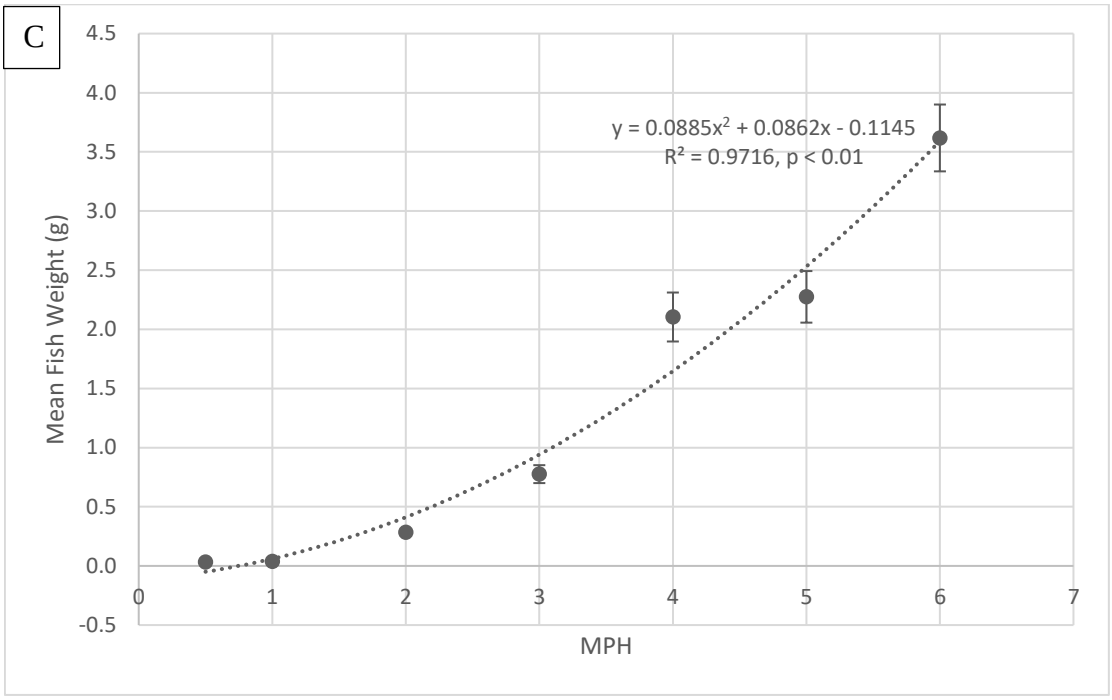

Figure 3. Mean length and weight of Lake Sturgeon during development

The mean length (mm) and weight (g) of the Lake Sturgeon reared in the UofM Animal Holding facility in the 2017 season from 0.5 to 29 MPH. Length measurements were taken from the tip of the snout to the end of the tail, measuring the total fish length, then averaged and plotted with standard error of the mean (error bars) for each point (A). A linear line of best fit was also plotted and had an R^2 value of 0.9857. The mean weight (g) of the Lake Sturgeon from 0.5 to 29 MPH was graphed (B); and the graph enlarged over range from 0.5 to 6 MPH (C). The number of fish sampled at each age group changed with the size of the fish at each age, and were as follows: 0.5 MPH, n = 35; 1 MPH, n = 40; 2 MPH, n = 41; 3 MPH, n = 22; 4 MPH, n = 22; 5 MPH, n = 20; 6 MPH, n = 18; 17 MPH, n = 5; 29 MPH, n = 5. For both length and weight there was a significant increase from 6 MPH to 17 MPH (as indicated by *, $p < 0.01$).

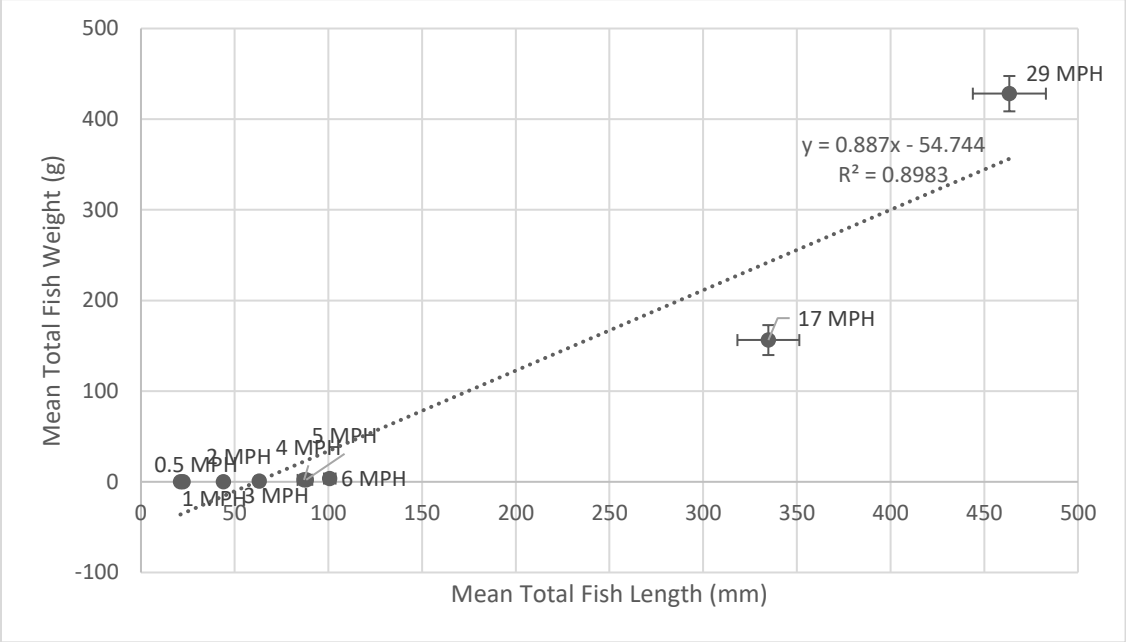

Figure 4. Linear regression between the mean fish weight and mean fish length

The linear regression between the total fish weight (g) and the total fish length (mm) of Lake Sturgeon reared at the UofM in 2017 (df = 8). Values for length and weight were taken from figure 3. There was a very high correlation between the length and weight, with a Pearson correlation of 0.948 and an adjusted R^2 value of 0.884 ($p < 0.001$).

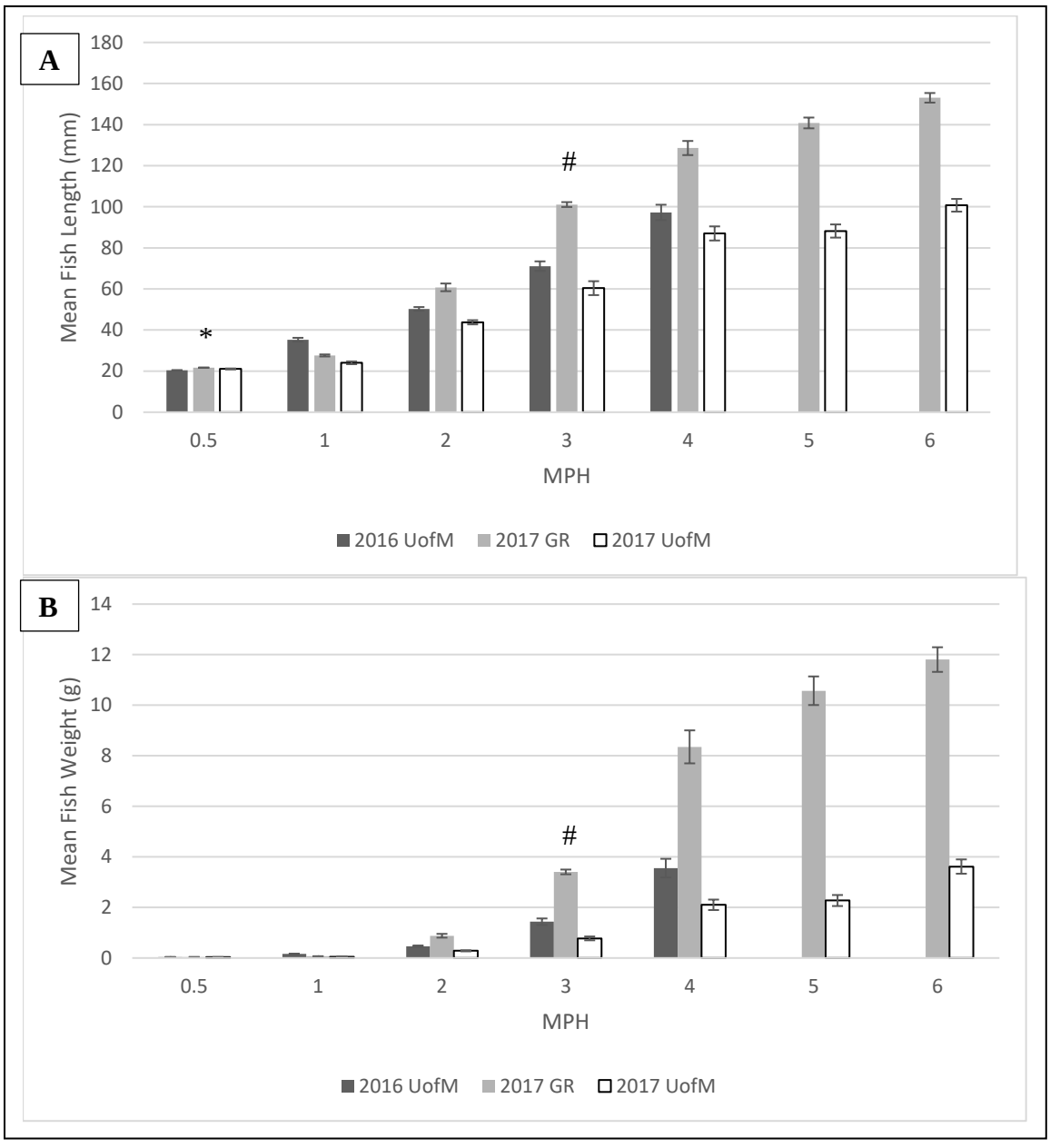
A
Mean Fish Length (mm)
180
160
140
120
100
80
60
40
20
0
*
#
0.5
1
2
3
4
5
6
MPH
2016 UofM
2017 GR
2017 UofM
B
Mean Fish Weight (g)
14
12
10
8
6
4
2
0
#
0.5
1
2
3
4
5
6
MPH
2016 UofM
2017 GR
2017 UofM

Figure 5. Variation in length and weight between different years and locations

Histograms of the differences in Lake Sturgeon growth (length in millimeters and weight in grams) reared at the University of Manitoba (UofM) from between 2016 and 2017 hatching seasons and from the Grand Rapid (GR) Manitoba Hydro hatchery in 2017 (df = 392, 194 and 326 respectfully). Both length (A) and weight (B) were shown to be greater in 2016 than in 2017, and greater at the GR hatchery than at the UofM ($p < 0.01$). There was a significant difference in length and weight between all locations and ages, except for the weight between locations and years at 1 MPH (ANOVA, $p < 0.01$). The length data at 0.5 MPH looks rather similar on the graph, but there is a statistically significant difference between them (* indicates significant difference in length between years and locations at 0.5 MPH, ANOVA, $p < 0.01$). At 3 MPH there is an observable and statistical difference between the groups in both length and weight (# indicates significant difference in length and weight between years and locations at 3 MPH, ANOVA, $p < 0.01$). Note, data for fish length and weight from GR and 2016 UofM, provided by Cat Brandt (Dr. Gary Anderson's lab).

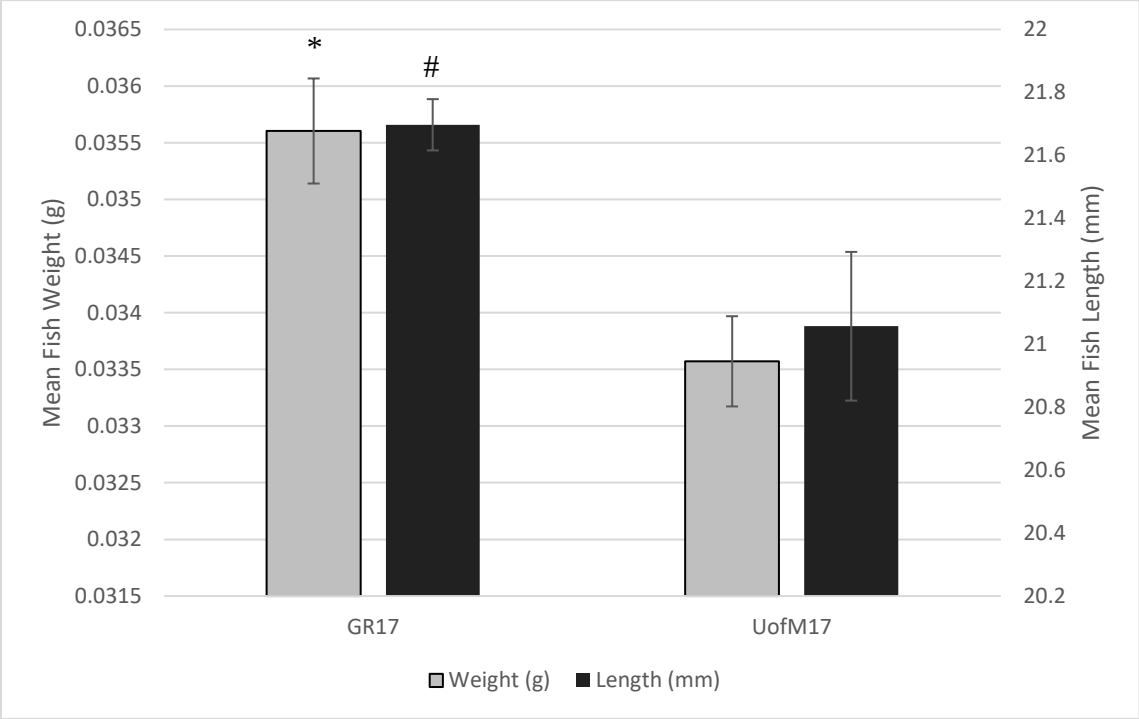

Figure 6. Variation in length and weight across locations at 0.5 MPH

Bar graph of the differences of Lake Sturgeon at 0.5 MPH reared at the UofM and Grand Rapids hatchery in 2017. Length is shown on the right y-axis and weight is shown on the left y-axis. Measurements were taken at 0.5 MPH (n=271 for GR; n=35 for UofM) to compare. Length and weight were both significantly greater at the GR location in 2017 than the UofM location (* indicates significant differences in weight, and # indicates significance in length between locations, $p < 0.05$).

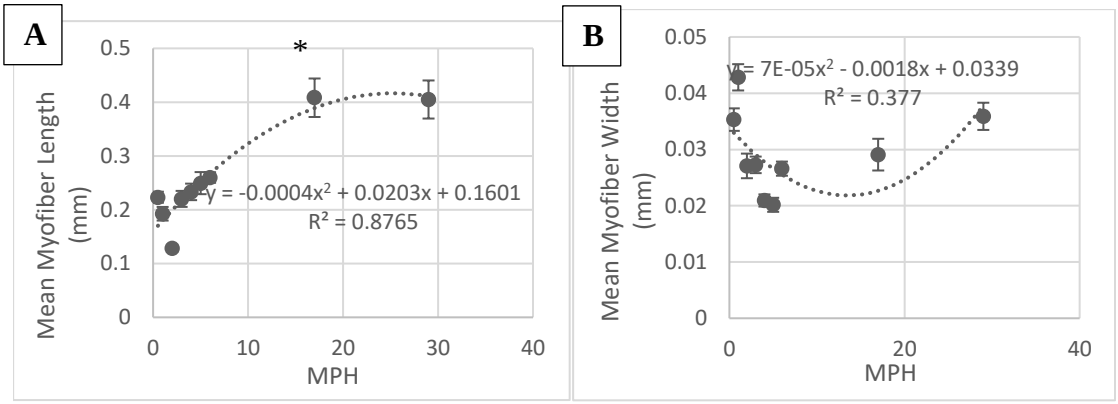

Figure 7. Changes in myofiber dimensions with increasing age in fibers from the Lake Sturgeon

Muscle fibers were isolated from Lake Sturgeon reared at the UofM from 0-29 months post-hatch (MPH). Pictures were taken of the fibers using the 20x objective lens, and the fibers were measured in both length (A) and width (B). From 6 MPH to 17 MPH there was a significant increase in the myofiber length (as indicated by *, post-hoc, $p < 0.05$); however, there was no significant difference in myofiber width between 6 and 17 MPH (df = 351 for each). There was a high correlation between myofiber length and MPH (A) with a Pearson correlation coefficient (r) of 0.892 ($p < 0.01$). There was only a negligible linear correlation between myofiber width and MPH (B), with an r value of 0.157 that was not significant ($p > 0.05$).

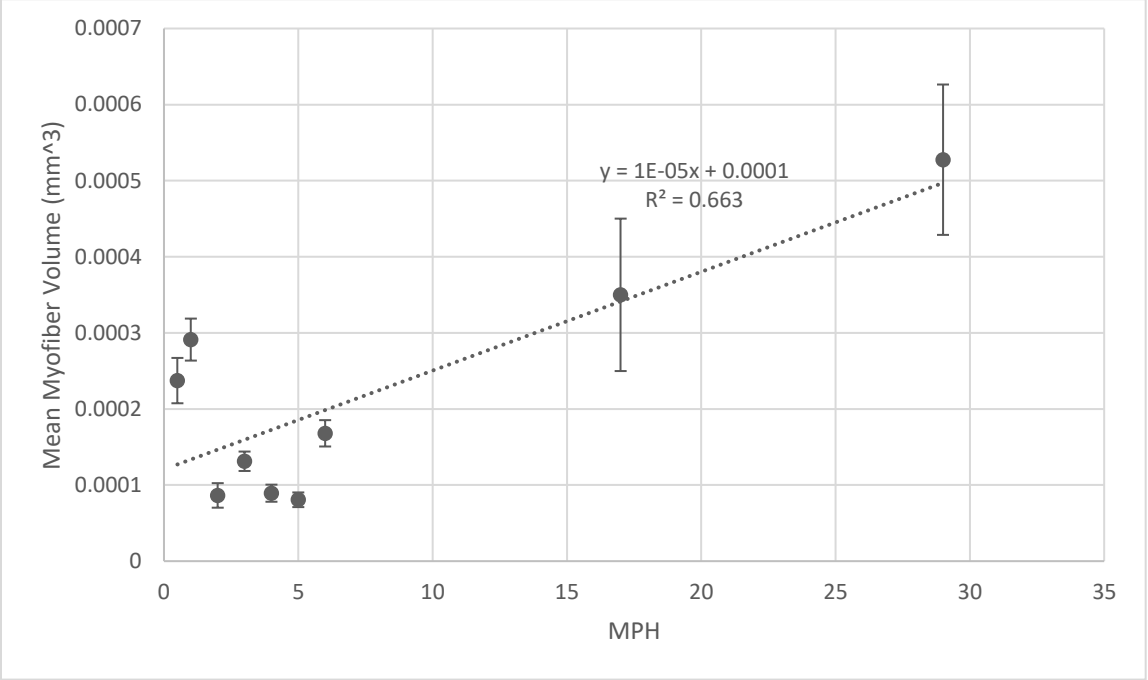

Figure 8. Growth in myofiber volume with increasing age

Myofiber length and width measurements were taken from 40 fibers at each age (0.5, 1, 2, 3, 4, 5, 6, 17, and 29 MPH; df = 8) and used to calculate volume. Volume was calculated by using the following equation (π*(width/2)^2*length). This scatterplot shows the mean volumes (mm^3) of the myofibers at each MPH with a linear trendline denoting a R^2 value of 0.663, and a high Pearson correlation coefficient (r) of 0.814 ($p < 0.01$).

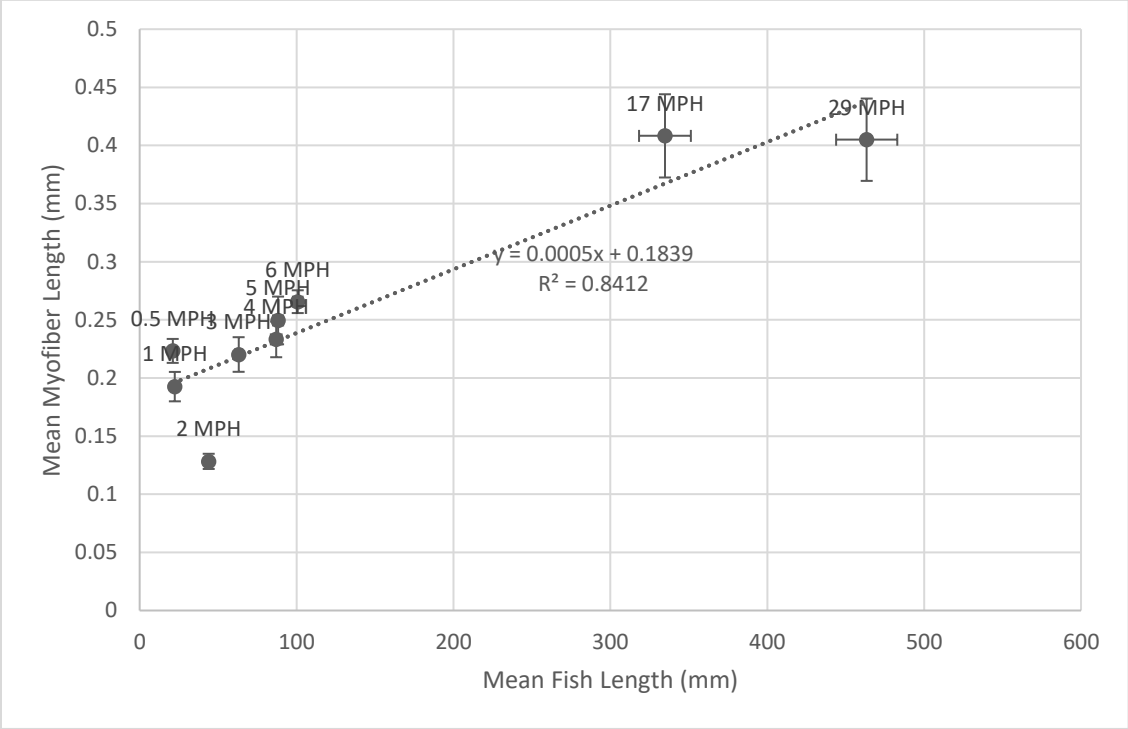

Figure 9. Linear regression of myofiber length versus fish length

The myofiber length (mm) was measured from end to end of the myofiber from the pictures taken using the 20x objective lens, and the fish length (mm) was measured from the tip of the snout to the end of the tail (df = 8). There was a strong linear correlation (r) between these two variables ($r = 0.917$, $p < 0.01$) and an adjusted R^2 value of 0.818 ($p < 0.01$).

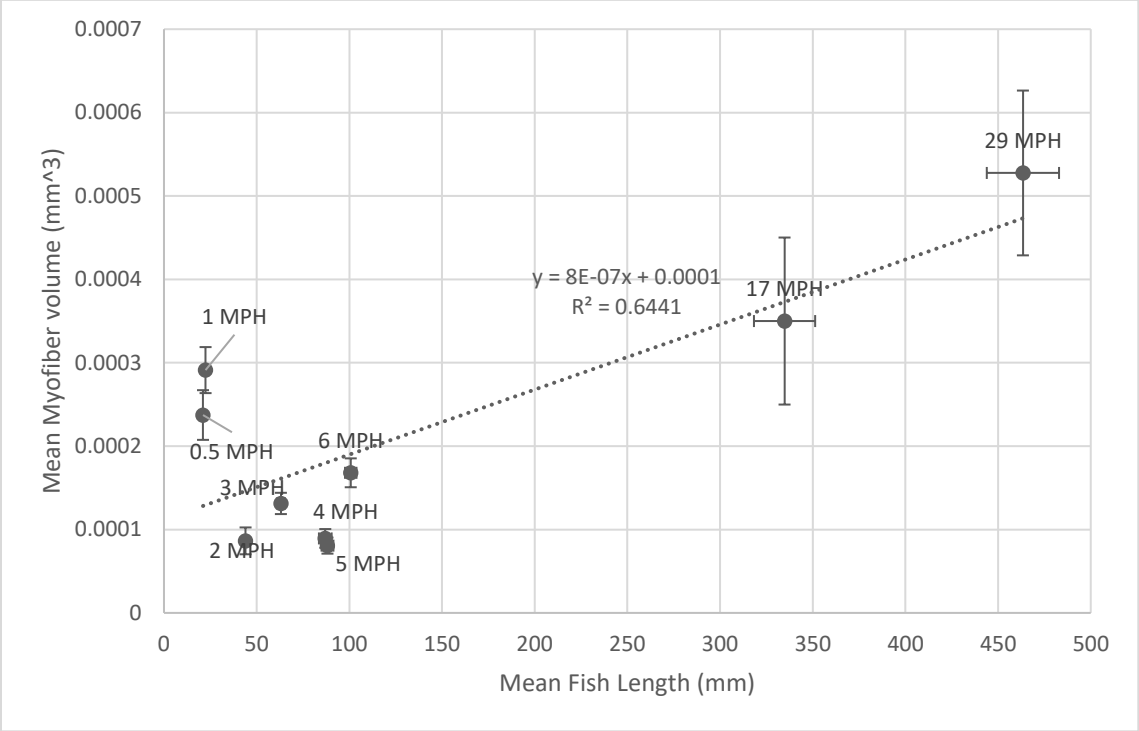

Figure 10. Linear regression of myofiber volume and fish length

Scatterplot denoting the linear regression of mean myofiber volume (mm^3) and mean fish length (mm). Fiber volume was calculated by using the equation $\pi*(width/2)^2*length$, and the total length of the fish was measured from the tip of the snout to the end of the tail (df = 8). There was a high correlation between these variables, with a Pearson correlation coefficient (r) of 0.803 ($p < 0.01$).

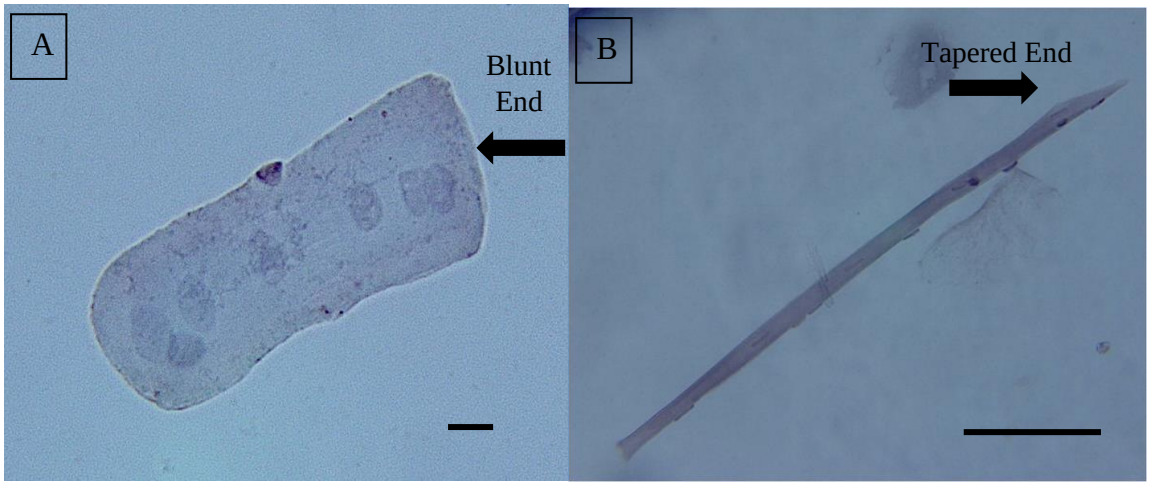

Figure 11. Myofiber terminal characteristics

Representative fibers were isolated from A. 2 MPH and B. 5 MPH Lake Sturgeon and stained for BrdU using the HRP-DAB method. These fibers display the differences in terminal characteristics. A blunt end was flat and not pointed (arrow in A), whereas a tapered end was notably pointed, with one side a lot longer than the other (arrow in B). The scale bars are representative of 10 µm (panel A) and 100 µm (panel B).

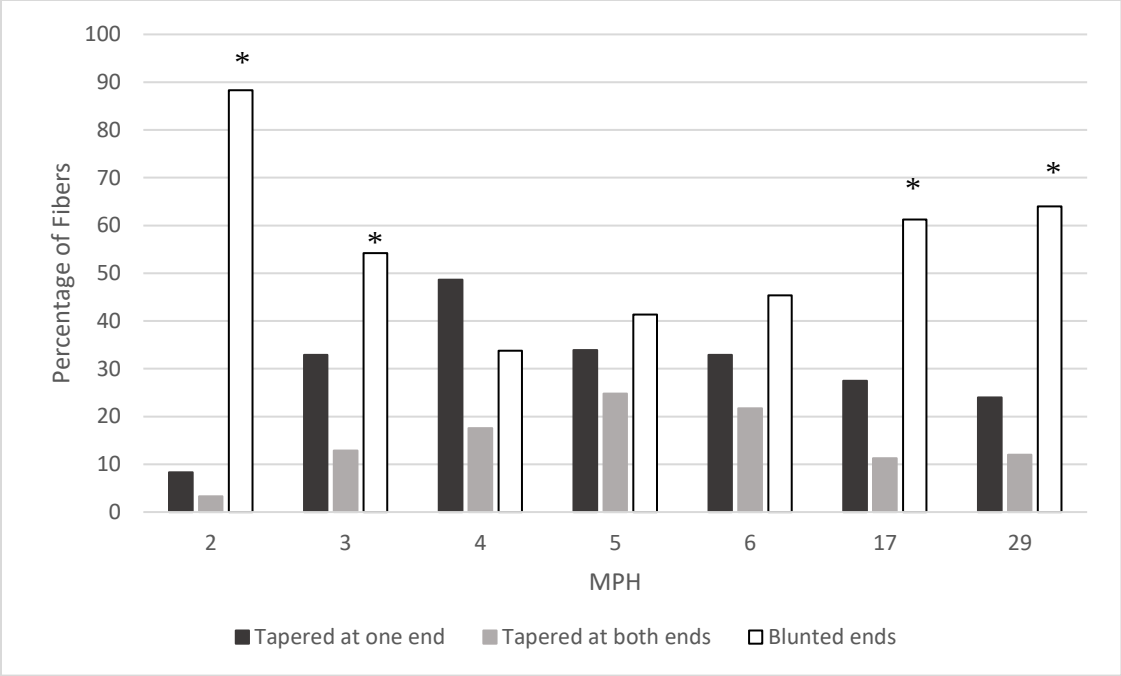

Figure 12. Myofiber terminal characteristics divided by age

Bar graph showing the distribution of the percentage of fibers at each age that had two blunt ends or one or both ends tapered in some way. The sample size for each age varied (2MPH, n = 60; 3MPH, n = 155; 4MPH, n = 74; 5MPH, n = 121; 6MPH, n = 152; 17MPH, n = 80; and 29MPH, n = 25 fibers. Fibers were analyzed from dishes with the same chase times indicated in figure 15C. There were significant differences (by Chi-square (χ^2) statistics) in fiber-end characteristics at nearly every age: 2, 3, 4, 6, 17 and 29 MPH ($p < 0.001$ ($\chi^2 = 81.9$); $p < 0.001$ ($\chi^2 = 39.652$); $p = 0.005$ ($\chi^2 = 10.73$); $p = 0.002$ ($\chi^2 = 12.80$); $p < 0.001$ ($\chi^2 = 31.23$); and $p = 0.004$ ($\chi^2 = 11.12$) respectively), as well as within fiber characteristics between ages ($p < 0.001$ ($\chi^2 = 75.07$); $p < 0.001$ ($\chi^2 = 58.76$); $p < 0.001$ ($\chi^2 = 66.88$) for tapered at one end, tapered at both ends and blunted at both ends myofibers, respectively). The * indicate significant differences between terminal characteristics at the same ages.

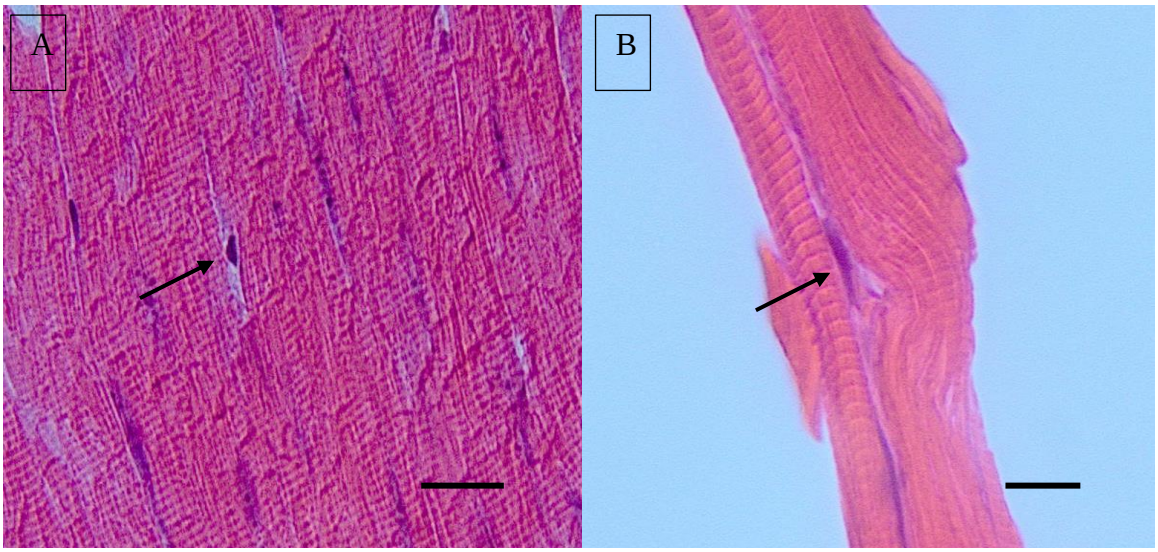

Figure 13. Longitudinal muscle sections from Lake Sturgeon

Longitudinal sections of muscle cut from a 1MPH (A) and 6 MPH (B) Lake Sturgeon and stained with haematoxylin and eosin viewed at 40x objective lens. The scale bars are representative of 10 µm. The nuclei are stained purple and the myofibers are stained pink. Due to their location adjacent the myofiber, the nuclei indicated by the arrows could be possible SCs. At this magnification the sarcomeres are visible within the fiber.

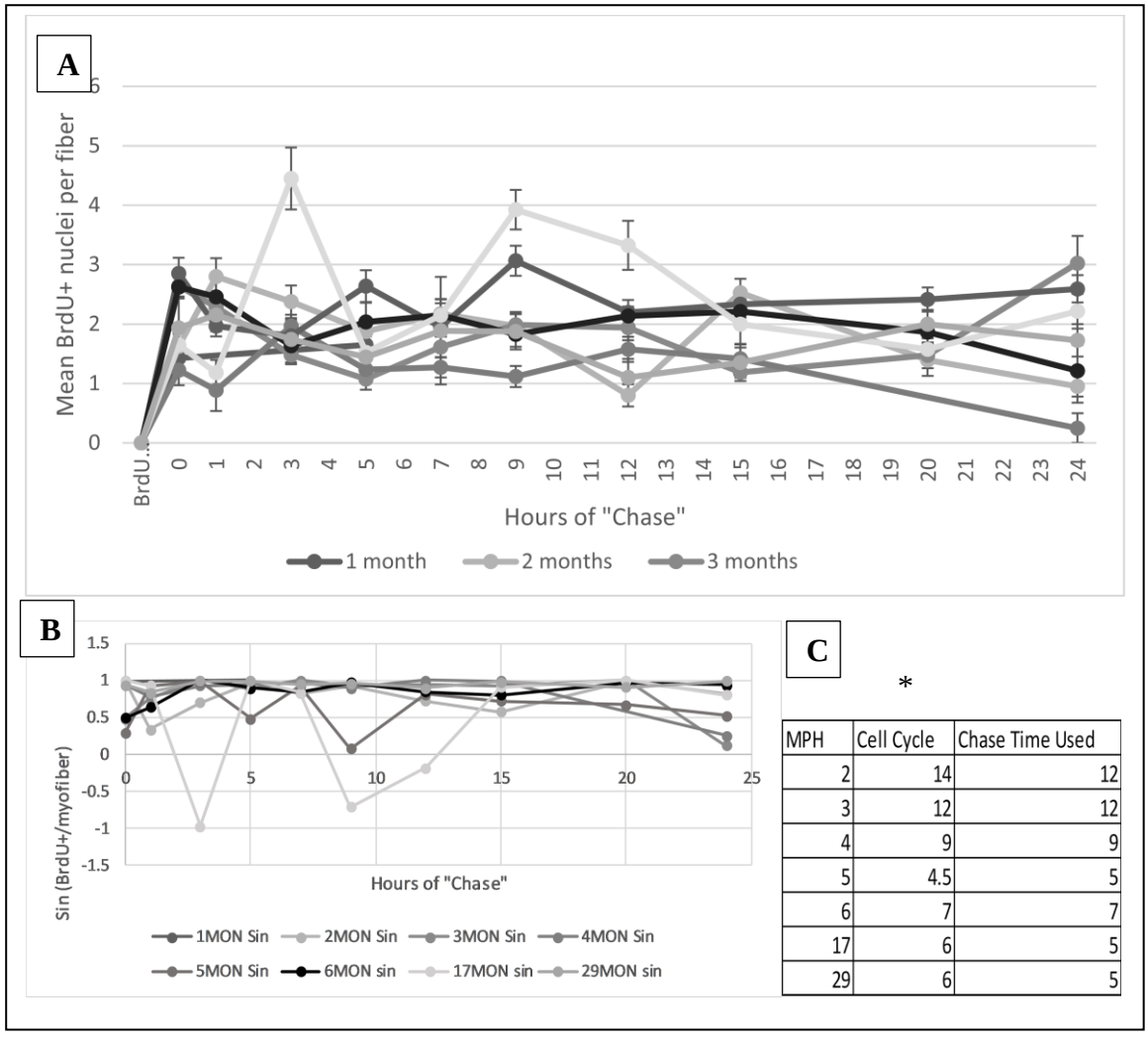

MPH	Cell Cycle	Chase Time Used
2	14	12
3	12	12
4	9	9
5	4.5	5
6	7	7
17	6	5
29	6	5

Figure 14. SC cell cycle changes as age increases

A pulse-chase experiment was conducted where the isolated fibers were incubated in a solution containing BrdU for 2 hours (the "Pulse"), then a medium without BrdU for up to 24 hours (the "Chase"). During the chase, fibers were fixed at various time points to study the state of their SCs as time progressed. The time points chosen were 0,1,3,5,7,9,12,15,20 and 24 hours. The number of BrdU+ nuclei per fiber was counted on the fixed fibers at each time point and those values were plotted against time (A). This gave a sinusoidal-type pattern in the graph of BrdU+ nuclei for each age of fish, shown by the flattening of the line when sin (BrdU+ nuclei per fiber) was plotted against chase time (B). The time between peaks in each graph in A was used to represent cell-cycle time (C). There was a statistical difference in cell-cycle time among different age groups (as indicated by *, one sample t-test, $p < 0.01$).

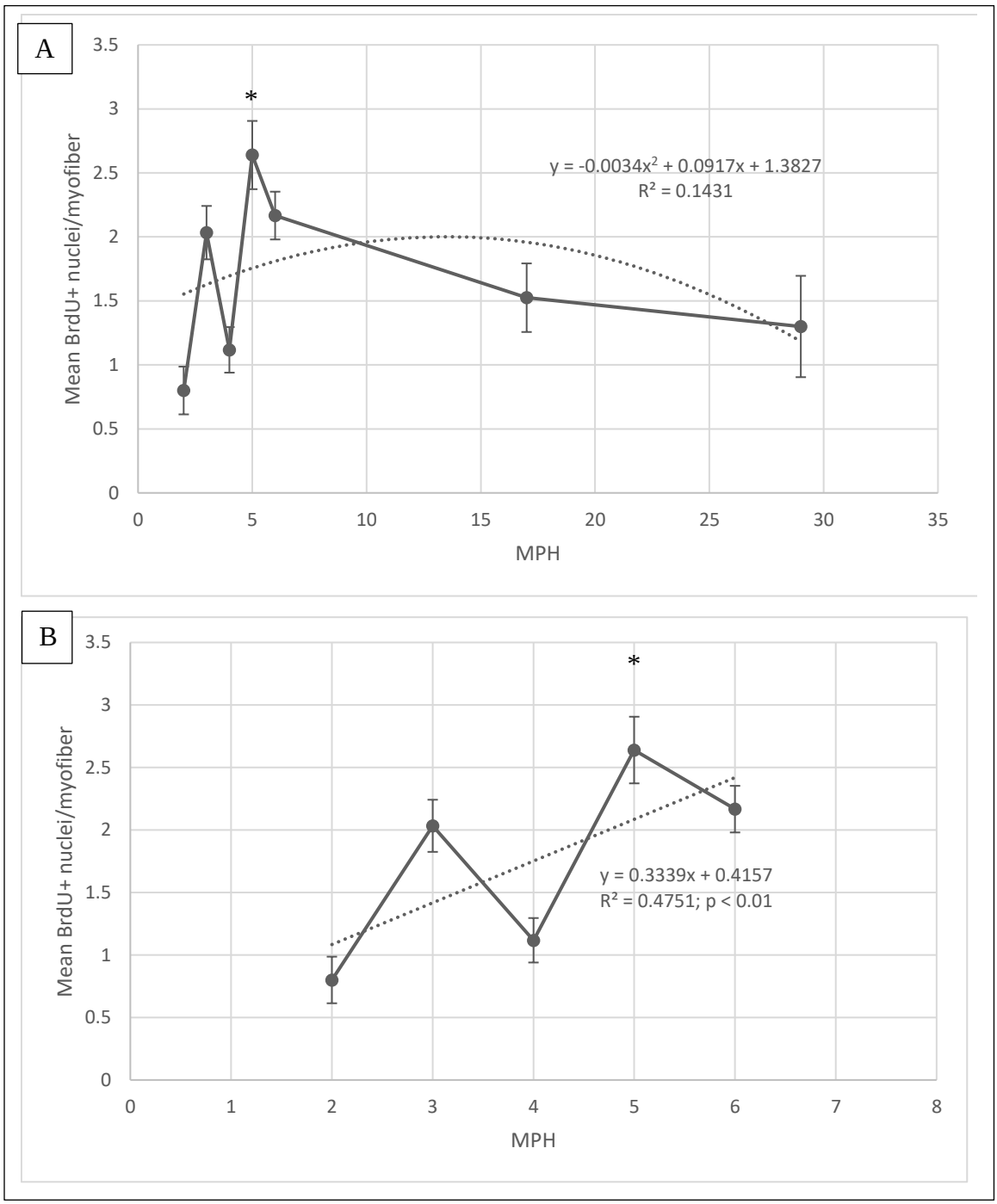
A
Mean BrdU+ nuclei/myofiber
MPH
y = -0.0034x² + 0.0917x + 1.3827
R² = 0.1431
*
B
Mean BrdU+ nuclei/myofiber
MPH
y = 0.3339x + 0.4157
R² = 0.4751; p < 0.01
*

Figure 15. Populations of dividing (BrdU+) SCs

The populations of dividing SCs was determined detecting BrdU uptake using the HRP-DAB staining method. Counts of DAB-positive nuclei were completed using a light microscope and a 40x objective (2 MPH, n = 20; 3 MPH, n = 60; 4 MPH, n = 34; 5 MPH, n = 61; 6 MPH, n = 72; 17 MPH, n = 40; 29 MPH, n = 10). There was a significant difference overall (ANOVA, $p < 0.01$) in the number of BrdU+ nuclei/myofiber at different months post-hatch (A). There was a significant increase in the BrdU+ SC population per myofiber from 4 MPH to 5 MPH (as indicated by *, t-test $p < 0.05$), and there was no significant change in BrdU+ SCs/myofiber between any two age groups 5 MPH or higher. These findings did not fit a linear or polynomial regression well, as there was a low negative correlation ($r = -0.185$, non-significant), and a linear R^2 value of only 0.034 (non-significant, $p > 0.05$). The 17 and 29 MPH data points were removed to observe what was occurring from 2 to 6 MPH (B), and although there is variability between ages, a positive linear trend is still observed with an R^2 value of 0.4571 ($p < 0.01$).

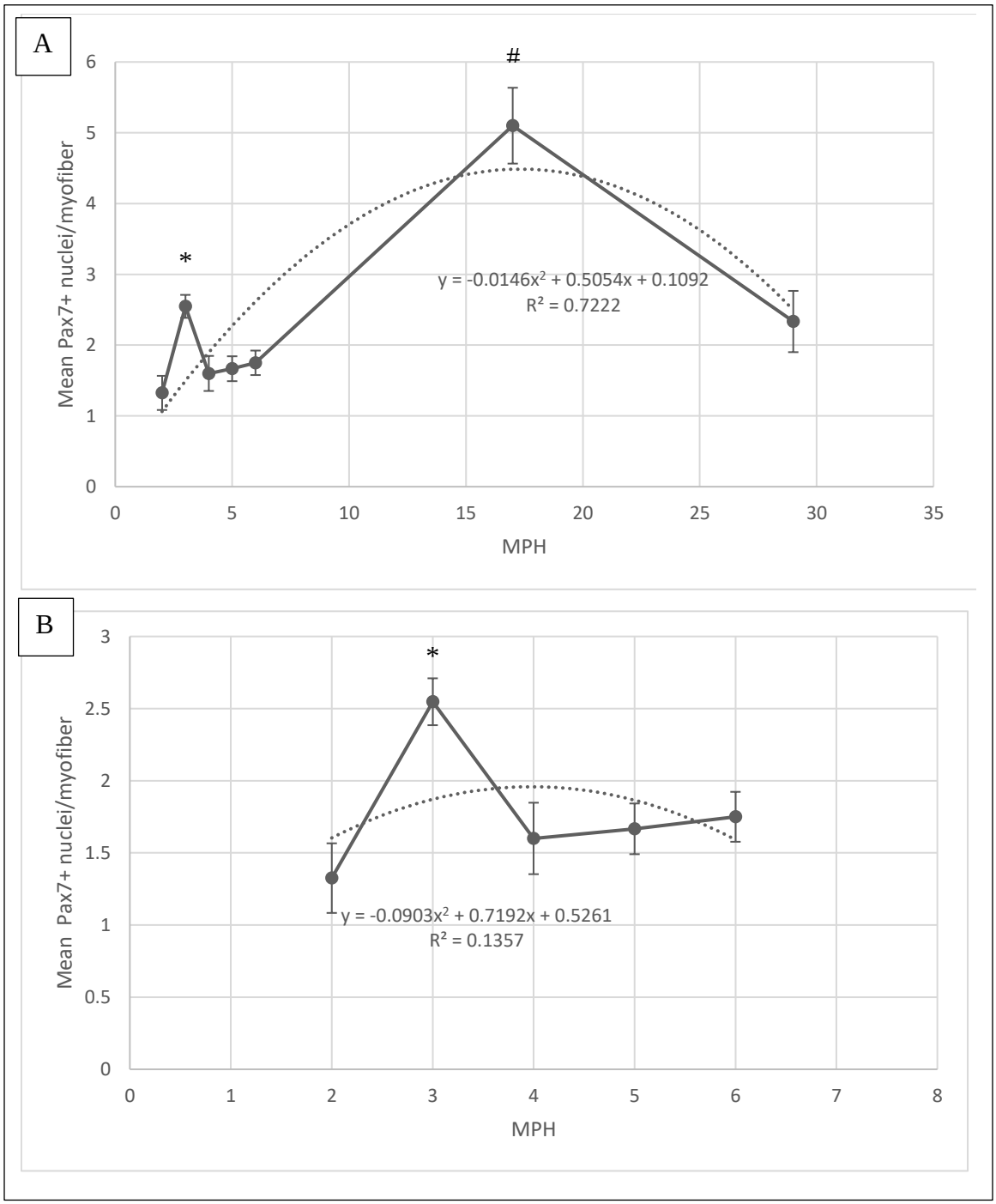
A
Mean Pax7+ nuclei/myofiber
MPH
y = -0.0146x² + 0.5054x + 0.1092
R² = 0.7222
*
#
B
Mean Pax7+ nuclei/myofiber
MPH
y = -0.0903x² + 0.7192x + 0.5261
R² = 0.1357
*

Figure 16. Populations of Pax7+ SCs

The population of Pax7+ SCs was determined on fibers from each age by using HRP-DAB detection of immunostaining for Pax7. Counts of DAB-positive nuclei were completed using a light microscope and a 40x objective lens to visualize fibers (Graph A; 2 MPH, n = 40; 3 MPH, n = 95; 4 MPH, n = 40; 5 MPH, n = 60; 6 MPH, n = 80; 17 MPH, n = 40; 29 MPH, n = 15). There was a significant difference overall (ANOVA, $p < 0.01$), though particular pairwise comparisons were only significant (t-test, $p < 0.01$) between ages 2 vs. 3 MPH (*), 3 vs. 4 MPH, 6 vs. 17 MPH (#) and 17 vs. 29 MPH (t-test, $p < 0.01$). Between 4 and 5 MPH and 5 and 6 MPH there was no significant change in the Pax7 population per myofiber ($p > 0.05$). These findings showed a significant polynomial regression ($R2=0.7272$, $p < 0.05$, as indicated on the graph) but did not fit a linear regression line well ([ow positive correlation ($r = 0.465$, non-significant), with a linear R^2 value of only 0.088 ($p < 0.05$)]. Since there was a large change at 17 MPH, the data up to 6 MPH was also graphed separately (B). There was a significant increase at 3 MPH in the population of Pax7+ SCs (indicated by *; t-test, $p < 0.01$). A polynomial regression showed an R^2 value of 0.1357

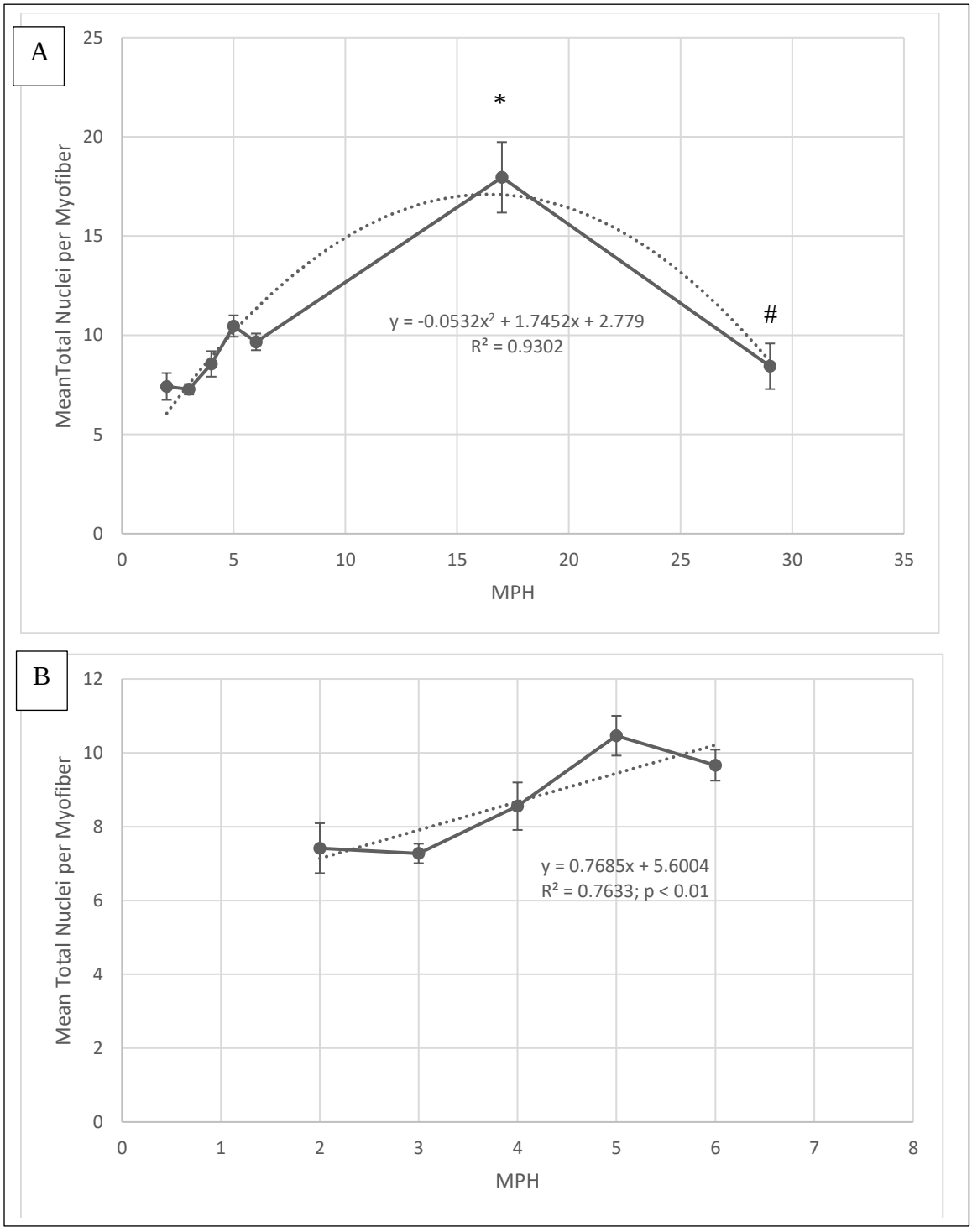
A
MeanTotal Nuclei per Myofiber
MPH
y = -0.0532x² + 1.7452x + 2.779
R² = 0.9302
*
#
B
Mean Total Nuclei per Myofiber
MPH
y = 0.7685x + 5.6004
R² = 0.7633; p < 0.01

Figure 17. Population of total nuclei versus fish age

The population of total nuclei (SC plus myonuclei) was plotted against age (MPH). In general, the graph shows a positive linear trend up to 17 MPH, then a decrease to 29 MPH (A). Overall, there was a significant increase in total nuclei per myofiber with increasing age (ANOVA, asterisk (*) indicates $p < 0.01$), with a significant decrease at 29 MPH (ANOVA, # indicates $p < 0.01$). Since there was such a change at the older ages (17 and 29 MPH), the data for total nuclei was graphed for 2 to 6 MPH only (B). Removing the older ages showed a statistically significant linear increase in nuclei populations as the fish age with an R^2 value of 0.7633 ($p < 0.01$).

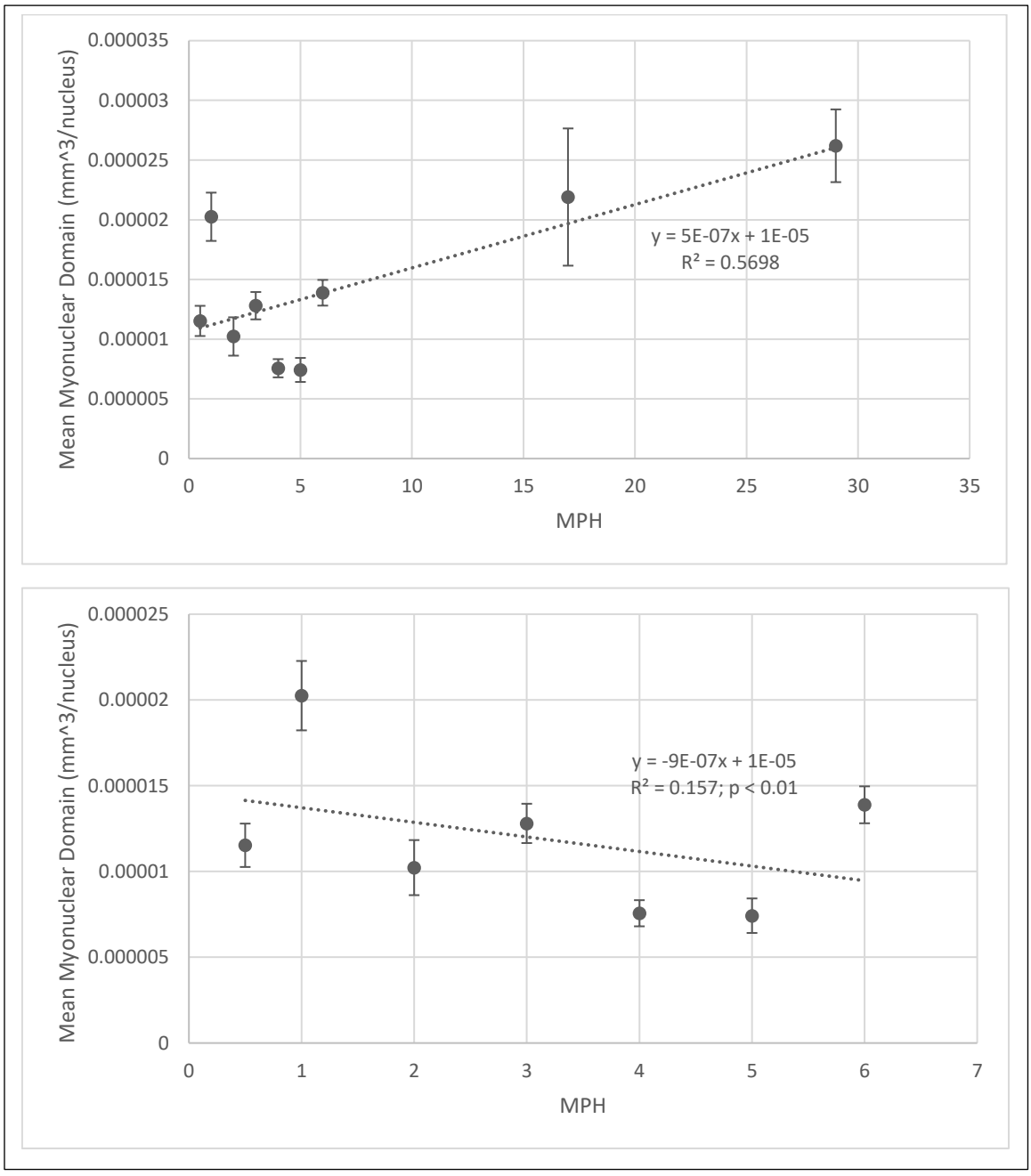
Mean Myonuclear Domain (mm^3/nucleus)
0.000035
0.00003
0.000025
0.00002
0.000015
0.00001
0.000005
0
0
5
10
15
20
25
30
35
MPH
y = 5E-07x + 1E-05
R² = 0.5698
Mean Myonuclear Domain (mm^3/nucleus)
0.000025
0.00002
0.000015
0.00001
0.000005
0
0
1
2
3
4
5
6
7
MPH
y = -9E-07x + 1E-05
R² = 0.157; p < 0.01

Figure 18. Myonuclear domain with increasing age

Scatterplot of the myonuclear domain of Lake Sturgeon myofibers by age (0.5, 1, 2, 3, 4, 5, 6, 17, and 29 MPH; df = 8). Myonuclear domain, or the amount of sarcoplasm regulated by a single nucleus, was determined by taking the calculated volume of a fiber (π*(width/2)^2*length) and dividing by the number of nuclei in that fiber. The domain volume was averaged from 40 fibers at each age group. There was a low correlation between myonuclear domain and age, with a Pearson correlation of 0.329 with an R^2 value of 0.5698 ($p < 0.05$). Since there was such a change at the older ages (17 and 29 MPH), the data for myonuclear domain was graphed for 2 to 6 MPH only (B). Removing the older ages showed a statistically significant linear decrease in myonuclear domain as the fish age with an R^2 value of 0.157 ($p < 0.01$).

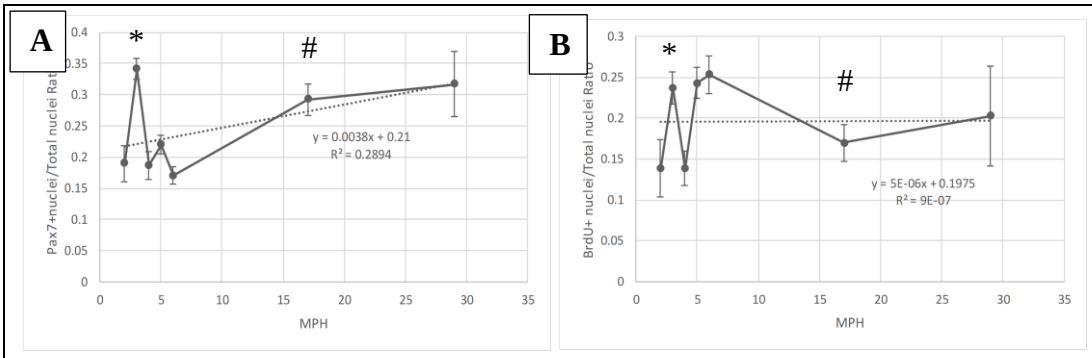

Figure 19. Ratio of satellite cells (by lineage and by proliferative status) to total nuclei/myofiber with increasing age.

The ratio of all satellite cells (Pax7+ SC nuclei) to total nuclei (A) and dividing satellite cells (BrdU+ SC nuclei) to total nuclei (B) plotted against age (months post hatch, MPH). Ratios were calculated by taking the number of DAB+ SC nuclei (Pax7 or BrdU, respectively) and dividing by the total number of nuclei in the same fiber. The ratios were then averaged for each age group and plotted. Overall, there was a significant difference in the Pax7+/total myonucleus ratio (ANOVA, $p < 0.01$). Though there was no significant difference between the ages of 4 and 5 MPH, or between 17 and 29 MPH ($p > 0.05$), there was statistical difference between all other pairs of age groups ($p < 0.05$). For results shown in B, there was an overall significant difference in the BrdU+/myonucleus ratio (ANOVA, $p < 0.01$). Though there is no significant difference between the ages of 5 and 6 MPH, as well as 17 and 29 MPH ($p > 0.05$), there is statistical difference between all other age-group pairs ($p < 0.05$). The * indicates the statistical differences between 2 and 3 MPH, and # indicates the statistical difference between 6 and 17 MPH in both lineage and proliferative SCs.

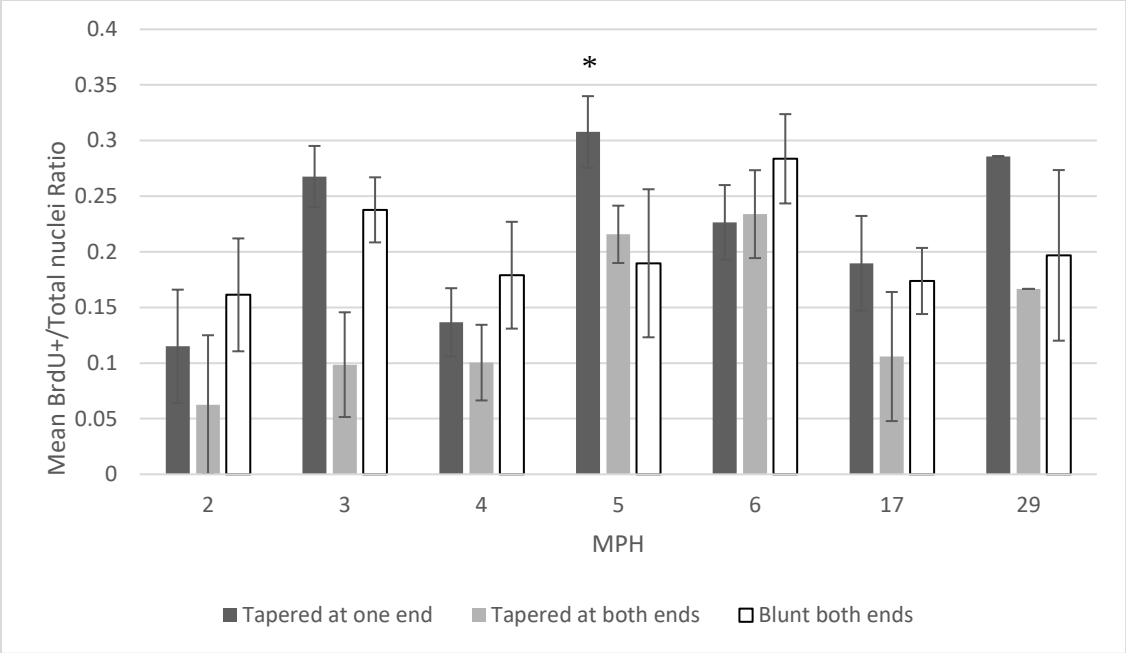

Figure 20. The ratio of dividing SCs to total nuclei plotted with respect to myofiber terminal characteristics

Bar graph of the mean ratio of dividing (BrdU+) SCs to total myonuclei plotted against fish age with respect to myofiber-terminal characteristics. Namely, the mean ratio was plotted for fibers with one tapered end, with two tapered ends and with both blunt ends for each age group (2 MPH, n = 19; 3 MPH, n = 60; 4 MPH, n = 34; 5 MPH, n = 61; 6 MPH, n = 72; 17 MPH, n = 27; 29 MPH, n = 10). There was only a statistical difference in proliferative SC/total myonuclei at 5 MPH (as indicated by *, ANOVA, $p < 0.05$); there were no differences seen at any other age (ANOVA, $p > 0.05$). Between different age groups, the fibers tapered at one end and the fibers tapered at both ends showed overall significant differences in their ratio of BrdU+/total nuclei across ages (ANOVA, $p < 0.01$ and $p < 0.05$ respectfully); there was no statistical difference in the ratio of BrdU+/myonuclei between ages for the fibers that were blunted at both ends ($p > 0.05$).

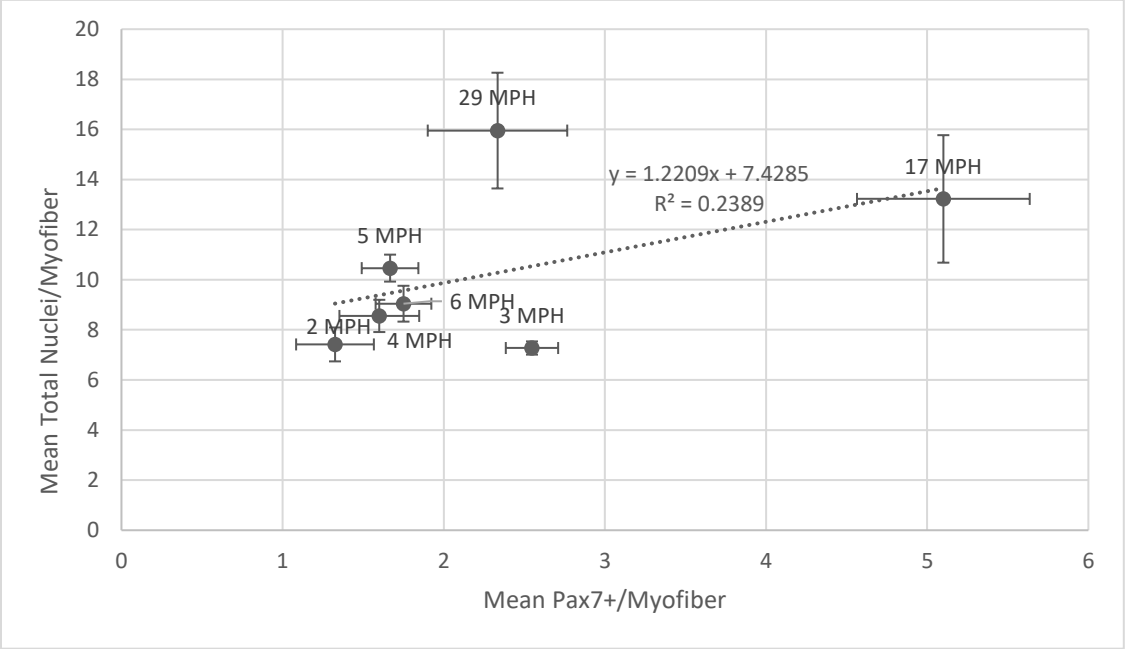

Figure 21. Linear regression of the total nuclei per myofiber and the number of Pax7+ SCs per myofiber

Scatterplot and regression of the total nuclei per myofiber (Pax7+ SCs and myonuclei) and the number of SCs (Pax7+) per myofiber. These values were determined from counts of different parameters on the same fibers and averaged for each age group. The regression was not significant, as there was a moderate Pearson correlation coefficient (r) of 0.489 ($p > 0.05$), and an adjusted R^2 of only 0.087 (non-significant).

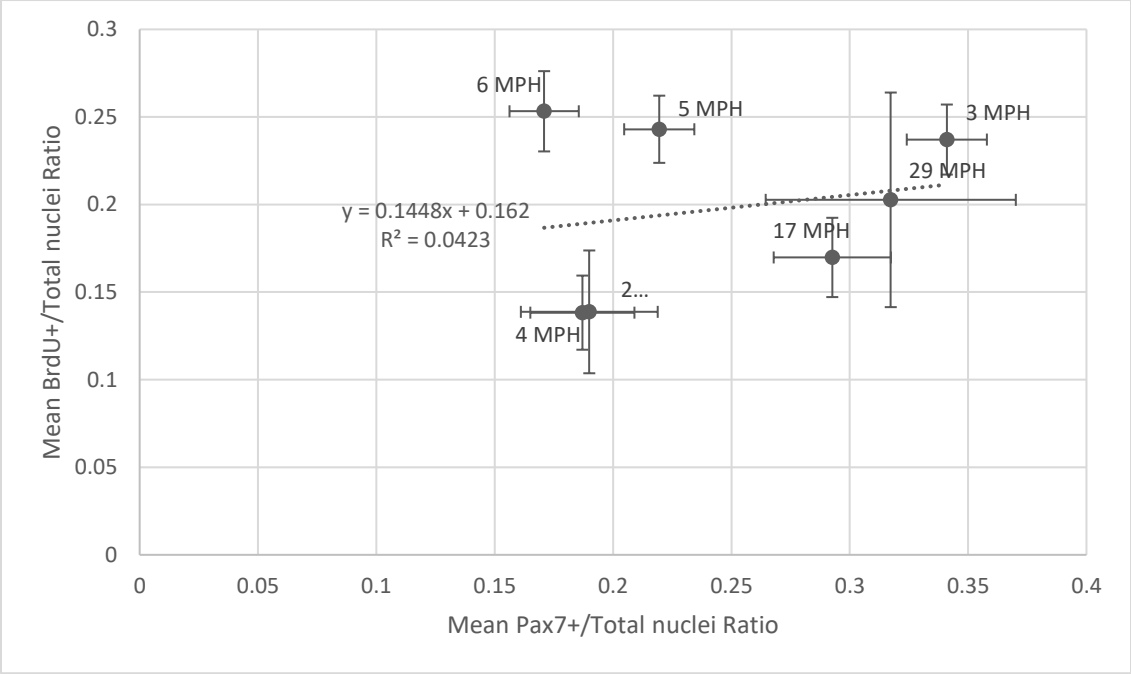

Figure 22. Linear regression between the ratio of proliferative BrdU+ SC nuclei to total nuclei and the ratio of Pax7+ SC nuclei to total myonuclei

Scatterplot denoting the linear regression between the ratio of dividing SCs to total nuclei and the ratio of Pax7+ SCs to total nuclei. Ratios were determined by dividing the number of BrdU+ and total nuclei or Pax7+ nuclei and total nuclei (total nuclei included SCs and myonuclei). The Pax7+ SCs and BrdU+ SCs were counted from immunostaining of fibers isolated from the same pool of fibers at each age, but fibers were only stained for one of BrdU uptake or Pax7. This regression was not significant and had a very small R^2 value of -0.149 (non-significant), and a low correlation, with a Pearson correlation coefficient (r) of only 0.206 (non-significant).

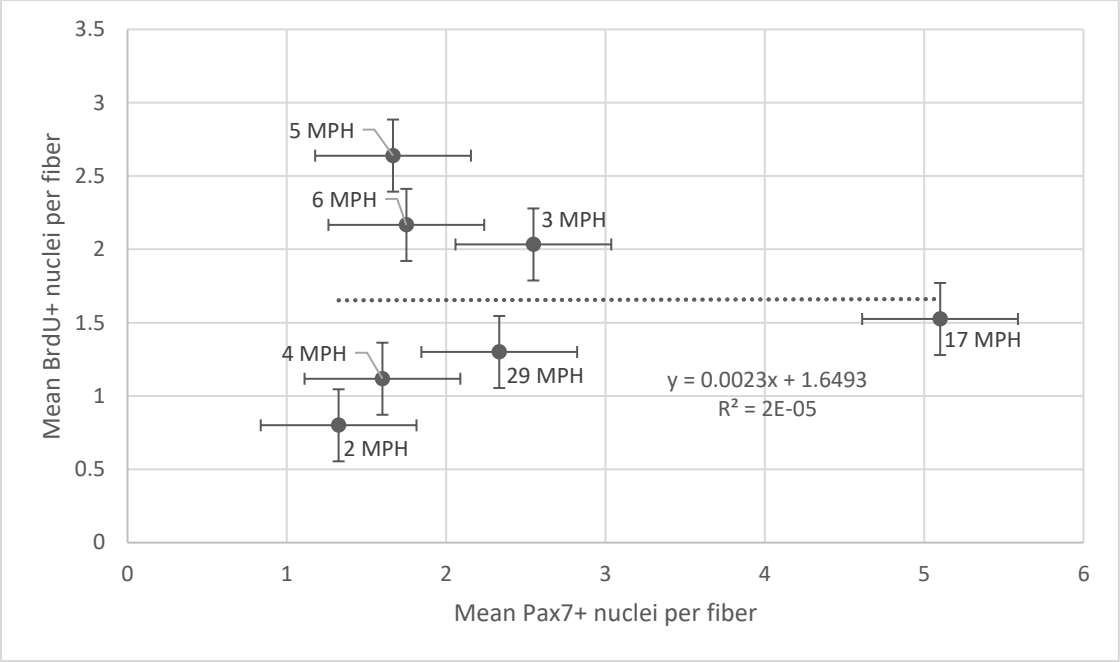

Figure 23. Linear regression between the mean number of dividing (BrdU+) SCs and the mean number of total (Pax7+) SCs per fiber

Scatterplot denoting the regression between the mean number of dividing SCs per myofiber (BrdU+ SC nuclei) and the mean number of SCs per myofiber (Pax7+ SC nuclei) on different fibers, although at each age (months post hatch, MPH), the fibers were aliquoted from the same pool of isolated fibers. The correlation between these two variables is negligible and not significant, with a Pearson correlation coefficient (r) of 0.072 (non-significant), and an adjusted R^2 value of -0.194 (non-significant).

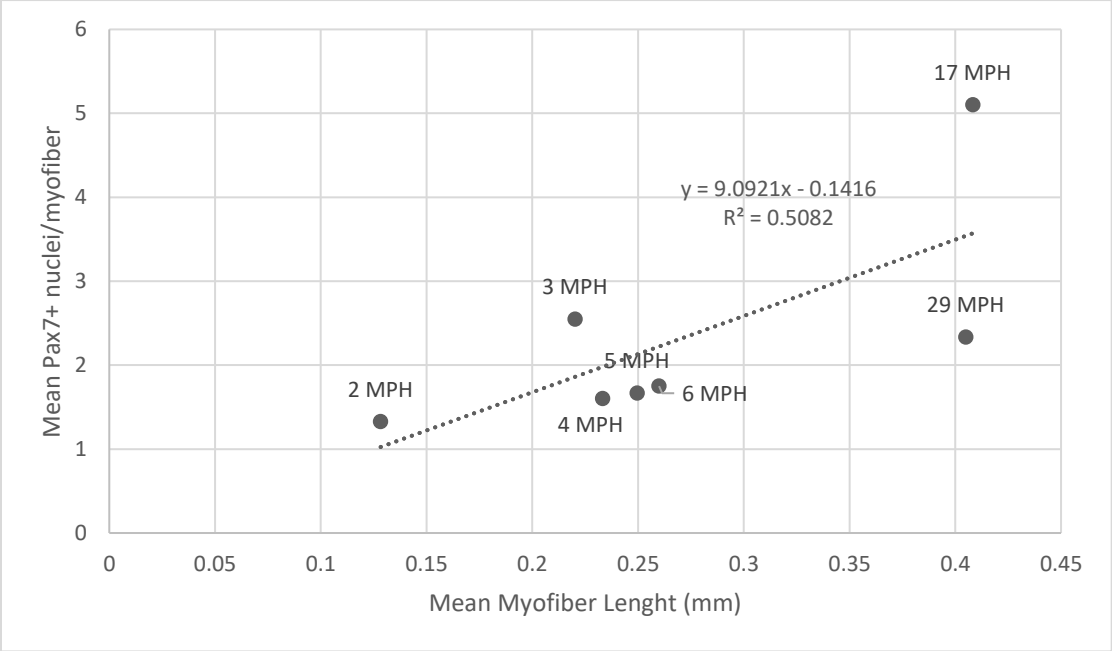

Figure 24. Linear regression between the mean number of Pax7 SCs and the mean myofiber length

Scatterplot denoting the regression between the mean number of SCs (Pax7) per myofiber and the mean length of different fibers, although at each age (months post hatch, MPH), the fibers were aliquoted from the same pool of isolated fibers. The correlation between these two variables is high, with a Pearson correlation coefficient (r) of 0.713 (non-significant), and an adjusted R^2 value of 0.410 (non-significant).

Chapter 4: Discussion

This project sought to describe the developmental process in the juvenile Lake Sturgeon, by determining the extent of satellite cell proliferation and incorporation into the muscle fiber via single -fiber isolation. It is crucial to determine the natural growth patterns of endangered species like the Lake Sturgeon, to assist in developing methods for optimal conservation and re-stocking programs. The results of this study will also increase our understanding of how evolutionarily older species, such as the Lake Sturgeon and the lamprey, are related to one another and to other, evolutionarily younger species, like teleosts, from a developmental perspective. With new findings coming out on lamprey and zebrafish muscle development, this study can contribute to muscle development interpretations in an evolutionary context (Zhang & Anderson, 2014; Anderson, Cunha and Docker, submitted, personal communication).

Lake sturgeon are very armoured fish which aids in protection against predators, though this armouring is not greatly required in captivity. The fish that were used in this study were sampled from tanks in the University of Manitoba facility, and it was noticeable that the scutes, or the boney-plated armouring, was developed in the 17 MPH, but not in the 6 MPH fish. The lack of predators brings about lower physical activity and a decrease in the physiological need to develop armouring. These could both contribute to differences between the muscle development of wild and captive juvenile Lake Sturgeon.

In the wild there are also several other additional variables that could contribute to changes in muscle characteristics over time. There are seasonal variations in the climates where Lake Sturgeon are found, resulting in changes in temperature, feeding, predation

and subsequent swimming activity. In the colder winter months there could be a possible loss to fiber diameter due to inactivity from lowered predation and temperature. These variables seen in wild environments may influence the growth patterns in muscle fibers and consequently the whole fish, but may not be seen in captive fish.

Fibers were isolated from Lake Sturgeon from 0.5 to 29 months post-hatch (MPH) and plated in single fiber culture for 24 hours. Following a pulse-chase experiment, fibers were stained Pax7 and BrdU, and the positively stained SCs counted. Since the muscle of many species of teleost grows by both hypertrophy (increases in muscle fiber size) and fiber hyperplasia (increases in the number of muscle fibers), the goal of this project was also to determine if Lake Sturgeon muscle developed similarly and determine chronological changes in the pattern of those two aspects of growth as the fish aged. Although the term "fiber hyperplasia" is problematic since the fibers themselves do not actually divide and multiply, and it's actually the addition of new fibers by the division of SCs and the fusion of myogenic myoblast daughter cells, this term will be used to describe the addition of new fibers by that process.

The overarching hypotheses were that the Lake Sturgeon muscle would grow by utilizing both hypertrophy and myofiber hyperplasia and that the cell cycle of the SCs would increase in duration as the fish aged; specifically, we hypothesized that with age, nuclei would be added to the myofibers, the domain of those myofibers would increase and the cell cycle of the resident satellite cells would increase in duration. Results were used to determine the rate of SC proliferation in the developing Lake Sturgeon as this is not a well-researched topic. Muscle growth is so critical to survival, and the information acquired from this study adds to our knowledge of the SC contributions and muscle growth

in the endangered Lake Sturgeon. This investigation provided evidence that the Lake Sturgeon myofiber anatomy changes and the SCs have a cell cycle that changes and gets shorter as development continues.

4.1 SC Cell-Cycle Variations

A classic pulse-chase experiment was used to identify the cells that incorporated BrdU, and therefore were proliferating; those cells were tracked in their proliferative state along isolated myofibers as time progressed from 0-24 hours of chase in each experiment. It was expected that there would be a certain number of SCs that were proliferating at the time of BrdU incubation, that SCs would incorporate the BrdU into their DNA and therefore be visible when stained. Those cells would then completely divide, resulting in two daughter cells that would stain positive for BrdU. This progressive step in SC hyperplasia would cause a direct doubling in the numbers of positively stained BrdU nuclei. This was not seen in the experiments that were conducted; as seen in figure 14, there were peaks and troughs observed with the pulse-chase experiment at each age group, and not the 'doubling' that was expected.

In prior experiments where continuous incubation or intermittent infusion with BrdU was used, a linear slope was produced when the number of BrdU+ cells was graphed against time until it reached a plateau, when presumably all activated SCs were labelled (Bower & Johnston, 2010; Nowakowski, et al., 1989). This experiment produced a slight variation in those continuous and long-term intermittent pulse-chase experiments, and since there was no additional BrdU in the media following the 2-hour incubation time in our experiment, the second peak is thought to be the condensed chromatin of the daughter cells from the first division.

Another explanation for the trend in the number of BrdU+ nuclei that was seen across all ages could have been due to some of the SCs being slower to proliferate than others. Specifically, that during the incubation period, all of the SCs that were proliferating at the time took up the BrdU, but a subpopulation proliferated slower and thus were preserving the SC lineage longer. This was described in a study by Schultz (1996) where rat muscle SCs were divided into two different subdivisions. "Producer" SCs constituted 80% of the total SC population, and were responsible for providing myogenic myoblasts that fuse to fibers, whereas "reserve" SCs were thought to be responsible for replenishing the SC populations and made up 20% of the total population (Schultz, 1996). These reserve cells, which divided much slower than the producer cells, were not completely labelled after 14 days of BrdU infusion, compared with the 32-hour cell cycle time that was determined for the producer SCs (Schultz, 1996).

It is interesting that the BrdU+ values did not continue to increase over time as is seen in other labelling studies (Bower & Johnston, 2010; Nowakowski et al., 1989). Even if only some of the cells were labelled, there should have still been a noticeable increase in the number of cells staining positive for BrdU, as the cells continue to proliferate. This was not the case, as after some time the population of BrdU+ nuclei decreased, then increased a second time. This decrease in BrdU+ nuclei after a proliferation event could have been due to a "quenching" of the BrdU levels, causing the level of DAB to not be up to the DAB-positive intensity used as the reference standard in the counts, and therefore wasn't counted. That could account for the number of BrdU+ having a peak when the SCs incorporated the BrdU, and a trough when most of them had divided, suggesting that the daughter cells weren't mitotic or were not positive enough to be included in the population

counts. Since the peaks were thought to be observed when the majority of proliferating SCs at that time were in mitosis, the time between peaks was determined to be a cell cycle.

There was variation in the number of BrdU+ nuclei observed between time points at one age, but there were also variations seen in the cell-cycle times among ages. When the graphs of populations of BrdU over time (pulse-chase) was observed, the cell-cycle times were determined to be 14, 12, 9, 4.5, 7, 6, and 6 hours for the ages 2, 3, 4, 5, 6, 17, and 29 MPH, respectively by measuring the average period cycle. These periods, as seen in figure 14, were noticeably, but also statistically decreasing as age increased. Since this data showed a trend of decreasing cell-cycle time as age increases, the hypothesis that the cell-cycle time would increase with age was rejected. This is different from the study done by Seigel et al. (2011) on adult mice (aged 80 to 130 days), where the average cell cycle was determined to be approximately 10 hours for the majority of daughter cells (Siegel, et al., 2011). The cell cycles that we determined in the juvenile Lake Sturgeon in our experiment were also all much shorter than the cell cycles of SCs observed in Atlantic salmon of 28.1 hours (Bower & Johnston, 2010). The difference and variability seen between the results of this study and previous studies on mice and salmon could be due to the nature of muscle growth in mammals versus fish, or evidence of one of the differences between determinate and indeterminate growth, respectively.

Previously described by Biga and Goetz (2006) when looking at giant Danio versus zebrafish, fish that increase size very rapidly and that grow to be very large in size increase in fiber size and fiber number faster than smaller, determinate growing fish (Biga & Goetz, 2006). Since the fibers would have to grow quicker in order to keep up with the continued growth rate of a much larger body size, the SCs would need to proliferate quicker, as that

is one of the ways in which the myofibers increase in size. Since the rate of body length growth was linear, as seen in figure 2A, the length of the fibers would grow at the same rate with age, but total fish weight increased in a polynomial fashion. Though this weight includes the full fish, and not just the muscle tissue, this could indicate that the number of fibers would need to increase, since the myofiber width also does not change with age.

The pattern of proliferation was demonstrated to be cyclical in nature by graphing the sine function of the BrdU+ populations of each age across time. If there was a single cycle within the graph, the curve would flatten out when the sine function was plotted. This was the case for most ages, though with 5 and 17 MPH, there was still a curve within the graph of the sine function that was plotted. This is thought to be due to more than one cycle present within the data for those age groups, as would be the case if the SCs were in synchrony as subsets on the population of fibers; the synchrony would be just enough to result in two or more noticeable cycles, but not so out of synchrony so as to abrogate a detectable cycle pattern.

4.2 Myofiber changes during development

Muscle fibers were isolated and combined from several fish at each age and subsequently plated and stained for markers of nuclei. Care was taken so that the fibers were not agitated to prevent the SCs becoming activated by physical means so they were only activated due to the natural timing of developmental activation. This allowed the rate of SC activation during development to be conserved and minimize the level of SC activation by the preparation protocol.

There was a great amount of heterogeneity amongst the fibers; under the microscope, several different shapes were observed. Some fibers were thin and long, while others were short and wider; any combination of those characteristics was also observed. Though there were different dimensions to the fibers, there was not an observable difference in characteristics between ages or within ages. It seemed to be quite random, without much of a trend observed in that aspect. As well as their size characteristics, the fibers did show differences in the characteristics of their termini, where they would attach to bone or connective tissue to exert force. There was a trend toward statistically more fibers at the younger and older ages that were blunted at both ends. By comparison, fish between the ages of 4 and 6 MPH had fibers that did not differ in the percentages of fibers with blunted or tapered ends.

In a study by Curzi et al. (2012), physically trained rats had several more tendon ends that developed finger-like projections connecting to muscle fibers allowing for increased contact area, which lessened the mechanical strain across the cell membrane (Curzi et al., 2012). The increase in mechanical strain caused morphological changes to the muscle-tendon junction (MTJ). Looking at the results of our investigation in Lake Sturgeon muscle development, the pointed terminals observed on a number of the myofibers could relate to the requirement to reduce strain on the muscle by increasing the surface area connected to the tendon.

It is possible that the fibers have a natural tendency to have blunt ends based on biophysical constraints, so when the ratio changes to show more tapered ends it could be indicative of MTJ strain. Though this strain is often thought to be due to muscular mechanical stretch and exercise, there is the potential that MTJ stress could also be

provoked by the addition of new myofibers, or hyperplasia. With this idea in mind, it could be proposed that at 4, 5, and 6 MPH there is an increase in the number of myofibers, with not much change in the fiber dimensions, as supported by results shown in figure 7.

This interpretation is also supported by the results of populations of proliferating SCs, as indicated by BrdU+ nuclei. At 5 MPH there is a large peak in the number of BrdU+ nuclei, showing that many SCs were actively proliferating at that age. The proliferating SCs could produce myogenic myoblast daughter cells that could incorporate into nearby existing fibers or fuse with other myogenic myoblasts to create new myofibers.

The number of nuclei within and around the fiber was counted at each age and was observed to significantly increase over time, then decrease at 29 MPH. As seen in figure 17 there was a positive linear trend observed in the number of nuclei with increasing age, with a peak at 17 MPH and a drop to 29 MPH. This is in accordance with the changes in myofiber length and volume, as they both increased with age. If the fibers increased in size, the growth could have come from the addition of nuclei and/or the increase in the myonuclear domain. At 29 MPH there could be a hyperplasic event, resulting in the increase in the number of new myofibers with low numbers of myonuclei, decreasing the average at that age. The average length of the myofibers is not statistically different between 17 and 29 MPH, but there is a large increase in the myonuclear domain, which could still allow for an interpretation of hyperplasia at 29 MPH. It seems to be the case that the growth occurred by both mechanisms of muscular growth (hypertrophy and hyperplasia), as there are peaks and troughs in myonuclear populations and variation in the myonuclear domain as well.

4.3 SC Population Variations

When the nuclei were stained for Pax7, the SC-specific marker chosen, there was not a definitive trend observed with age. When a trend line was applied to the plotted number of Pax7+ nuclei per myofiber as a function of age, it looked parabolic in nature with the peak of the line at 17 MPH. The increases in SCs surrounding the examined myofibers seen at 3 MPH could come from an increase in myogenic myoblast daughter cells, as indicated by the parallel increase in BrdU+ nuclei at the same age. At 17 MPH though, the BrdU+ nuclei are decreasing from the levels at earlier ages, so the increase in SC could have come from the migration of SC daughter cells from other fibers, or it is possible that there was a large proliferation event immediately prior to the sample collection. It is important to note as well, that the nuclei that stain positively for Pax7 could be quiescent SC and aren't necessarily activated SCs.

While investigating carp, Koumans et al. (1991) determined the populations of myosatellite cells to be consistent during growth and increasing myofiber length (Koumans, et al., 1991). This was different from what was evaluated from this study, as with increasing length, the number of Pax7+ nuclei per myofiber appeared to increase as well, though this trend was not significant (figure 24). This increasing population of myosatellite cells could be a result of the rapid growth that naturally occurs in the Lake Sturgeon and the requirement for the satellite cells to be available for growth consistently.

4.4 Regressions

A few regressions were completed to determine if there were correlations between different variables collected from the study. Though many of the regressions showed no statistical significance, it is still meaningful to take note of these findings, as they may suggest areas for further experimentation and help clarify the context of the study and direct inferences from the results that help interpretation of the findings. There is still scientific value in understanding a non-significant relationship, even if statistically it is not significant. It was expected that there would be a relationship between the length of the myofiber and the number of Pax7+ SC, as seen in carp by Koumans et al. (1991). This was not the case seen in this study, as there was not a strong correlation between those variables (figure 24). This area would be a good to explore in a bit more detail, such as the relationship of Pax7+ SCs to myofiber length within different fiber types, to confirm the findings of this study.

There was an expectation that the values of Pax7+ SC and the proliferating SCs would be correlated at any given age, though this was not what was observed (figure 22 and 23). Though the ratios of Pax7+/total nuclei and BrdU+/total nuclei as well as the raw numbers of BrdU+ and Pax7+ nuclei per myofiber showed no correlation, it may have been because the stains were completed on different sets of fibers (figure 22 and 23 respectively). If a double stain for Pax7 and BrdU had been done on the same sets of fibers, these data (Pax7+ SCs and BrdU+ SCs) could be directly compared, and the regression of those data may have looked different. Unfortunately, due to technical issues, the double stain could not be accomplished for this experiment; it would be good to be able to compare the Pax7+ and BrdU+ nuclei on the same fibers in the future. The possible relationship

between Pax7+ SCs and BrdU+ dividing SCs, with more data being added from additional future studies, is an important direction of further exploration.

4.5 Limitations and Future Directions

To make a more complete study of the muscle development in juvenile Lake Sturgeon, there are several more avenues of research to explore in future. Now that a general view of muscle development with respect to SCs has been achieved, SC activation, cycling, and pre- and post-natal muscle development should be examined in detail. It was assumed that given the location that the fibers were extracted from, and the method of dissection, that this experiment used fast type II, white muscle fibers. Although Schultz (1996) determined there was no difference in SC cell-cycle time between fast and slow muscle fibers in rat muscle, it would be interesting to assess differences in SC populations, activity and cycle time between the muscle types and with fiber size in the Lake Sturgeon.

The use of isolated and cultured fibers was ideal for this study, as it allowed the SCs to be observed in their natural position adjacent to the myofiber, and allowed enough space between fibers that SC could be recognized. If sections were used instead, the fibers would be packed too densely together, and it would be difficult to resolve the SCs as distinct from other proliferating non-myogenic cells in the interstitium without considerable additional immunostaining (SCs located between layers of laminin in ECM and dystrophin in the fiber-membrane cytoskeleton. In sections, the counts could not assess total numbers of myonuclei and labelled SCs per fiber without a huge amount of additional work involving serial sectioning. In previous research, viewing the myotome and other body structures such as the notochord, spinal cord and nerves in histological sections during Sturgeon development was modeled, though single muscle fibers and SCs are easier

viewed when isolated (Steinbacher et al., 2006). Another area of future study would be to see if there are differences in myofiber characteristics between sections and isolated fibers. Although sections are not ideal for looking at SCs, it would be useful to see which method would be easier or more accurate for characterizing fiber attributes, such as length, width, volume and myonuclear domain during growth.

Future research should examine SC activity in the ages between 6 and 17 MPH to get a more detailed idea of the period that was not examined in this study. As stated previously, there could have been a proliferation event or fiber growth (e.g., with hyperplasia and/or hypertrophy) that was not apparent, given the ages that were investigated. If experiments were conducted more frequently during the juvenile stage, a more thorough description of the developmental process could be achieved.

The results of this experiment give an understanding of the characterization of muscle growth and satellite cell populations as the Lake Sturgeon develop. Additional research to add on to this understanding would include: determining if the volume of sarcoplasm surrounding the myonuclei is uniform, look at the effect of caloric intake on muscle development, and examine the differences in SC morphology, contribution and activation between fast and slow muscle fibers. In this investigation, the myonuclear domain, as calculated by taking the volume divided by the number of total associated nuclei, was determined to increase with increasing age. Since Bruusgaard et al. (2006) determined that the distribution of myonuclei is not random, and that the distance between the nuclei in mammals is influenced by their so-called repulsive properties towards each other and works to minimize long distance travel of molecules, speculation would dictate it may be similar in fish (Bruusgaard et al, 2006). The method in which the domain was

calculated does not give any detail as to the homogeneity of the distance between nuclei, and it was assumed that it was equal, but that should be investigated further.

Salmon that had calorie-restrictive diets were shown to produce fewer myofibers, but had fibers with larger diameters than their satiated counterparts (Johnston, et al., 2014). Considering the possibility of restrictive diets in the cold, Manitoba winter, it would be interesting to investigate how both temperature and food availability affect growth and metabolism (Belghit, et al., 2014; Sfakianakis, et al., 2012).

The most interesting results were that the myofiber length had a very high correlation to the total fish length with a Pearson correlation coefficient (r) of 0.917 and an adjusted R^2 value of 0.818 ($p < 0.01$; figure 9). The other results that were interesting were that the SC cell cycle time significantly decreased as the fish aged ($p < 0.01$; figure 14C).

In most of the graphs, there was a large change from the 6 MPH to 17 and 29 MPH data, and the older ages had a high influence on the weight of the results. Because there was such an observed difference in data between the older (17 and 29 MPH) and younger (0.5 to 6 MPH) fish, future studies should directly consider the younger (< 1 year) and older (> 1 year) age groups separately. In future, more age-groups should be scrutinized to confirm the jump in data between the ages, as well as to determine where between 6 and 17 MPH there is a jump in development. Further research should look at the older and younger age groups separate from each other to determine more precise trends observed.

4.6 Significance

Lake Sturgeon *(Acipencer fulvescens*) are an evolutionarily and ecologically important species. Increasing our knowledge of their development could be a

big step in decreasing their rate of extinction in waterways, especially for some that are particularly prone to hydroelectric development.

The hypothesis that the cell cycle of the Lake Sturgeon SCs would increase in duration as the fish aged was rejected. The data showed that the SC cell cycle decreased in duration as the fish aged with only slight variation. The hypothesis that the domain of the myofibers would increase with increasing age was not rejected. There was a general trend observed that the myonuclear domain increased with increasing fish age, though variability was very high, and so the data was not conclusive. The final hypothesis, that the satellite cell to myonuclear ratio would decrease with increasing fish age was rejected. Over the course of the study, the Pax7+ SC to myonuclear ratio increased, dropped to a trough, then increased again gradually. If viewed in a small time-frame, this ratio could be observed to be increasing or decreasing. Since this ratio changes over time, and does not have a distinct trend from 0.5 to 29 MPH, this hypothesis was rejected.

The novel finings of this study include a) the decreasing duration of the SC cell cycle with increasing age of the juvenile fish, and b) the patterns of SC proliferation in relation to myofiber hypertrophy and changes in myonuclear domain. With these new insights into the natural developmental characteristics of muscle fibers in growing Lake Sturgeon, further research can be conducted to discover the influences of rearing and genetics, or the source of variation in their normal development and success (or not) of the fish as they age up to and past 29 MPH. With these results, research can determine how changes in water quality and human influences by more direct investigation of their effects on early Lake Sturgeon muscle development and survival. Finally, the evolutionary context of the findings on Lake Sturgeon muscle growth and SCs will be important to consider in

comparisons with other ancient species such as lamprey (*Icthyomyozon fossor*), teleosts, and mammals, in relation to the notion of determinate vs. indeterminate growth patterns in muscle fiber number.

.

References

Abmayr, S. M., & Pavlath, G. K. (2012). Myoblast fusion: lessons from flies and mice. *Development*, *139*(4), 641–656. https://doi.org/10.1242/dev.068353

Anderson, J., Cunha & Docker (2018). Novel "omega fibers" in superficial body-wall myotomes during metamorphosis in the northern brook lamprey, *Ichthyomyzon fossor*. Submitted for publication in J Exp Zool. B: Molecular and Cellular Evolution (MS#: B-2018-05-0027).

Anderson, J. E. (2000). A Role for Nitric Oxide in Muscle Repair : Nitric Oxide – mediated Activation of Muscle Satellite Cells. *Molecular Biology of the Cell*, *11*(May), 1859–1874.

Anderson, J. E., Garrett, K., Moor, A., McIntosh, L. M., & Penner, K. (1998). Dystrophy and Myogenesis in mdx Diaphragm Muscle. *Muscle & Nerve*, *21*(September), 1153–1165.

Anderson, J. E., Wozniak, A. C., & Mizunoya, W. (2012). Myogenesis, *798*, 85–102. https://doi.org/10.1007/978-1-61779-343-1

Barth, C. C., & Anderson, G. W. (2015). Factors influencing spatial distribution and growth of juvenile lake sturgeon (Acipenser fulvescens). *Canadian Journal of Zoology*, *93*, 823–831. https://doi.org/10.1139/cjz-2015-0058

Baylor, S. M., & Hollingworth, S. (1998). Model of Sarcomeric Ca2+ Movements, Including ATP Ca2+ Binding and Diffusion, during Activation of Frog Skeletal Muscle. *The Journal of General Physiology*, *112*(3).

Bekoff, B. Y. A., & Betz, W. (1977). Properties of Isolated Adult Rat Muscle Fibres Maintained in Tissue Culture. *Journal of Physiology*, *271*, 537–547.

Belghit, I., Skiba-Cassy, S., Geurden, I., Dias, K., Surget, A., Kaushik, S., … Seiliez, I. (2014). Dietary methionine availability affects the main factors involved in muscle protein turnover in rainbow trout (Oncorhynchus mykiss). *British Journal of Nutrition*, *112*(4), 493–503. https://doi.org/10.1017/S0007114514001226

Bevan, S., & Steinbach, J. H. (1977). The distribution of α-bungarotoxin binding sites on mammalian skeletal muscle developing *in vivo*. *The Journal of Physiology*, *267*(1), 195–213. https://doi.org/10.1113/jphysiol.1977.sp011808

Biga, P. R., & Goetz, F. W. (2006). Zebrafish and giant danio as models for muscle growth: determinate vs. indeterminate growth as determined by morphometric analysis. *American Journal of Physiology-Regulatory, Integrative and Comparative Physiology*, *291*(5), R1327–R1337. https://doi.org/10.1152/ajpregu.00905.2005

Boudreau-Larivière, C., Parry, D. J., & Jasmin, B. J. (2000). Myotubes originating from single fast and slow satellite cells display similar patterns of AChE expression. *American Journal of Physiology. Regulatory, Integrative and Comparative Physiology*, *278*(1), R140-8. Retrieved from http://www.ncbi.nlm.nih.gov/pubmed/10644632

Bower, N. I., & Johnston, I. A. (2010). Paralogs of Atlantic salmon myoblast determination factor genes are distinctly regulated in proliferating and differentiating myogenic cells. *AJP: Regulatory, Integrative and Comparative Physiology*, *298*(6), R1615–R1626. https://doi.org/10.1152/ajpregu.00114.2010

Braun, T., Bober, E., Rudnicki, M. a, Jaenisch, R., & Arnold, H. H. (1994). MyoD expression marks the onset of skeletal myogenesis in Myf-5 mutant mice. *Development (Cambridge, England)*, *120*(11), 3083–3092. https://doi.org/10.1091/mbc.E08

Brooke, M. H., & Kaiser, K. K. (1970). Muscle fiber types: how many and what kind? *Archives Neurology*, *23*, 369–379.

Brown, M. D., Cotter, M. A., Hudlickfi, O., & Vrbovfi, G. (1976). The Effects of Different Patterns of Muscle Activity on Capillary Density, Mechanical Properties and Structure of Slow and Fast Rabbit Muscles. *Pflugers Arch: European Journal of Physiology*, *361*, 241–250.

Bruusgaard, J. C., Johansen, I. B., Egner, I. M., Rana, Z. A., & Gundersen, K. (2010). Myonuclei acquired by overload exercise precede hypertrophy and are not lost on detraining. *Proceedings of the National Academy of Sciences*, *107*(34), 15111–15116. https://doi.org/10.1073/pnas.0913935107

Bruusgaard, J. C., Liestøl, K., & Gundersen, K. (2006). Distribution of myonuclei and microtubules in live muscle fibers of young, middle-aged, and old mice. *Journal of Applied Physiology*, *100*, 2024–2030. https://doi.org/10.1152/japplphysiol.00913

Buckingham, M., Bajard, L., Chang, T., Daubas, P., Hadchouel, J., Meilhac, S., … Relaix, F. (2003). The formation of skeletal muscle: from soma to limb. *Journal of Anatomy*, *202*, 59–68.

Cao, Y., Zhao, Z., Gruszczynska-Biegala, J., & Zolkiewska, A. (2003). Role of metalloprotease disintegrin ADAM12 in determination of quiescent reserve cells

during myogenic differentiation in vitro. *Molecular and Cellular Biology*, *23*(19), 6725–38. https://doi.org/10.1128/MCB.23.19.6725-6738.2003

Chakkalakal, J. V., Jones, K. M., Basson, M. A., & Brack, A. S. (2012). The aged niche disrupts muscle stem cell quiescence. *Nature*, *490*(7420), 355–360. https://doi.org/10.1038/nature11438

Chang, N. C., & Rudnicki, M. A. (2014). *Satellite Cells: The Architects of Skeletal Muscle*. *Current Topics in Developmental Biology* (1st ed., Vol. 107). Elsevier Inc. https://doi.org/10.1016/B978-0-12-416022-4.00006-8

Chargé, S. B. P., & Rudnicki, M. (2004). Cellular and molecular regulation of muscle regeneration. *Physiological Reviews*, *84*(1), 209–238. https://doi.org/10.1152/physrev.00019.2003

Cheung, T. H., Quach, N. L., Charville, G. W., Liu, L., Park, L., Edalati, A., … Rando, T. A. (2012). Maintenance of muscle stem-cell quiescence by microRNA-489. *Nature*, *482*(7386), 524–8. https://doi.org/10.1038/nature10834

Choi, J., Costa, M. L., Mermelstein, C. S., Chagas, C., Holtzer, S., & Holtzer, H. (1990). MyoD converts primary dermal fibroblasts, chondroblasts, smooth muscle, and retinal pigmented epithelial cells into striated mononucleated myoblasts and multinucleated myotubes. *Proceedings of the National Academy of Sciences of the United States of America*, *87*(20), 7988–92. Retrieved from http://www.ncbi.nlm.nih.gov/pubmed/2172969

Close, R. I. (1972). Dynamic Properties of Mammalian Skeletal Muscles. *Physiological Reviews*, *52*(1), 129–197.

Collins, C. A., Olsen, I., Zammit, P. S., Heslop, L., Petrie, A., Partridge, T. A., & Morgan, J. E. (2005). Stem cell function, self-renewal, and behavioral heterogeneity of cells from the adult muscle satellite cell niche. *Cell*, *122*(2), 289–301. https://doi.org/10.1016/j.cell.2005.05.010

Conboy, M. J., Karasov, A. O., & Rando, T. A. (2007). High Incidence of Non-Random Template Strand Segregation and Asymmetric Fate Determination In Dividing Stem Cells and their Progeny. *PLoS Biology*, *5*(5), e102. https://doi.org/10.1371/journal.pbio.0050102

Cornelison, D. D. W., & Wold, B. J. (1997). Single-Cell Analysis of Regulatory Gene Expression in Quiescent and Activated Mouse Skeletal Muscle Satellite Cells. *Developmental Biology*, *191*, 270–283. https://doi.org/10.1006/dbio.1997.8721

Crist, C. G., Montarras, D., & Buckingham, M. (2012). Muscle Satellite Cells Are Primed for Myogenesis but Maintain Quiescence with Sequestration of Myf5 mRNA Targeted by microRNA-31 in mRNP Granules. *Cell Stem Cell*, *11*(1), 118–126. https://doi.org/10.1016/j.stem.2012.03.011

Curzi, D., Salucci, S., Marini, M., Esposito, F., Agnello, L., Veicsteinas, A., … Falcieri, E. (2012). How physical exercise changes rat myotendinous junctions: An ultrastructural study. *European Journal of Histochemistry*, *56*(2), 117–122. https://doi.org/10.4081/ejh.2012.e19

Deasy, B. M., Jankowski, R. J., Payne, T. R., Cao, B., Goff, J. P., Greenberger, J. S., & Huard, J. (2003). Modeling Stem Cell Population Growth: Incorporating Terms for Proliferative Heterogeneity. *Stem Cells*, *21*(5), 536–545.

https://doi.org/10.1634/stemcells.21-5-536

Delfini, M. C., Hirsinger, E., Pourquié, O., & Duprez, D. (2000). Delta 1-activated notch inhibits muscle differentiation without affecting Myf5 and Pax3 expression in chick limb myogenesis. *Development (Cambridge, England)*, *127*, 5213–5224. Retrieved from http://dev.biologists.org/content/develop/127/23/5213.full.pdf

Dietrich, S., Abou-Rebyeh, F., Brohmann, H., Bladt, F., Sonnenberg-Riethmacher, E., Yamaai, T., … Birchmeier, C. (1999). The role of SF/HGF and c-Met in the development of skeletal muscle. *Development (Cambridge, England)*, *126*(8), 1621–1629.

Dumont, N. A., Wang, Y. X., von Maltzahn, J., Pasut, A., Bentzinger, C. F., Brun, C. E., & Rudnicki, M. A. (2015). Dystrophin expression in muscle stem cells regulates their polarity and asymmetric division. *Nature Medicine*, *21*(12), 1455–1463. https://doi.org/10.1038/nm.3990

Ellisman, M. H., Rash, J. E., Staehelin, A., & Porter, K. R. (1976). Studies of Excitable Membranes: II. A Comparison of Specializations at Neuromuscular Junctions and Nonjunctional Sarcolammas. *The Journal of Cell Biology*, *68*, 752–774.

Engler, A. J., Griffin, M. A., Sen, S., Bönnemann, C. G., Sweeney, H. L., & Discher, D. E. (2004). Myotubes differentiate optimally on substrates with tissue-like stiffness. *The Journal of Cell Biology*, *166*(6), 877–887. https://doi.org/10.1083/jcb.200405004

Epstein, J. A., Shapiro, D. N., Cheng, J., Lam, P. Y. P., & Maas, R. L. (2017). Pax3 Modulates Expression of the c-Met Receptor during Limb Muscle Development.

Proceedings of the National Academy of Sciences of the United States of America, *93*(9), 4213–4218.

Franchi, M. V., Reeves, N. D., & Narici, M. V. (2017). Skeletal muscle remodeling in response to eccentric vs. concentric loading: Morphological, molecular, and metabolic adaptations. *Frontiers in Physiology*, *8*(JUL), 1–16. https://doi.org/10.3389/fphys.2017.00447

Fukada, S., Uezumi, A., Ikemoto, M., Masuda, S., Segawa, M., Tanimura, N., … Takeda, S. (2007). Molecular Signature of Quiescent Satellite Cells in Adult Skeletal Muscle. *Stem Cells*, *25*(10), 2448–2459. https://doi.org/10.1634/stemcells.2007-0019

Gabillard, J. C., Sabin, N., & Paboeuf, G. (2010). In vitro characterization of proliferation and differentiation of trout satellite cells. *Cell and Tissue Research*, *342*(3), 471–477. https://doi.org/10.1007/s00441-010-1071-8

Grifone, R., Demignon, J., Houbron, C., Souil, E., Niro, C., Seller, M. J., … Maire, P. (2005). Six1 and Six4 homeoproteins are required for Pax3 and Mrf expression during myogenesis in the mouse embryo. *Development*, *132*(9), 2235–49. https://doi.org/10.1242/dev.01773

Gros, J., Manceau, M., Thomé, V., & Marcelle, C. (2005). A common somitic origin for embryonic muscle progenitors and satellite cells. *Nature*, *435*(7044), 954–958. https://doi.org/10.1038/nature03572

Halevy, O., Piestun, Y., Allouh, M. Z., Rosser, B. W. C., Rinkevich, Y., Reshef, R., … Yablonka-Reuveni, Z. (2004). Pattern of Pax7 expression during myogenesis in the

posthatch chicken establishes a model for satellite cell differentiation and renewal. *Developmental Dynamics*, *231*(3), 489–502. https://doi.org/10.1002/dvdy.20151

Hardy, R. S., & Litvak, M. K. (2004). Effects of temperature on the early development, growth, and survival of shortnose sturgeon, Acipenser brevirostrum, and Atlantic sturgeon, Acipenser oxyrhynchus, yolk-sac larvae. *Environmental Biology of Fishes*, *70*, 145–154.

Harel, I., Nathan, E., Tirosh-Finkel, L., Zigdon, H., Guimarães-Camboa, N., Evans, S. M., & Tzahor, E. (2009). Distinct Origins and Genetic Programs of Head Muscle Satellite Cells. *Developmental Cell*, *16*(6), 822–832. https://doi.org/10.1016/j.devcel.2009.05.007

Holmes, K. C., & Geeves, M. (2000). The structural basis of muscle contraction. *The Royal Society*, *355*, 419–431.

Houmard, J. A., Weidner, M. L., Gavigan, K. E., Tyndall, G. L., Hickey, M. S., & Alshami, A. (1998). Fiber type and citrate synthase activity in the human gastrocnemius and vastus lateralis with aging. *Journal Of Applied Physiology (Bethesda, Md.: 1985)*, *85*(4), 1337–1341. Retrieved from http://search.ebscohost.com.delfos.uem.es/login.aspx?direct=true&db=cmedm&AN=9760325&lang=es&site=ehost-live

Huxley, A. F., & Niedergerke, R. (1954). Structural Changes in Muscle During Contraction. *Nature*, *173*, 971–973.

Imaoka, Y., Kawai, M., Mori, F., & Miyata, H. (2015). Effect of eccentric contraction on satellite cell activation in human vastus lateralis muscle. *The Journal of*

Physiological Sciences, *65*(5), 461–469. https://doi.org/10.1007/s12576-015-0385-4

Johnston, I. A. (1999). Muscle development and growth: Potential implications for flesh quality in fish. *Aquaculture*, *177*(1–4), 99–115. https://doi.org/10.1016/S0044-8486(99)00072-1

Johnston, I. A. (2006). Environment and plasticity of myogenesis in teleost fish. *Journal of Experimental Biology*, *209*(12), 2249–2264. https://doi.org/10.1242/jeb.02153

Johnston, I. A., de la serrana, D. G., & Devlin, R. H. (2014). Muscle fibre size optimisation provides flexibility for energy budgeting in calorie-restricted coho salmon transgenic for growth hormone. *Journal of Experimental Biology*, *217*(19), 3392–3395. https://doi.org/10.1242/jeb.107664

Johnston, I. A., Kristjánsson, B. K., Paxton, C. G. P., Vieira, V. L. A., Macqueen, D. J., & Bell, M. A. (2012). Universal scaling rules predict evolutionary patterns of myogenesis in species with indeterminate growth. *Source: Proceedings: Biological Sciences Proc. R. Soc. B*, *279*(279), 2255–2261. https://doi.org/10.1

Johnston, I. a, Bower, N. I., & Macqueen, D. J. (2011). Growth and the regulation of myotomal muscle mass in teleost fish. *The Journal of Experimental Biology*, *214*(10), 1617–1628. https://doi.org/10.1242/jeb.038620

Kablar, B., Krastel, K., Ying, C., Tapscott, S. J., Goldhamer, D. J., & Rudnicki, M. A. (1999). Myogenic determination occurs independently in somites and limb buds. *Developmental Biology*, *206*(2), 219–31. https://doi.org/10.1006/dbio.1998.9126

Kassar-Duchossoy, L., Giacone, E., Gayraud-Morel, B., Jory, A., Gom??s, D., &

Tajbakhsh, S. (2005). Pax3/Pax7 mark a novel population of primitive myogenic cells during development. *Genes and Development*, *19*(12), 1426–1431. https://doi.org/10.1101/gad.345505

Kelly, A. M., & Zacks, S. I. (1969). The Histogenesis of Rat Intercostal Muscle. *The Journal of Cell Biology*, *42*, 135–153.

Kern, H., Barberi, L., Löfler, S., Sbardella, S., Burggraf, S., Fruhmann, H., … Musaro, A. (2014). Electrical stimulation counteracts muscle decline in seniors, *6*(July), 1–11. https://doi.org/10.3389/fnagi.2014.00189

Kirkpatrick, L. J., Allouh, M. Z., Nightingale, C. N., Devon, H. G., Yablonka-Reuveni, Z., & Rosser, B. W. C. (2008). Pax7 shows higher satellite cell frequencies and concentrations within intrafusal fibers of muscle spindles. *Journal of Histochemistry and Cytochemistry*, *56*(9), 831–840. https://doi.org/10.1369/jhc.2008.951608

Koumans, J. T. ., Akster, H. A., Booms, G. H. ., & Osse, J. W. . (1993). Growth of carp (Cyprinus carpio) white axial muscle; hyperplasia and hypertrophy in relation to the myonucleus/sarcoplasm ratio and the occurence of different subclasses of myogenic cells.pdf. Journal of Fish Biology.

Koumans, J. T. M., Akster, H. A., Booms, G. H. R., Lemmens, C. J. J., & Osse, J. W. M. (1991). Numbers of myosatellite cells in white axial muscle of growing fish: Cyprinus carpio L. (teleostei). *American Journal of Anatomy*, *192*(4), 418–424. https://doi.org/10.1002/aja.1001920409

Kuang, S., Kuroda, K., Le Grand, F., & Rudnicki, M. A. (2007). Asymmetric Self-Renewal and Commitment of Satellite Stem Cells in Muscle. *Cell*, *129*(5), 999–

1010. https://doi.org/10.1016/j.cell.2007.03.044

Larsson, L., Edström, L., Lindegren, B., Gorza, L., & Schiaffino, S. (1991). MHC composition and enzyme-histochemical and physiological properties of a novel fast-twitch motor unit type. *The American Journal of Physiology*, *261*(1), 93–101. Retrieved from http://www.ncbi.nlm.nih.gov/pubmed/1858863

Leiter, J. R. S., & Anderson, J. E. (2010). Satellite cells are increasingly refractory to activation by nitric oxide and stretch in aged mouse-muscle cultures. *International Journal of Biochemistry and Cell Biology*, *42*(1), 132–136. https://doi.org/10.1016/j.biocel.2009.09.021

Leiter, J. R. S., Upadhaya, R., & Anderson, J. E. (2012). Nitric oxide and voluntary exercise together promote quadriceps hypertrophy and increase vascular density in female 18-mo-old mice. *AJP: Cell Physiology*, *302*(9), C1306–C1315. https://doi.org/10.1152/ajpcell.00305.2011

Leshem, Y., Spicer, D. B., Gal-Levi, R., & Halevy, O. (2000). Hepatocyte growth factor (HGF) inhibits skeletal muscle cell differentiation: A role for the bHLH protein Twist and the cdk inhibitor p27. *Journal of Cellular Physiology*, *184*(1), 101–109. https://doi.org/10.1002/(SICI)1097-4652(200007)184:1<101::AID-JCP11>3.0.CO;2-D

Lieber, R. L. (1993). Skeletal Muscle Architecture: Implications for Muscle Function and Surgical Tendon Transfer. *Journal of Hand Therapy*, *6*(2), 105–113. https://doi.org/10.1016/S0894-1130(12)80291-2

Lieber, R. L., & Friden, J. (2000). Functional and clinical significance of skeletal muscle

architecture. *Muscle & Nerve*, *23*(11), 1647–1666. https://doi.org/10.1002/1097-4598(200011)23:11<1647::AID-MUS1>3.0.CO;2-M

Lin, W., Burgess[2], R. W., Dominguez, B., Pfaff, S. L., Sanes[2], J. R., & Lee, K.-F. (2001). Distinct roles of nerve and muscle in postsynaptic differentiation of the neuromuscular synapse. *Nature*, *410*(26).

Maeda, N., Miyoshi, S., & Toh, H. (1983). First observation of a muscle spindle in fish. *Nature*. https://doi.org/10.1038/302061a0

Mankoo, B. S., Collins, N. S., Ashby, P., Grigorieva, E., Pevny, L. H., Candia, a, … Pachnis, V. (1999). Mox2 is a component of the genetic hierarchy controlling limb muscle development. *Nature*, *400*(6739), 69–73. https://doi.org/10.1038/21892

Marics, I., Padilla, F., Guillemot, J.-F., Scaal, M., & Marcelle, C. (2002). FGFR4 signaling is a necessary step in limb muscle differentiation. *Development*, *129*(19).

Mauro, A. (1961). Satellite cell of skeletal muscle fibers. *The Journal of Biophysical and Biochemical Cytology*, *9*, 493–5. Retrieved from http://www.ncbi.nlm.nih.gov/pubmed/13768451

McLoon, L. K., & Wirtschafter, J. D. (2002). Continuous myonuclear addition to single extraocular myofibers in uninjured adult rabbits. *Muscle and Nerve*, *25*(3), 348–358. https://doi.org/10.1002/mus.10056

Miller, J. B., & Stockdale, F. E. (1986). Developmental origins of skeletal muscle fibers: Clonal analysis of myogenic cell lineages based on expression of fast and slow myosin heavy chains (myoblast/myotube/muscle cell culture/chicken embryo/fast

and slow muscle fibers). *Developmental Biology*, *83*, 3860–3864.

Mizunoya, W., Upadhaya, R., Burczynski, F. J., Wang, G., & Anderson, J. E. (2011). Nitric oxide donors improve prednisone effects on muscular dystrophy in the mdx mouse diaphragm. https://doi.org/10.1152/ajpcell.00482.2010.

Mootoosamy, R. C., & Dietrich, S. (2002). Distinct regulatory cascades for head and trunk myogenesis. *Development (Cambridge, England)*, *129*(3), 573–83. Retrieved from http://www.ncbi.nlm.nih.gov/pubmed/11830559

Motohashi, N., & Asakura, A. (2014). Muscle satellite cell heterogeneity and self-renewal. *Front Cell Dev Biol.*, *2*(1), 1–21. https://doi.org/10.3389/fcell.2014.00001

Mukaka, M. M. (2012). A guide to appropriate use of Correlation coefficient in medical research. *Malawi Medical Journal*, *24*(3), 69–71. https://doi.org/10.1016/j.cmpb.2016.01.020

Nowak, S. J., Nahirney, P. C., Hadjantonakis, A.-K., & Baylies, M. K. (2009). Nap1-mediated actin remodeling is essential for mammalian myoblast fusion. *Journal of Cell Science*, *122*(Pt 18), 3282–93. https://doi.org/10.1242/jcs.047597

Nowakowski, R. S., Lewin, S. B., & Miller, M. W. (1989). Bromodeoxyuridine immunohistochemical determination of the lengths of the cell cycle and the DNA-synthetic phase for an anatomically defined population. *Journal of Neurocytology*, *18*(3), 311–318. https://doi.org/10.1007/BF01190834

Peterson, D. L., Vacsei, P., & Jennings, C. A. (2007). Ecology and Biology of the Lake Sturgeon: A Synthesis of Current Knowledge of a Threatened North American

Acipenseridae. *Reviews in Fish Biology and Fisheries*, *17*, 59–76.

Pollock, M. S., Carr, M., Kreitals, N. M., & Phillips, I. D. (2015). Review of a species in peril: what we do not know about lake sturgeon may kill them. *Environmental Reviews*, *23*, 30–43. Retrieved from http://www.nrcresearchpress.com.uml.idm.oclc.org/doi/pdf/10.1139/er-2014-0037

Przewoźniak, M., Czaplicka, I., Czerwińska, A. M., Markowska-Zagrajek, A., Moraczewski, J., Stremińska, W., … Brzoska, E. (2013). Adhesion Proteins - An Impact on Skeletal Myoblast Differentiation. *PLoS ONE*, *8*(5), e61760. https://doi.org/10.1371/journal.pone.0061760

Puthucheary, Z., Skipworth, J. R. A., Rawal, J., Loosemore, M., Van Someren, K., & Montgomery, H. E. (2011). Genetic Influences in Sport and Physical Performance. *Sports Medicine*, *41*(10), 845–859. https://doi.org/10.2165/11593200-000000000-00000

Qu-Petersen, Z., Deasy, B., Jankowski, R., Ikezawa, M., Cummins, J., Pruchnic, R., … Huard, J. (2002). Identification of a novel population of muscle stem cells in mice: potential for muscle regeneration. *J.Cell Biol.*, *157*(0021–9525 (Print)), 851–864. https://doi.org/10.1083/jcb.200108150

Rescan, P. Y. (2005). Muscle growth patterns and regulation during fish ontogeny. *General and Comparative Endocrinology*, *142*(1–2 SPEC. ISS.), 111–116. https://doi.org/10.1016/j.ygcen.2004.12.016

Rome, Lawrence, C. (1997). Testing a Muscle's Design: Animals Jump, Swim and Communicate by using muscles that are Anatomically and Physiologically well-

adapted to Specific Functions. *American Scientist*, *85*(4), 356–363.

Rosser, B. W. C., Dean, M. S., & Bandman, E. (2002). Myonuclear domain size varies along the lengths of maturing skeletal muscle fibers. *International Journal of Developmental Biology*, *46*(5), 747–754. https://doi.org/10.1387/IJDB.12216987

Rossi, G., & Messina, G. (2014). Comparative myogenesis in teleosts and mammals. *Cellular and Molecular Life Sciences*, *71*(16), 3081–3099. https://doi.org/10.1007/s00018-014-1604-5

Rui, Y., Pan, F., & Mi, J. (2016). Composition of Muscle Fiber Types in Rat Rotator Cuff Muscles. *The Anatomical Record*, *299*(10), 1397–1401. https://doi.org/10.1002/ar.23384

Schäfer, K., & Braun, T. (1999). Early specification of limb muscle precursor cells by the homeobox gene Lbx1h. *Nature Genetics*, *23*(2), 213–216. https://doi.org/10.1038/13843

Schultz, E. (1996). Satellite cell proliferative compartments ingrowing skeletal muscles. *Developmental Biology*, *94*(175), 84–94.

Seale, P., Sabourin, L. A., Girgis-Gabardo, A., Mansouri, A., Gruss, P., & Rudnicki, M. A. (2000). Pax7 Is Required for the Specification of Myogenic Satellite Cells skeletal muscle are mitotically quiescent and are acti- vated in response to diverse stimuli, including stretch- ing, exercise, injury, and electrical stimulation. *Cell*, *102*, 777–786. https://doi.org/10.1016/S0092-8674(00)00066-0

Sfakianakis, D. G., Leris, I., & Kentouri, M. (2012). Exercise-related muscle lactate

metabolism in zebrafish juveniles: The effect of early life temperature. *Italian Journal of Zoology*, *79*(4), 568–573. https://doi.org/10.1080/11250003.2012.713032

Shea, K. L., Xiang, W., LaPorta, V. S., Licht, J. D., Keller, C., Basson, M. A., & Brack, A. S. (2010). Sprouty1 regulates reversible quiescence of a self-renewing adult muscle stem cell pool during regeneration. *Cell Stem Cell*, *6*(2), 117–29. https://doi.org/10.1016/j.stem.2009.12.015

Siegel, A. L., Kuhlmann, P. K., & Cornelison, D. (2011). Muscle satellite cell proliferation and association: new insights from myofiber time-lapse imaging. *Skeletal Muscle*, *1*(1), 7. https://doi.org/10.1186/2044-5040-1-7

Sjogaard, G. (1982). Capillary Supply and Cross-Sectional Area of Slow and Fast Twitch Muscle Fibres in Man. *Histochemistry*, *76*, 547–555.

Soukup, T., Zachařová, G., & Smerdu, V. (2002). Fibre type composition of soleus and extensor digitorum longus muscles in normal female inbred Lewis rats. *Acta Histochemica*, *104*(4), 399–405. https://doi.org/10.1078/0065-1281-00660

Staron, R. S., Leonardi, M. J., Karapondo, D. L., Malicky, E. S., Falkel, J. E., Hagerman, F. C., & Hikida, R. S. (1991). Strength and skeletal muscle adaptations in heavy-resistance-trained women after detraining and retraining. *Journal of Applied Physiology (Bethesda, Md. : 1985)*.

Steinbacher, P., Haslett, J. R., Sänger, A. M., & Stoiber, W. (2006). Evolution of myogenesis in fish: A sturgeon view of the mechanisms of muscle development. *Anatomy and Embryology*, *211*(4), 311–322. https://doi.org/10.1007/s00429-006-0082-4

Tajbakhsh, S., & Buckingham, M. E. (2017). Mouse Limb Muscle is Determined in the Absence of the Earliest Myogenic Factor myf-5. *Proceedings of the National Academy of Sciences of the United States of America*, *91*(2), 747–751.

Tajbakhsh, S., Rocancourt, D., Cossu, G., & Buckingham, M. (1997). Redefining the genetic hierarchies controlling skeletal myogenesis: Pax-3 and Myf-5 act upstream of MyoD. *Cell*, *89*(1), 127–138. https://doi.org/10.1016/S0092-8674(00)80189-0

Thiem, J. D., Hatin, D., Dumont, P., Van Der Kraak, G., & Cooke, S. J. (2013). Biology of Lake Sturgeon (Acipenser fulvescens) Spawning Below a Dam on the Richelieu River, Quebec: Behaviour, Egg Deposition, and Endocrinology. *Canadian Journal of Zoology*, *91*, 175–186.

Thompson, W. J. (1986). Changes in the innervation of mammalian skeletal muscle fibers during postnatal development. *Trends in Neuroscience*, *January*, 25–28.

Walro, J. M., & Kucera, J. (1999). Why adult mammalian intrafusal and extrafusal fibers contain different myosin heavy-chain isoforms. *Trends in Neurosciences*, *22*(4), 180–184. https://doi.org/10.1016/S0166-2236(98)01339-3

Watt, F. M., & Hogan, B. L. M. (2000). Out of Eden: Stem Cells and Their Niches Out of Eden: Stem Cells and Their Niches. *Science*, *287*, 1427–1430. Retrieved from http://www.jstor.org/stable/3074534

White, R. B., Biérinx, A.-S., Gnocchi, V. F., & Zammit, P. S. (2010). Dynamics of muscle fibre growth during postnatal mouse development. *BMC Developmental Biology*, *10*, 21. https://doi.org/10.1186/1471-213X-10-21

Winemiller, K. 0, & Rose, K. A. (1992). Patterns of Life-History Diversification in North American Fishes: Implicatibns for Population Regulation. *Canadian Journal of Fish and Aquatic Science*, *49*, 2196–2218.

Winter, F. De, Vo, T., Stam, F. J., Wisman, L. A. B., Bär, P. R., Niclou, S. P., … Verhaagen, J. (2006). The expression of the chemorepellent Semaphorin 3A is selectively induced in terminal Schwann cells of a subset of neuromuscular synapses that display limited anatomical plasticity and enhanced vulnerability in motor neuron disease. *Molecular and Cellular Neuroscience*, *32*(1–2), 102–117. https://doi.org/10.1016/j.mcn.2006.03.002

Wood, S. J., & Slater, C. R. (1995). Action potential generation in rat slow-and fast-twitch muscles. *Journal of Physiology*, *486*(2), 401–410.

Wozniak, A. C., & Anderson, J. E. (2007). Nitric oxide-dependence of satellite stem cell activation and quiescence on normal skeletal muscle fibers. *Developmental Dynamics*, *236*(1), 240–250. https://doi.org/10.1002/dvdy.21012

Wozniak, A. C., Kong, J., Bock, E., Pilipowicz, O., & Anderson, J. E. (2005). Signaling satellite-cell activation in skeletal muscle: Markers, models, stretch, and potential alternate pathways. *Muscle and Nerve*, *31*(3), 283–300. https://doi.org/10.1002/mus.20263

Yamada, M., Sankoda, Y., Tatsumi, R., Mizunoya, W., Ikeuchi, Y., Sunagawa, K., & Allen, R. E. (2008). Matrix metalloproteinase-2 mediates stretch-induced activation of skeletal muscle satellite cells in a nitric oxide-dependent manner. *International Journal of Biochemistry and Cell Biology*, *40*(10), 2183–2191.

https://doi.org/10.1016/j.biocel.2008.02.017

Yin, H., Price, F., & Rudnicki, M. a. (2013). Satellite cells and the muscle stem cell niche. *Physiological Reviews*, *93*(1), 23–67. https://doi.org/10.1152/physrev.00043.2011

Zammit, P. S., Golding, J. P., Nagata, Y., Hudon, V., Partridge, T. A., & Beauchamp, J. R. (2001). Muscle satellite cells adopt divergent fates : a mechanism for self-renewal ?, 347–357. https://doi.org/10.1083/jcb.200312007

Zhang, H., & Anderson, J. E. (2014). Satellite cell activation and populations on single muscle-fiber cultures from adult zebrafish (Danio rerio). *Journal of Experimental Biology*, *217*(11), 1910–1917. https://doi.org/10.1242/jeb.102210

Zhang, H., & Anderson, J. E. (2014). Satellite cell activation and populations on single muscle-fiber cultures from adult zebrafish (Danio rerio). *The Journal of Experimental Biology*, *217*(Pt 11), 1910–7. https://doi.org/10.1242/jeb.102210

Appendix

Antibodies

Antibody	Company	Location	Catalogue #
Anti-Pax7 in Mouse	DSHB	Iowa City, IA	178570
Biotin-conjugated Goat α Mouse 2º antibody	Jackson ImmunoResearch	West Grove, PA	115-067-003
Anti-BrdU in Mouse	Sigma-Aldrich	Oakville, ON	11170376001

Solutions

Basal Medium (BM) – L-15 medium + 1% Antibiotic/Antimycotic + 2% Fetal Bovine Serum (FBS). pH 7.4

Collagenase – 0.2% collagenase in L-15 medium

BrdU solution – 500 µg/ml BrdU in BM (diluted from a 10 mg/ml Brdu stock)

PBS (10x) – 80g NaCl + 2g KCl + 26.8g $Na_2HPO_4.7H_2O$ + 2.4g KH_2PO_4 + enough ddH_2O to make a 1000mL solution. pH to 7.4 using NaOH and HCl. Diluted 1:10 before using.

TBST (10x) – 61g Tris base + 90g NaCl + enough ddH_2O to make a 1000mL solution. pH to 8.4 using HCl and NaOH. Diluted 1:10 before using.

Collagen – 10% 0.01 NaOH + 10% 0.1M PBS + 80% CORNING Collagen

Acid Alcohol – 90% Absolute ethanol (100%) + 5% glacial acetic acid + 5% ddH_2o

TBS + HS – 0.01M TBS + 1% Horse Serum

DAB working solution – 1xPBS, 2% DAB stock (25mg/ml), 0.2% colour intensifier, 0.4% of 3% H_2O_2. – Solution was made fresh in the order stated and used right away

Disposal

- DAB
    - Some bleach was poured into a large container and the used DAB solution, as well as the first 3 ddH_2O rinse solutions were added to it. This solution needs to sit for at least 10 minutes and then it was poured down the drain using a large amount of water. Only a small amount of bleach needs to be added (when the DAB and water is added to it, it ends up being 10-20% bleach). Anything that came in contact with the DAB had to be rinsed with diluted bleach (10-20%) and then washed thoroughly with water.